Standard Model Results in *pp* Collisions by ATLAS & CMS

Yuri Kulchitsky

JINR, Dubna, Russia

B.I.Stepanov Institute of Physics NAS, Minsk, Belarus

XV-th International School-Conference "The Actual Problems of Microworld Physics"

27 August – 3 September 2023, Minsk, Belarus

STANDARD MODEL

- **The SM describes the fundamental constituents of matter and their interactions**
- The **SM** of particle physics is the theory describing **3 of the 4 known fundamental forces (electromagnetic, weak and strong interactions** — *excluding gravity*) in the universe and classifying all known elementary particles

- **Quantum chromodynamics sector** $\mathcal{L}_{\mathrm{QCD}} = \sum_{\psi} \bar{\psi}_i \left(i\gamma^\mu (\partial_\mu \delta_{ij} - i g_s G^a_\mu T^a_{ij}) \right) \psi_j - \frac{1}{4} G^a_{\mu\nu} G^{\mu\nu}_a,$
- **Electroweak sector** $\mathcal{L}_{\mathrm{EW}} = \sum_{\psi} \bar{\psi} \gamma^\mu \left(i\partial_\mu - g' \tfrac{1}{2} Y_{\mathrm{W}} B_\mu - g \tfrac{1}{2} \vec{\tau}_{\mathrm{L}} \vec{W}_\mu \right) \psi - \tfrac{1}{4} W^{\mu\nu}_a W^a_{\mu\nu} - \tfrac{1}{4} B^{\mu\nu} B_{\mu\nu},$
- **Higgs sector** $\mathcal{L}_{\mathrm{H}} = \left| \left(\partial_\mu + \frac{i}{2} \left(g' Y_{\mathrm{W}} B_\mu + g \vec{\tau} \vec{W}_\mu \right) \right) \varphi \right|^2 - \frac{\lambda^2}{4} \left(\varphi^\dagger \varphi - v^2 \right)^2.$
- **Yukawa sector** $\mathcal{L}_{\mathrm{Yukawa}} = \overline{U}_{\mathrm{L}} G_{\mathrm{u}} U_{\mathrm{R}} \varphi^0 - \overline{D}_{\mathrm{L}} G_{\mathrm{u}} U_{\mathrm{R}} \varphi^- + \overline{U}_{\mathrm{L}} G_{\mathrm{d}} D_{\mathrm{R}} \varphi^+ + \overline{D}_{\mathrm{L}} G_{\mathrm{d}} D_{\mathrm{R}} \varphi^0 + \mathrm{h.c.},$

Interaction	Gravitational	Weak	Electromagnetic	Strong	
Property		Electroweak		Fundamental	Residual
Acts on:	Mass - Energy	Flavor	Electric charge	Color charge	Atomic nuclei
Particles experiencing:	All particles	quarks, leptons	Electrically charged	Quarks, Gluons	Hadrons
Particles mediating:	Graviton (Not yet observed)	W^+, W^- and Z^0	γ (photon)	Gluons	Mesons
Strength at the scale of quarks:	10^{-41} (predicted)	10^{-4}	1	60	Not applicable to quarks
Strength at the scale of protons/neutrons:	10^{-36} (predicted)	10^{-7}	1	Not applicable to hadrons	20

QUANTUM CHROMODYNAMICS (QCD)

QCD: Quantum field theory of strong interactions (C.N. Yang, R. Mills; H. Fritzsch, M. Gell-Mann, H. Leutwyler)

- **Interaction carried by gluons acting on quarks and gluons**
- QCD-charge: colour of three types (red, blue, green)

❖ **QCD coupling strength α_s depends on energy**

$$f = f_0 + \alpha_s f_1 + \alpha_s^2 f_2 + \alpha_s^3 f_3 + \ldots$$

- **high energy** (= short distance or time): **α_s is small** (asymptotic freedom): **perturbative regime of QCD**
- **low energy** (= long distance or time): **α_s is large (confinement): non-perturbative regime of QCD**

❖ **The Renormalization Group Equation (RGE)**

$$\alpha_s(\mu^2) = \frac{\alpha_s(\mu_0^2)}{1 + b_0\alpha_s(\mu_0^2)\ln\frac{\mu^2}{\mu_0^2}} = \frac{1}{b_0 \ln\frac{\mu^2}{\Lambda^2}}$$

$$b_0 = \frac{11C_A - 2n_f}{12\pi}$$

n_f: number of light quarks;
C_A: QCD colour factors

❑ **$\alpha_s(\mu^2)$** can be expressed:

- in terms of coupling **$\alpha_s(\mu_0^2)$** at reference scale **μ_0**
- or by introducing non-perturbative constant **$\Lambda \approx 200$ MeV**, corresponding to the divergence (Landau pole) of **$\alpha_s(\mu_0^2)$**

❖ **Behaviour of $\alpha_s(\mu^2)$ as a function of energy Q (= 1/R) determines the properties of QCD and the dynamics of quarks and gluons**

- **Large Q (small distance R): α_s small:: QCD weakly interacting**; quarks and gluons asymptotically free; **regime of perturbative QCD**
- **Small Q ≈Λ (large distance R): α_s large::** QCD strongly interacting, quarks and gluons form colour-less bound states: baryons (qqq) and mesons (qq) and do not exist as free particles, **regime of non-perturbative QCD**

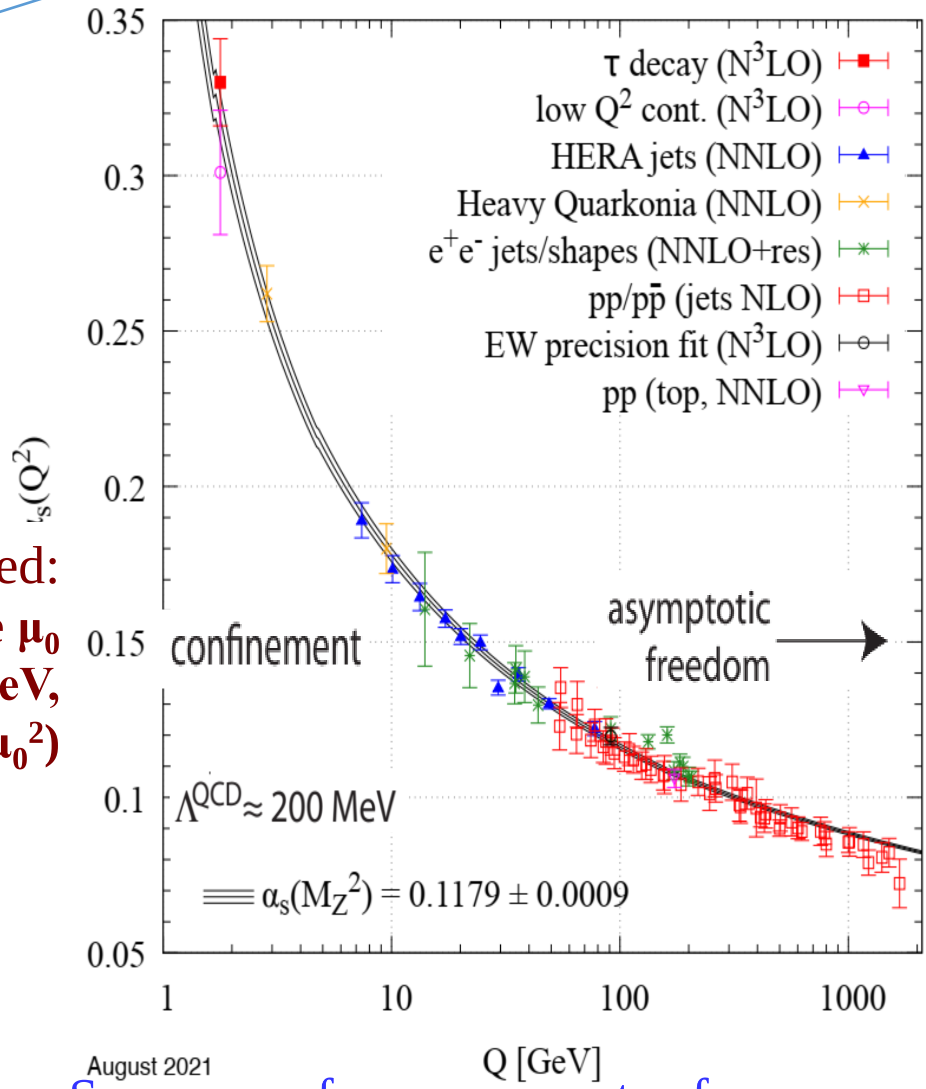

Summary of measurements of α_s as a function of the energy scale Q

QCD MEASUREMENTS AT THE LHC

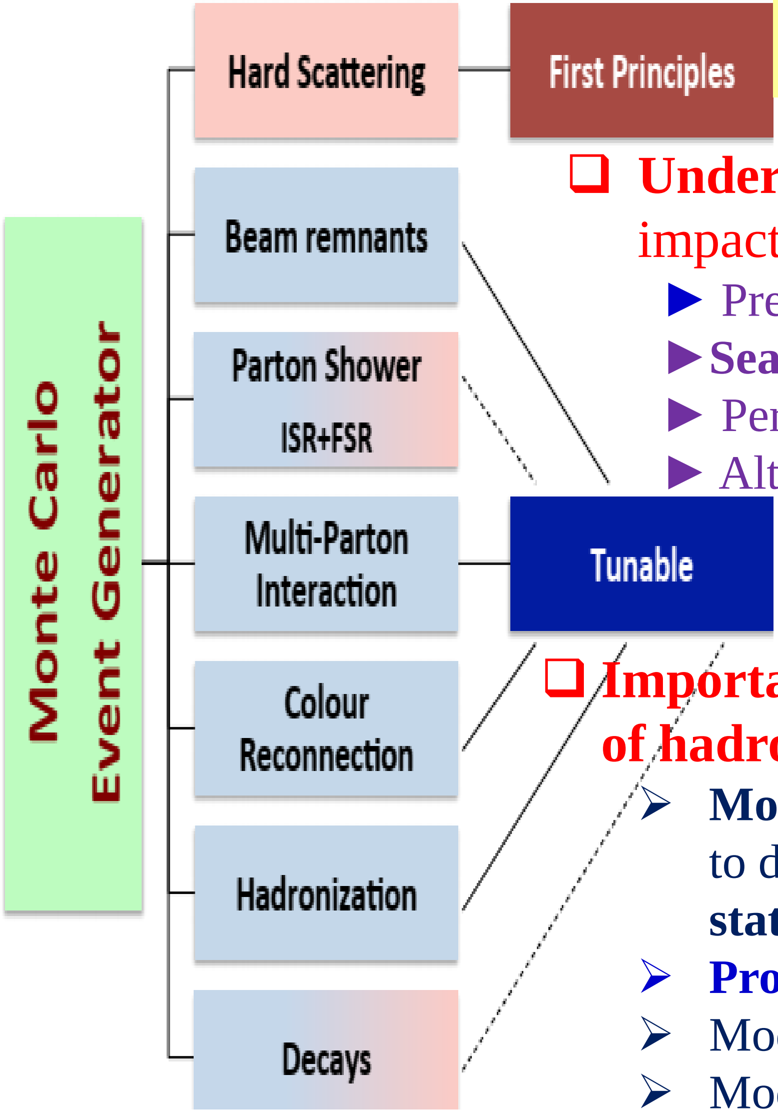

- **Understanding of soft QCD interactions** has direct impact on
  - ▶ Precision measurements,
  - ▶ **Searches for new physics,**
  - ▶ Perturbative ***Multi-Parton Interactions*** (MPI),
  - ▶ Alternative evolution equations and factorisation schemes

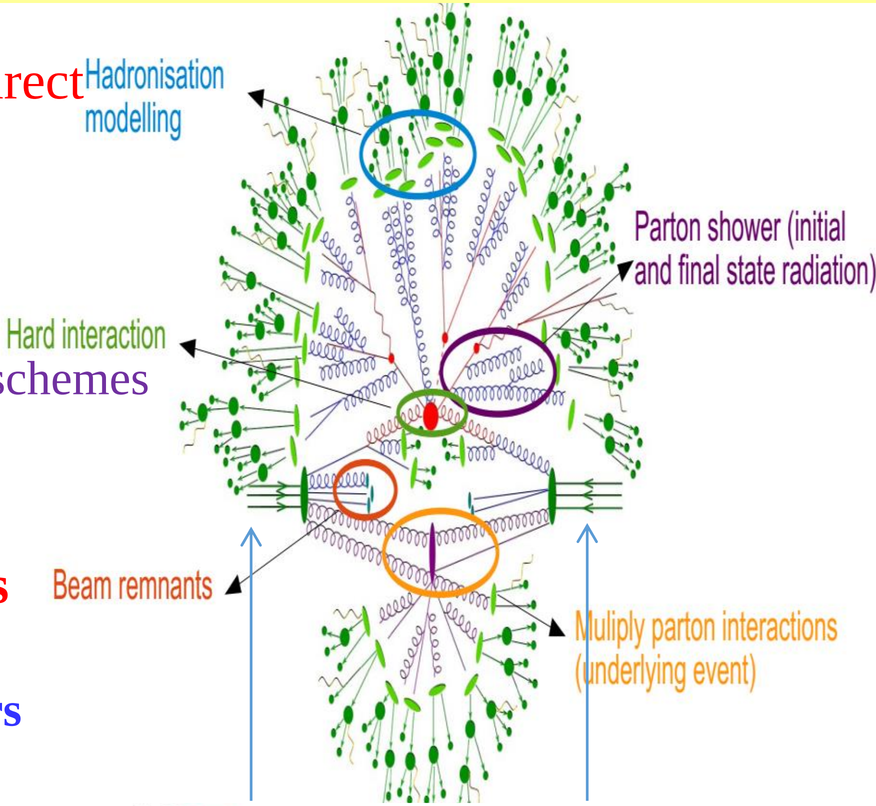

- **Importance of good modelling soft QCD aspects of hadron collisions:**
  - ➢ **Models developed** with set of **tunable parameters** to describe the **hadron-level properties** of **final states dominated** by QCD
  - ➢ **Probing parton distribution functions** (PDF)
  - ➢ Modelling **initial state of heavy ion collisions**
  - ➢ Modelling **of backgrounds for electroweak**

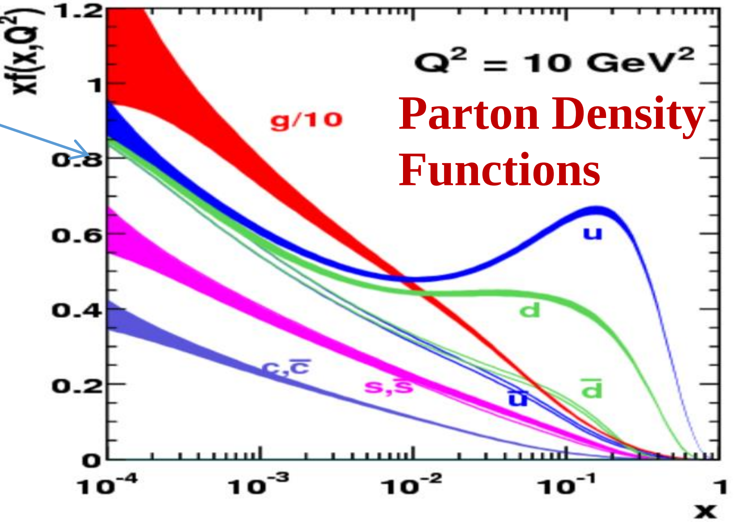

- **Soft QCD measurements are:**
  - ➢ **Crucial** for success of ongoing LHC measurements and R&D for ATLAS upgrades
  - ➢ **Crucial** for the **tuning of the Monte Carlo event generator**
  - ➢ **Essential** to **understand and correctly simulate** any other more complex phenomena
  - ➢ **Ideal** to study **tracking performance** in the "early" stage of a new data taking

SM PRODUCTION CROSS SECTION MEASUREMENTS

ATL-PHYS-PUB-2022-009

http://cern.ch/go/pNj7

Probing SM

Motivation:

- *Probing different aspects of Standard Model*
- *Sensitivity to New Physics*

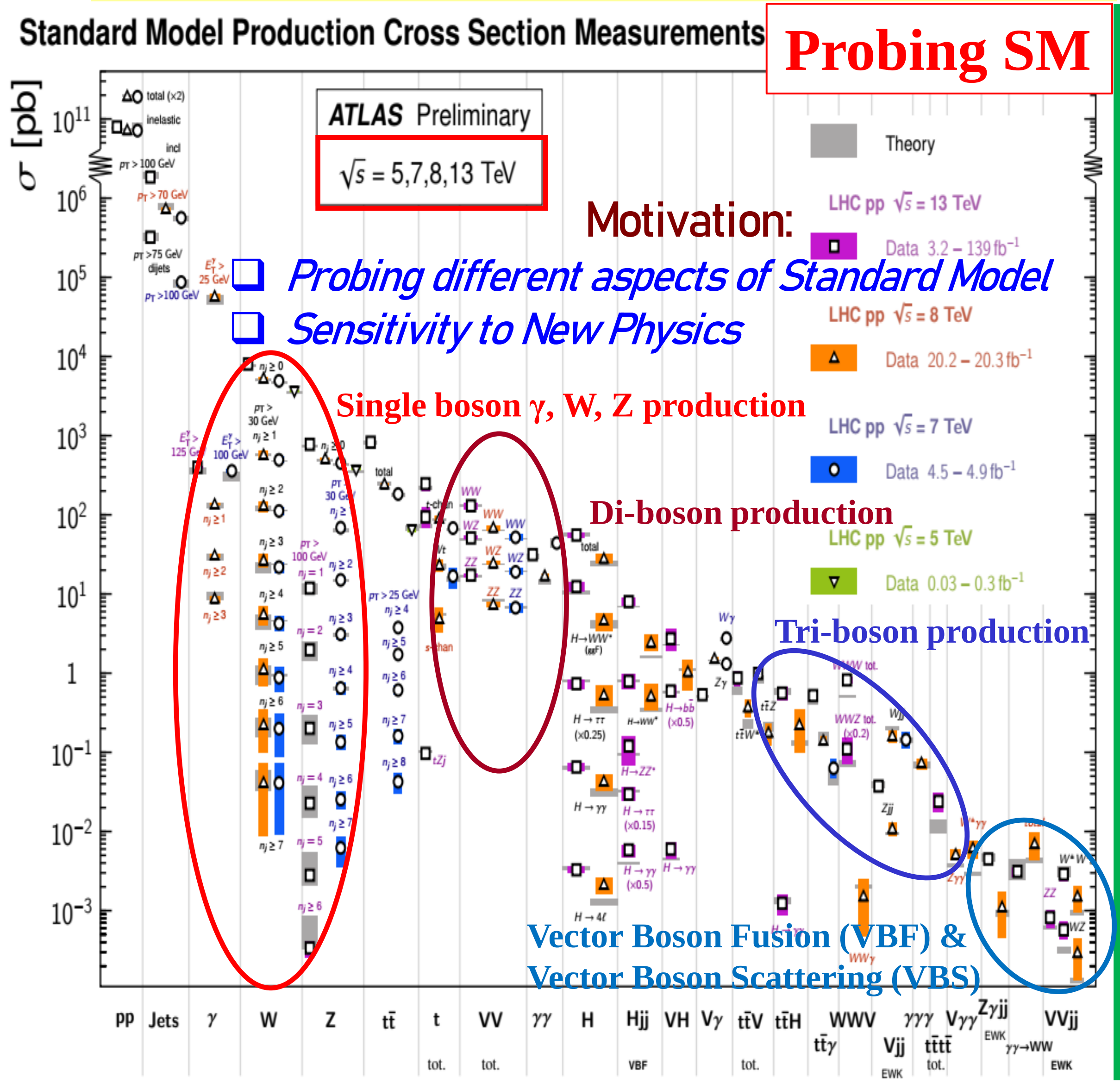

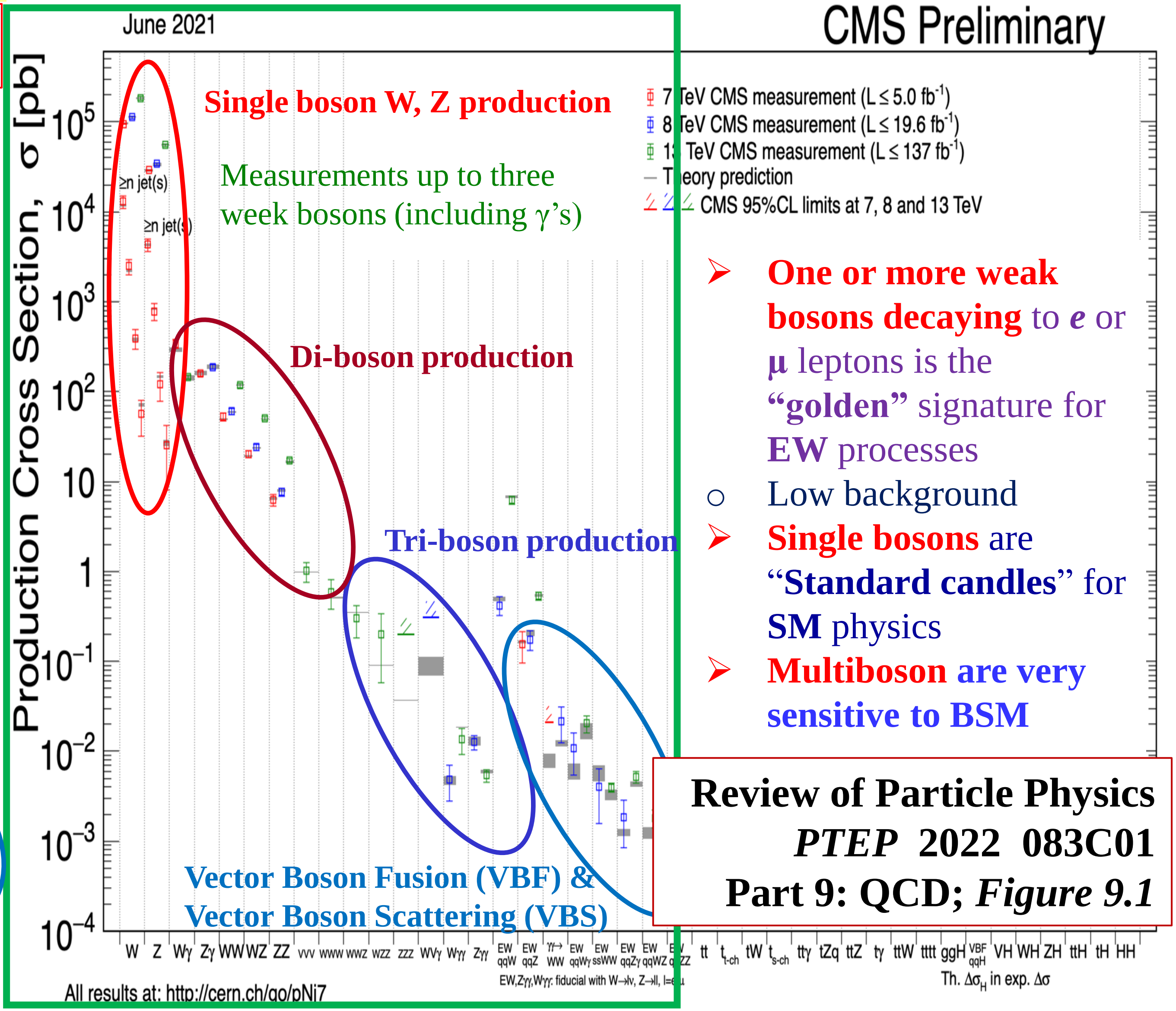

- **One or more weak bosons decaying** to ***e*** or **μ** leptons is the **"golden"** signature for **EW** processes
  - Low background
- **Single bosons** are **"Standard candles"** for **SM** physics
- **Multiboson are very sensitive to BSM**

Review of Particle Physics
***PTEP* 2022 083C01**
Part 9: QCD; *Figure 9.1*

ATLAS & CMS: Summary of SM and fiducial production cross-section measurements in **pp** interactions at **√s=5, 7, 8, 13 TeV**, corrected for branching fractions, compared to the corresponding **theoretical expectations**

A TOROIDAL LHC APPARATUS (ATLAS)

Subdetector	Operational Fraction
AFP	93.8%
ALFA	99.9%
CSC Cathode Strip Chambers	95.3%
Forward LAr Calorimeter	99.7%
Hadronic End-Cap Lar Cal	99.5%
LAr EM Calorimeter	100 %
LVL1 Calo Trigger	99.9%
LVL1 Muon RPC Trigger	99.8%
LVL1 Muon TGC Trigger	99.9%
MDT Muon Drift Tubes	99.7%
Pixels	97.8%
RPC Barrel Muon Chambers	94.4%
SCT Silicon Strips	98.7%
TGC End-Cap Muon Cha	99.5%
Tile Calorimeter	99.2%
TRT Transit Rad Tracker	97.2%

Air-core Muon spectrometer
(*μ Trigger/tracking and* ***Toroid Magnets***)
Precision Tracking:
MDT (Monitored Drift Tubes)
CSC (Cathode Strip Chambers) |η| >2.4
Trigger:
RPC (Resistive Plate Chamber) barrel
TGC (Thin Gas Chamber) endcap

Longitudinally segmented Calorimeter:
EM and Hadronic energy
LiquidAr EM barrel and End-cap & Hadronic End-cap
Tile calorimeter (Fe-scintillator) Hadronic barrel

46 m

7 000 tons

25 m

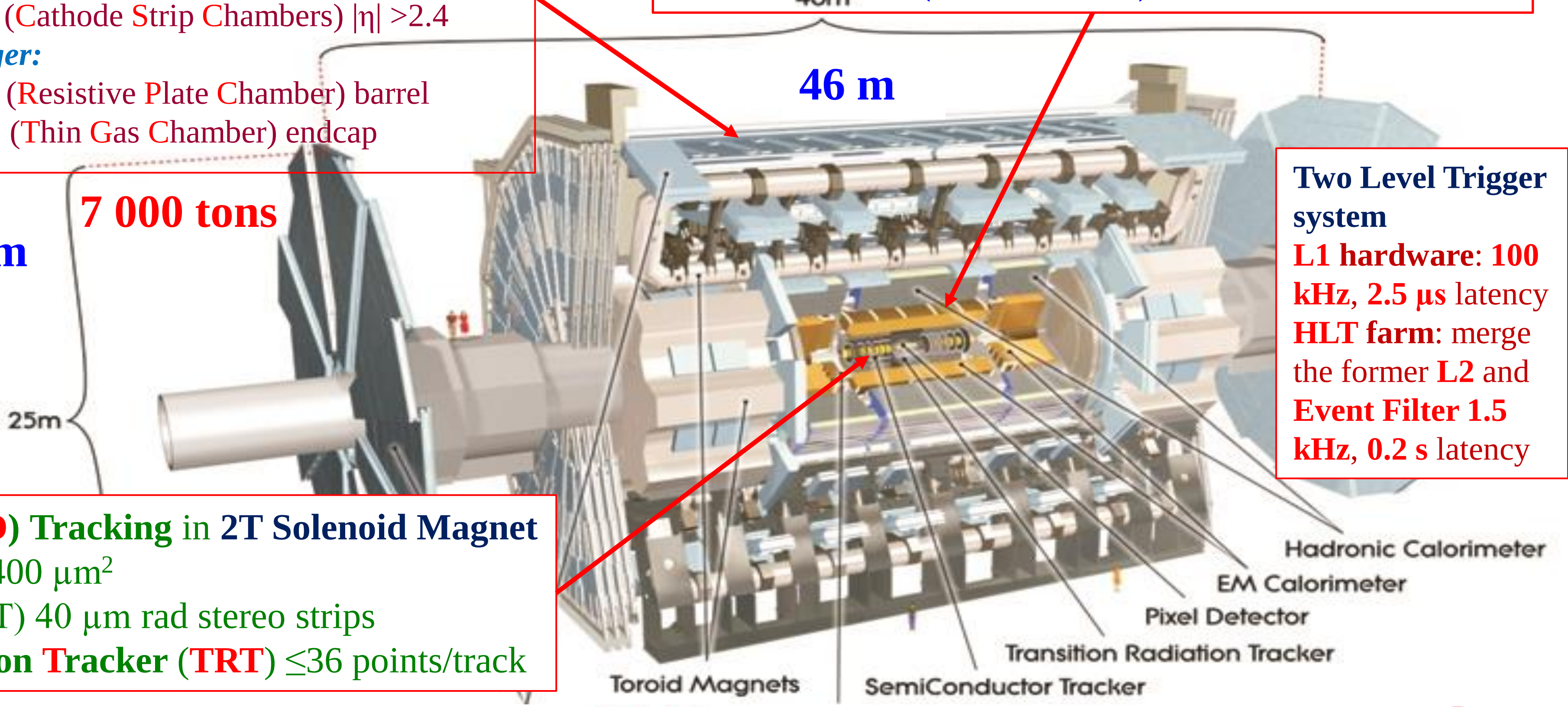

Two Level Trigger system
L1 hardware: **100 kHz**, **2.5 μs** latency
HLT farm: merge the former **L2** and **Event Filter 1.5 kHz**, **0.2 s** latency

Inner Detector (ID) Tracking in **2T Solenoid Magnet**
Silicon Pixels 50x400 μm^2
Silicon Strips (SCT) 40 μm rad stereo strips
TransitionRadiation Tracker (**TRT**) ≤36 points/track

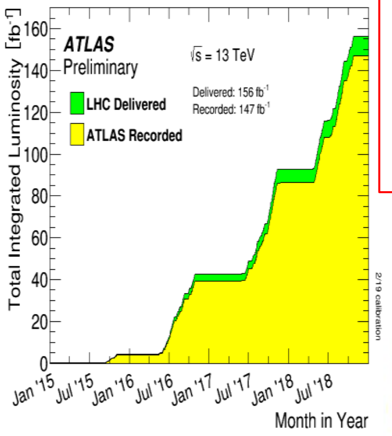

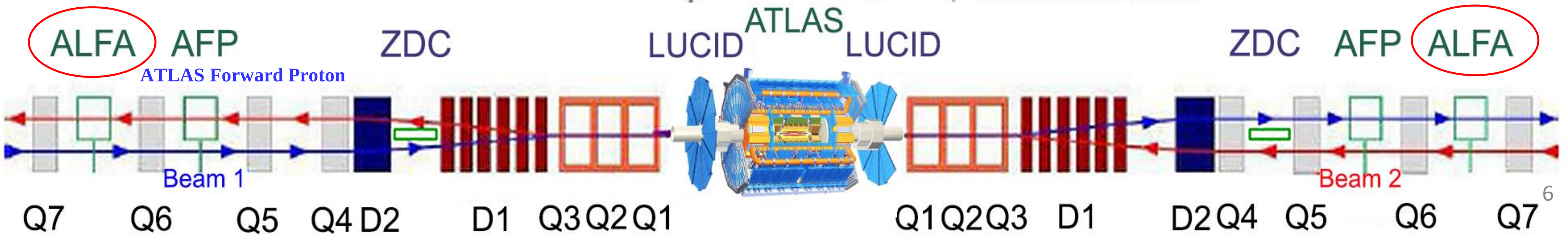

COMPACT MUON SOLENOID (CMS) + TOTEM

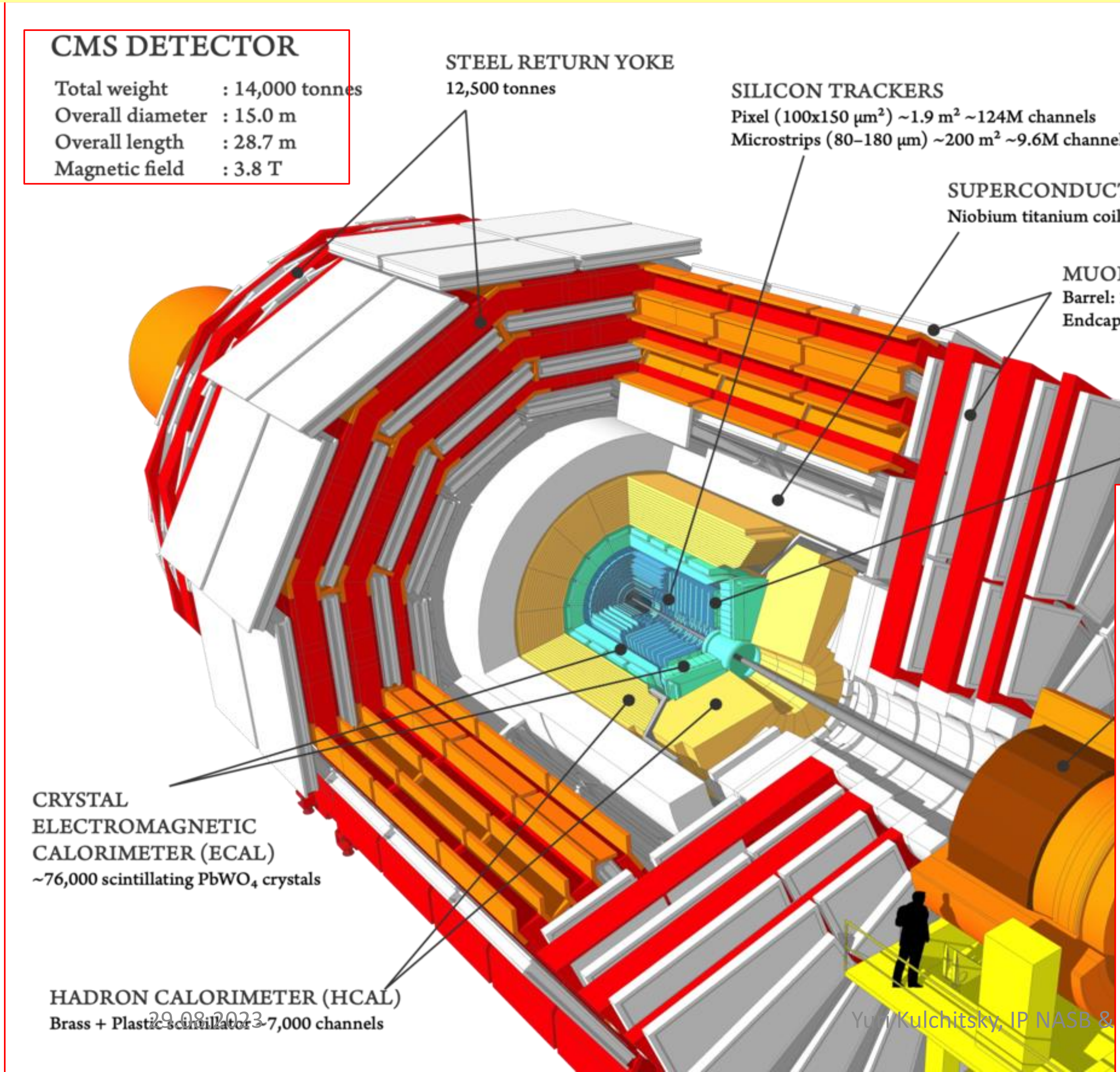

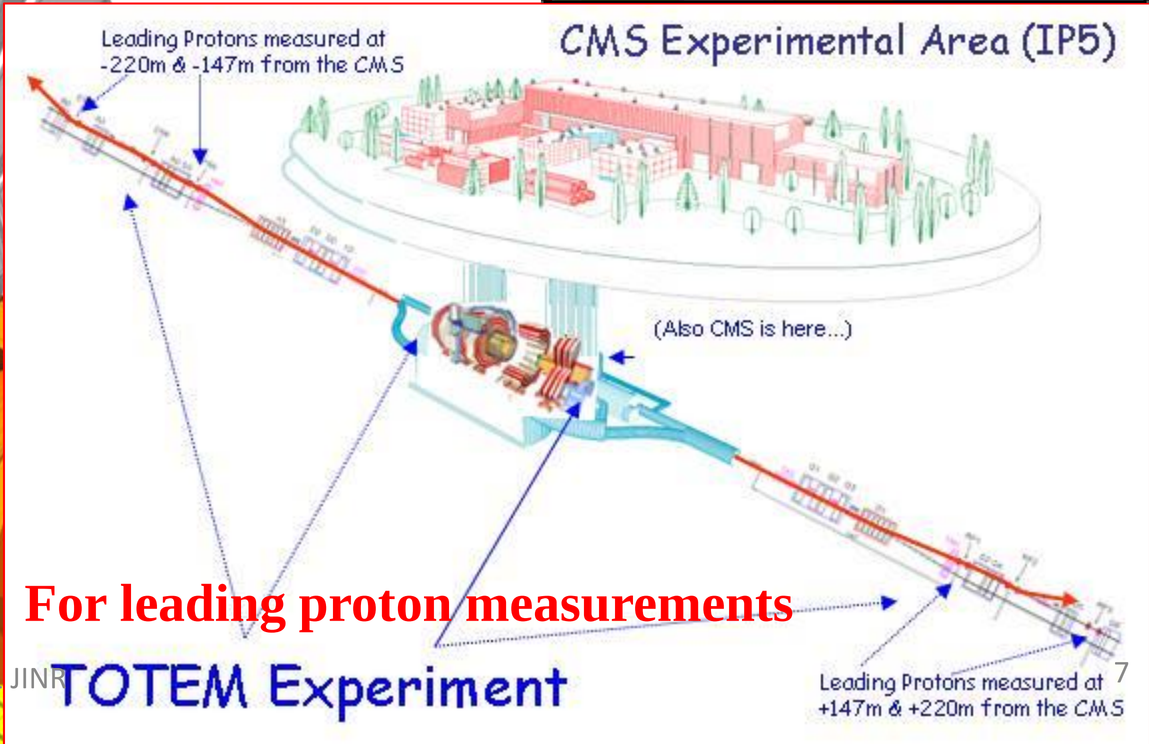

SM PRODUCTION CROSS SECTION MEASUREMENTS @ 13 TEV

- **Total Cross-sections**
  1. $pp \to X$
- **Diboson cross sections**
  1. $pp \to \gamma\gamma + X$
  2. $pp \to 4l + X$
- **WW-boson cross sections**
  1. $pp \to (\gamma\gamma \to W^+W^-) + X$
  2. $pp \to W^+W^- + \geq 1\ jet + X$
- Measurements of the **rarest processes**
  1. $pp \to Z(\to \nu\bar{\nu})\gamma + 2\ jets + X$
  2. $pp \to Z(\to ll)\gamma + 2\ jets + X$
  3. $pp \to WWW + X$
- **EW Z-boson cross sections**
  1. $pp \to Z + jet(high\text{-}p_T) + X$
  2. $pp \to Z + large\ R\text{-}jet + X$
- **The b-quark fragmentation** properties
  1. $pp \to jet(B^\pm \to J/\psi\ K^\pm \to \mu^+\mu^-\ K^\pm) + X$
- **Forward Proton Scattering**
  1. $pp \to p\,(\gamma\gamma \to \ell^+\ell^-)\,p^{(*)}$
- Soft QCD: **Bose-Einstein correlations**
  1. $pp \to h^\pm h^\pm + X$
- Bonus: **W-mass**

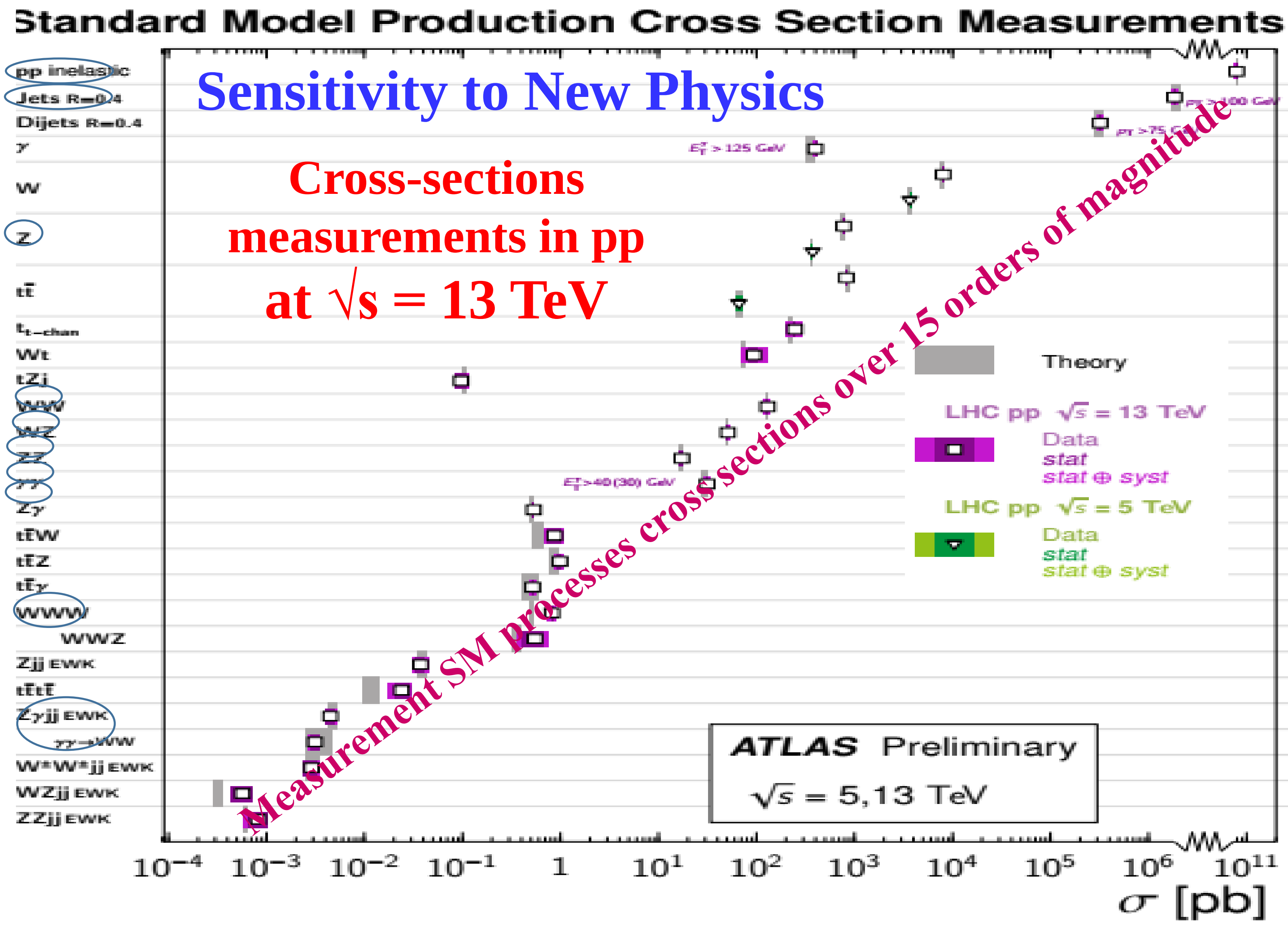

ATLAS: SM and fiducial production cross-section measurements in **pp** interactions at **5, 13 TeV**, corrected for branching fractions, compared to the corresponding **theoretical expectations**

- **ATLAS** measurements of elastic scattering can be linked to other processes occurring on hadronic pp-interactions
- **Calculation the total pp cross section σ_{tot}** & the **ρ-ratio**
- The **ρ-ratio** determines the complex phase between the **Coulomb** and the **nuclear amplitudes**

- **σ_{tot} (TOTEM) > σ_{tot} (ALFA) on 5.8 mb (2.2σ)**

$$\rho = \left.\frac{\mathrm{Re}[f_{\mathrm{el}}(t)]}{\mathrm{Im}[f_{\mathrm{el}}(t)]}\right|_{t\to 0}$$

where $f_{el}(t)$ is the **elastic-scattering amplitude**, t stands for the four-momentum transfer in the reaction

- **ρ = 0.0978 ±0.0085 (exp) ±0.0064 (th)**

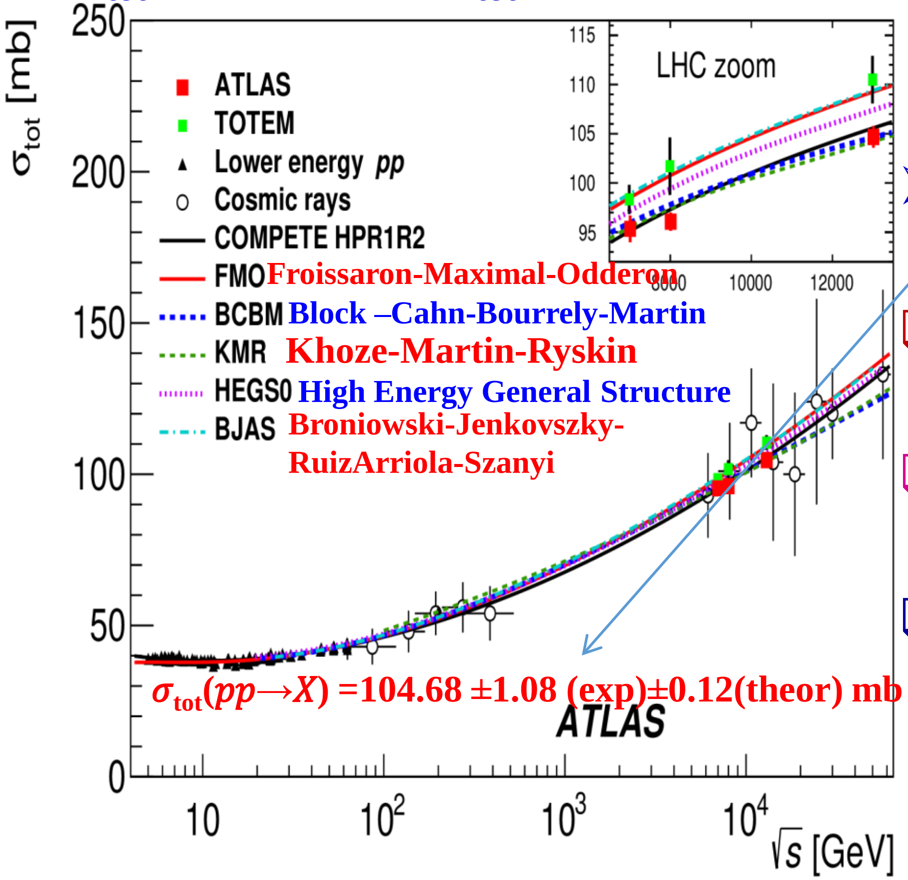

- **The most precise measurement of the total cross section**
- **The confirms the trend** of **σ_{tot} increase** with **√s**
- The **ρ-ratio** is in **disagreement** with **pre-LHC theoretical expectations**
- **σ_{tot}** and **ρ** together with other measurements of these parameters compared to **model predictions** in dependence of √s

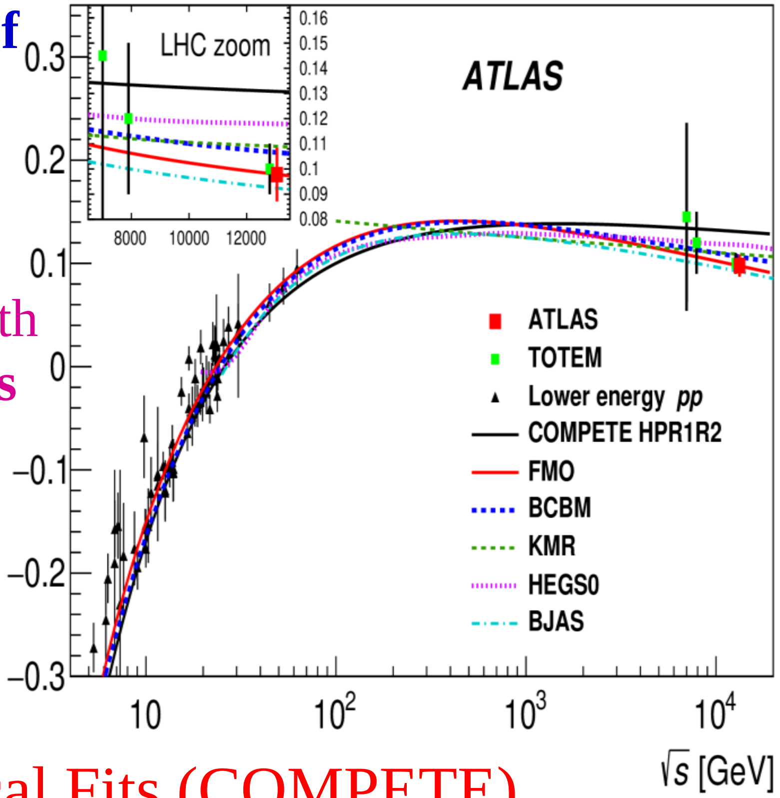

σ_{tot} and **ρ incompatible** with Community-Standard Semi-Empirical Fits (COMPETE) indicating **Odderon** exchange or a slowdown of σ_{tot} rise at high √s

σ_{TOT} pp elastic-scattering at 13 TeV #2

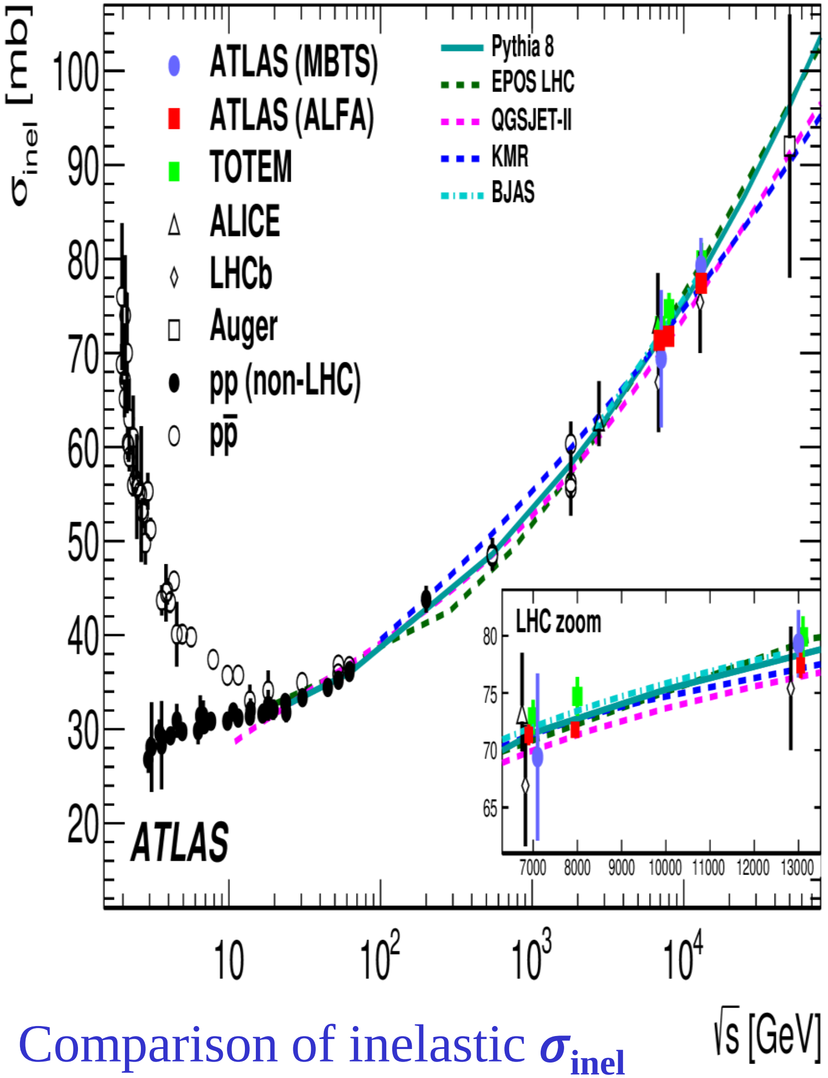

Comparison of inelastic σ_{inel} measurements with other published measurements and model predictions as a function of the $\sqrt{s}$

- **Total inelastic** cross section $\boldsymbol{\sigma_{tot}}$ is in **agreement** with previous **ATLAS** measurements using **MBTS** detectors
- **The ratio $\sigma_{inel}/\sigma_{tot}$, a measure of the opaqueness of the proton, continues to grow slowly** with $\sqrt{s}$, and its evolution is well described by the **Khoze-Martin-Ryskin** (KMR) **model.** (This is a two-channel eikonal model with few parameters and it uses all available high-energy data **for ρ and σ_{tot}**, as well as the corresponding differential elastic cross sections, and also all available measurements of low-mass diffraction.)
- The measurement remains far from **probing the black-disc limit**, i.e. a **totally opaque proton**
- **Ratio of elastic to total cross section σ_{el}/σ_{tot} in tension** with the values from **TOTEM** and lower energies

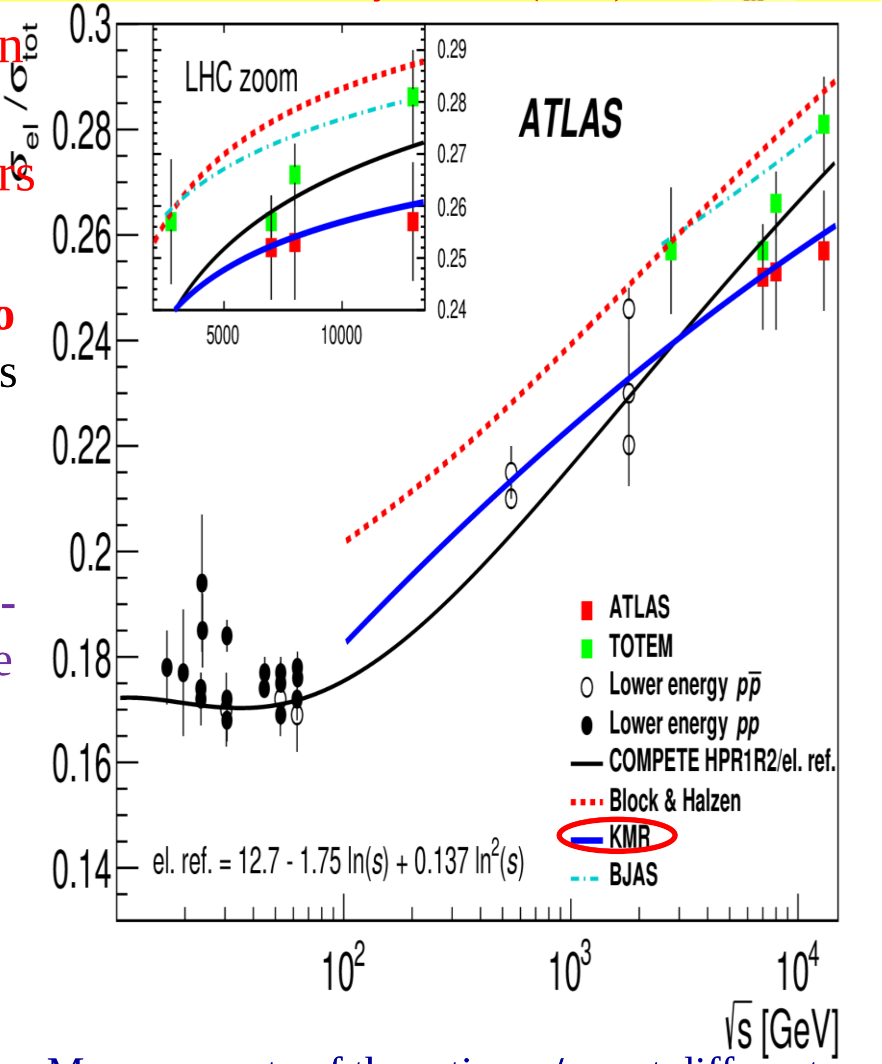

Measurements of the ratio σ_{el}/σ_{tot} at different $\sqrt{s}$ compared to model predictions and for illustrative purposes the **COMPETE** prediction of σ_{tot} divided by a conventional parameterization of the **elastic cross section**

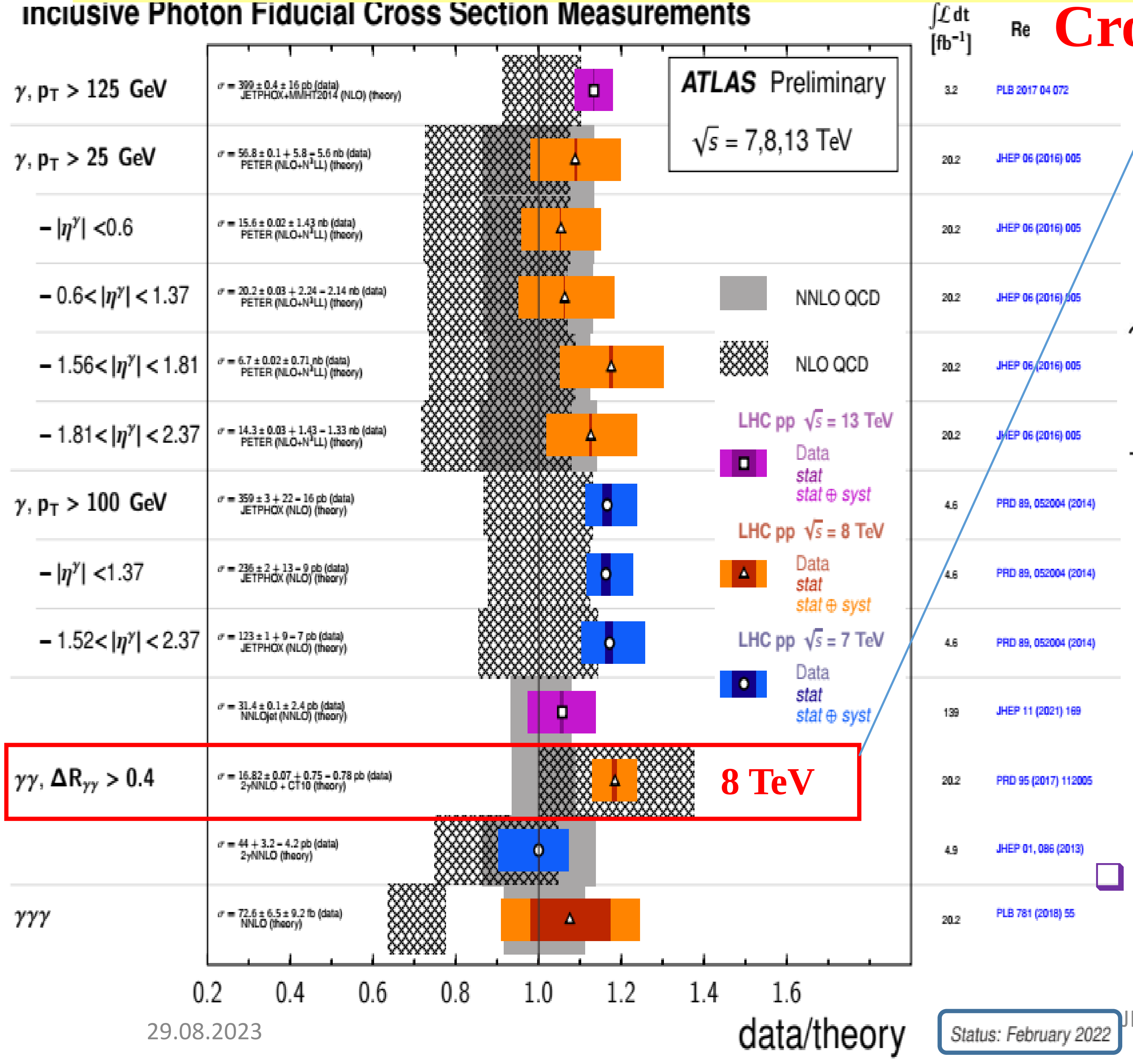

Cross section of pp→$\gamma\gamma(\Delta R_{\gamma\gamma}>0.4)$+X

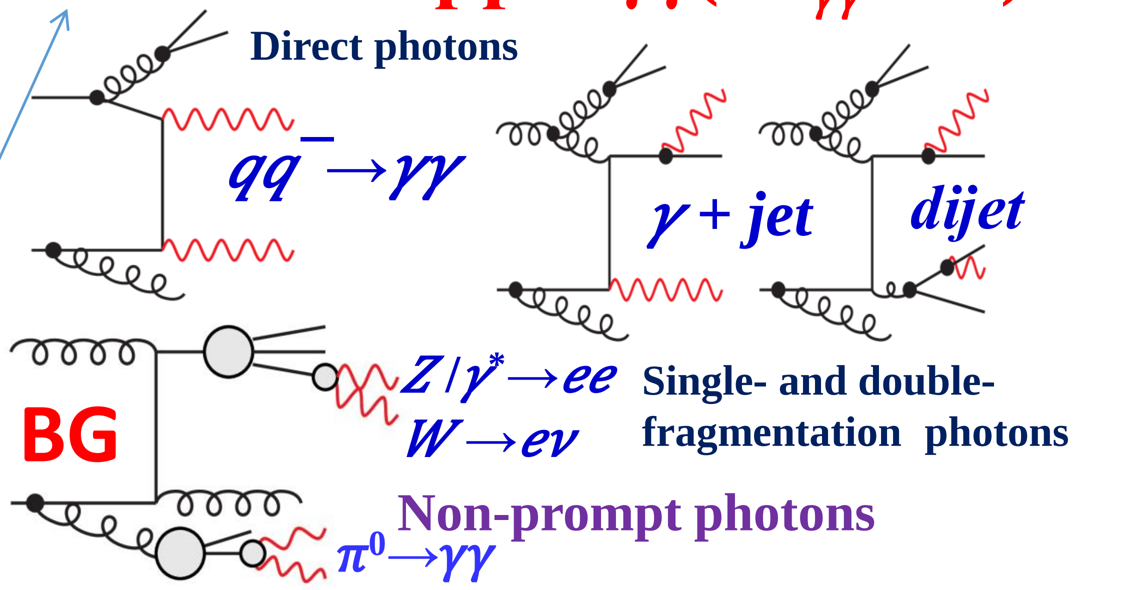

Selection	Detector level	Particle level
Photon kinematics	$p_{T,\gamma_{1(2)}} > 40\,(30)$ GeV, $\lvert\eta_\gamma\rvert < 2.37$ excluding $1.37 < \lvert\eta_\gamma\rvert < 1.52$	
Photon identification	tight	stable, not from hadron decay
Photon isolation	$E_{T,\gamma}^{iso,0.2} < 0.05 \cdot p_{T,\gamma}$	$E_{T,\gamma}^{iso,0.2} < 0.09 \cdot p_{T,\gamma}$
Diphoton topology	$N_\gamma \geq 2$, $\Delta R_{\gamma\gamma} > 0.4$	

- Overview of the event selection at the detector level and at the particle level (fiducial phase space)

Process	Event fraction [%]
$\gamma\gamma$ signal	60.4 ± 3.0
γj	20.0 ± 1.3
$j\gamma$	10.1 ± 1.1
jj	6.3 ± 1.2
Electron	2.6 ± 0.1
$\gamma\gamma$ pile-up	0.6 ± 0.4

Diphoton production fiducial & differential cross sections

Low-invariant mass diphoton event

$\Delta R_{\gamma\gamma} > 0.4$

$\sigma_{\gamma\gamma}$ = 31.4±0.1 (stat) ±2.4 (syst) pb

The measured integrated cross section compatible with the NNLO predictions and multileg-merged calculations

Fiducial cross section [pb]	$\sigma_{\gamma\gamma}$	± unc.
Sherpa MEPS@NLO	33.2	$^{+7.7}_{-5.6}$
Nnlojet NNLO	29.7	$^{+2.4}_{-2.0}$
NLO	19.6	$^{+1.6}_{-1.3}$
LO	5.3	$^{+0.5}_{-0.5}$
Diphox NLO	20.8	$^{+3.2}_{-2.9}$
Data	31.4	2.4

A comparison of the measured cross section with the theoretical predictions shows the importance of higher-order QCD contributions even for such an inclusive $\gamma\gamma$ measurement

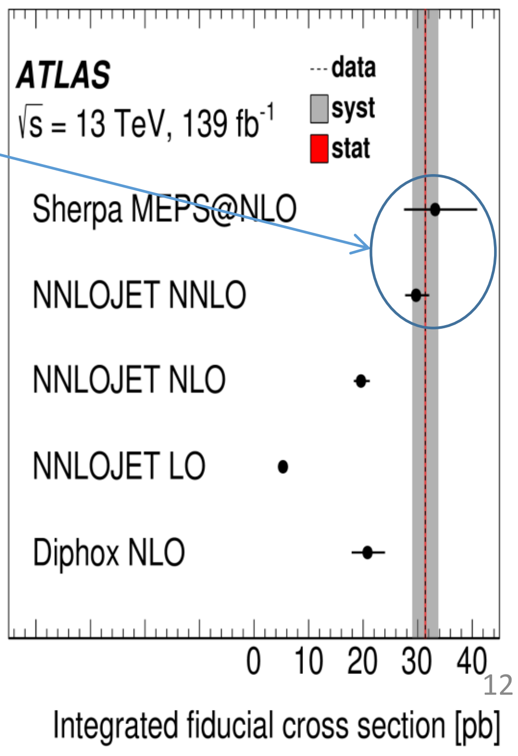

CROSS SECTION OF $pp \to \gamma\gamma + X$ AT 13 TEV #3

7 TeV: Eur.Phys.J.C 74 (2014) 3129;
JHEP 01 (2012) 133

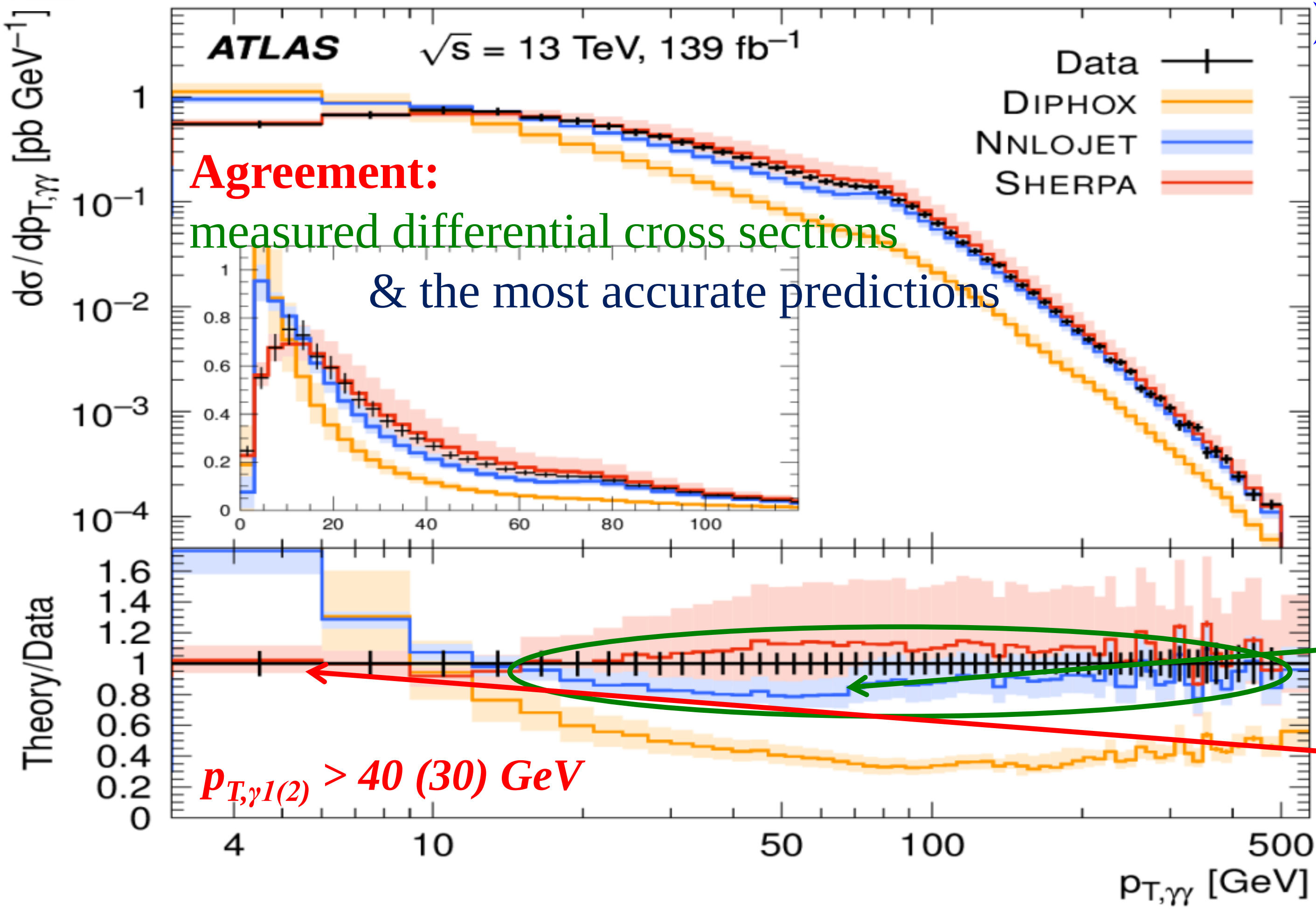

Differential cross sections measured as functions of $p_{T,\gamma\gamma}$ (also as functions of ϕ^*_{η}, $\pi - \Delta\phi_{\gamma\gamma}$, $a_{T,\gamma\gamma}$) compared with the predictions from **Diphox NLO**, **Nnlojet NNLO** and **Sherpa MEPS@NLO**. At the bottom, the ratio of the prediction to the data is shown. **Uncertainty bars** on the data represent the **total uncertainty**, while **uncertainty bands** on the predictions represent perturbative scale (**statistical**) uncertainties.

➢ Higher-order perturbative QCD corrections are crucial for $pp \to \gamma\gamma + X$

- In the **Leading Order** (LO) the **γγ** momenta balance each other perfectly, resulting in a $p_{T,\gamma\gamma}$ of zero. This obviously doesn't match the measured distribution, which shows that most of the **γ**-pairs have $p_{T,\gamma\gamma}$ values different from 0
- In the **Diphox NLO** and the **Nnlojet NNLO** physicists include the **production of the extra quarks and gluons** in the prediction.
- The **Nnlojet NNLO** prediction (**blue line**) gives a **good description** of the measured values at **high-**$p_{T,\gamma\gamma}$

➢ The **Sherpa** (red line) combine calculations with additional techniques, which involve the simulations of arbitrarily many quark and gluon emissions, especially relevant at low energies

❖ **Sherpa** provide the **best description** of the **entire measured distribution**, including the **low-**$p_{T,\gamma\gamma}$

DIBOSON CROSS SECTION MEASUREMENTS

ATL-PHYS-PUB-2022-009

https://twiki.cern.ch/twiki/bin/view/CMSPublic/PhysicsResultsCombined

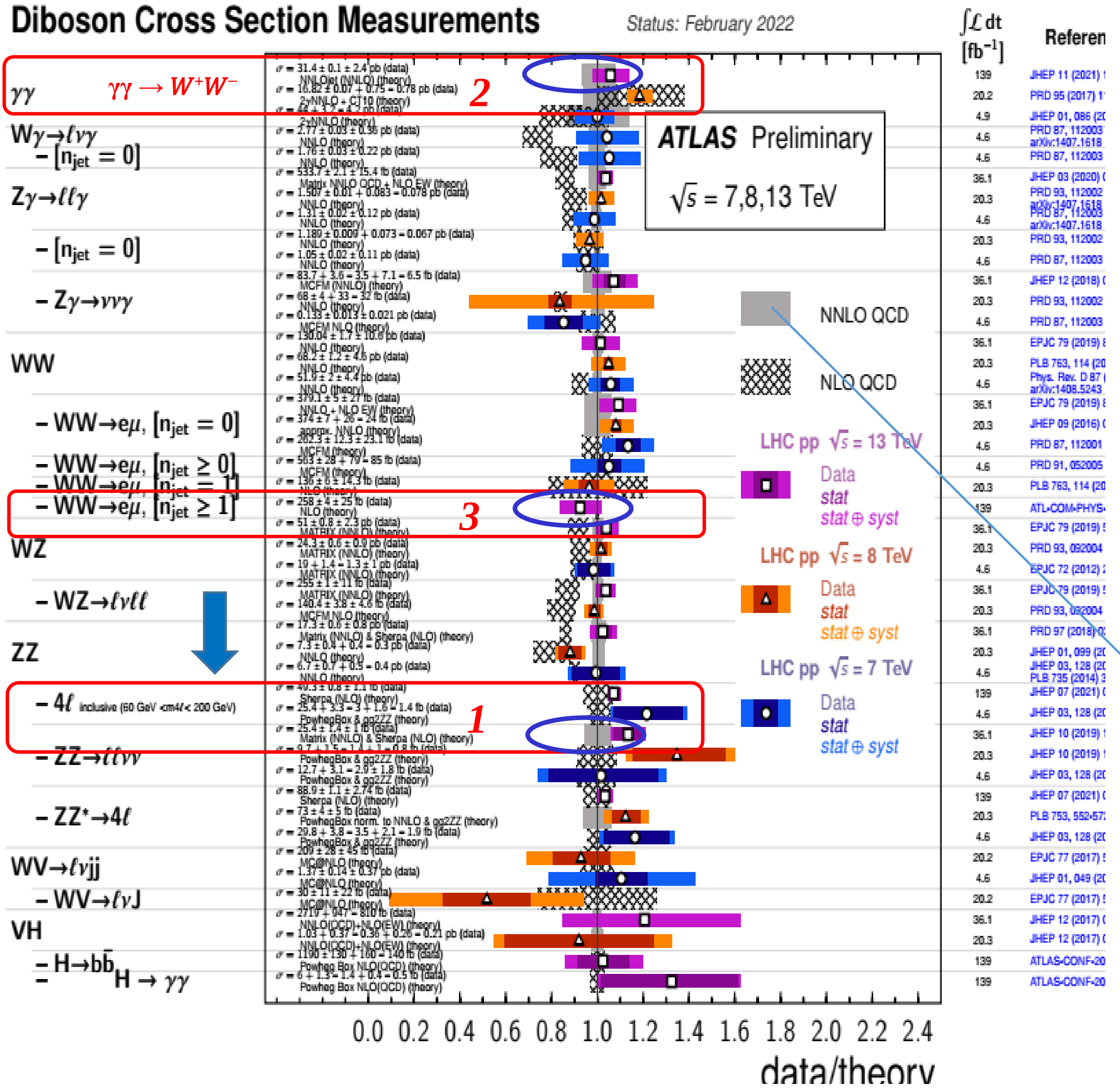

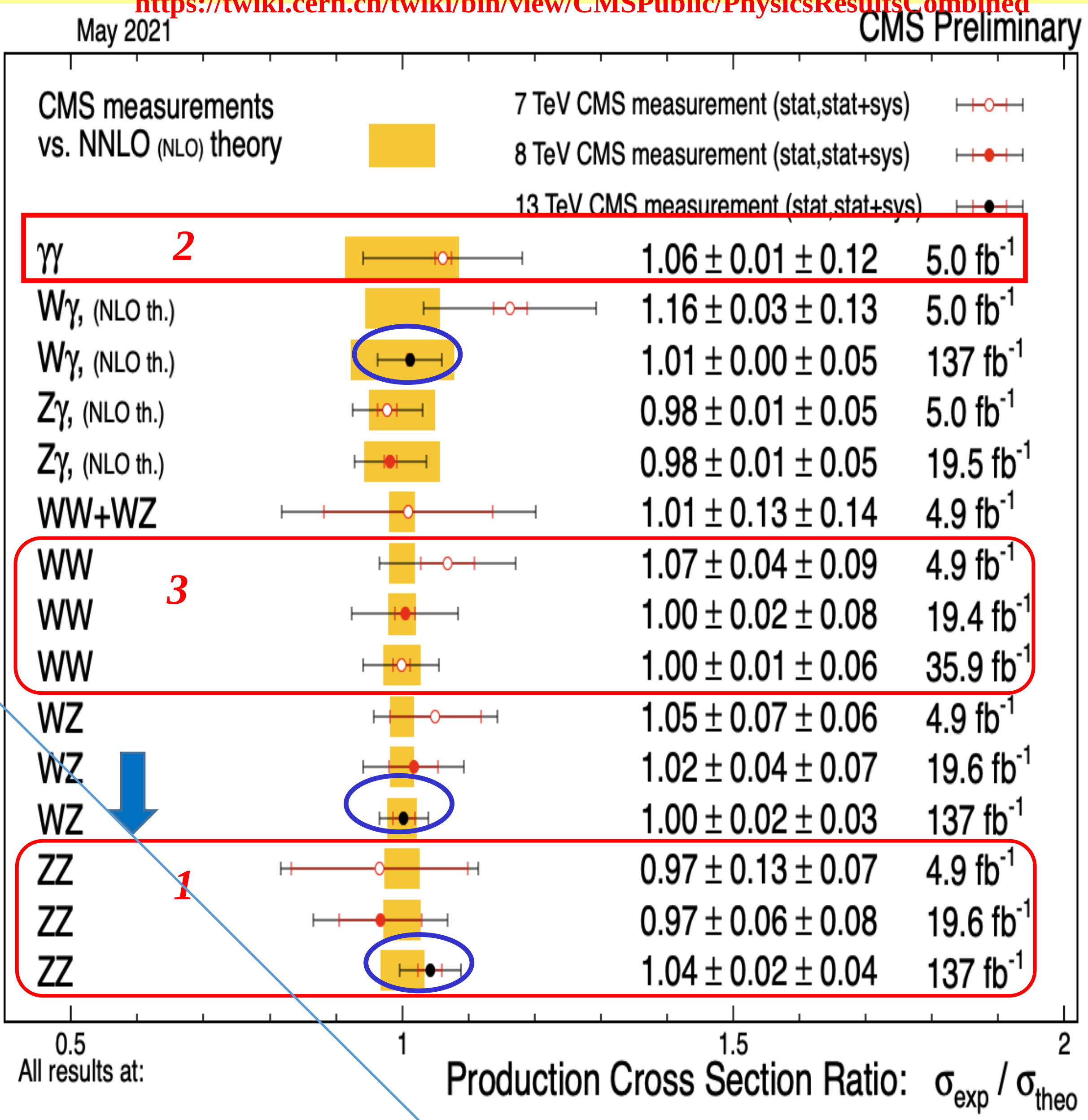

- **Diboson** cross section ratio comparison to theory: **Theory predictions updated to latest NNLO calculations.**

1. CROSS SECTION OF *PP→4 LEPTONS+X* AT 13 TEV *#1*

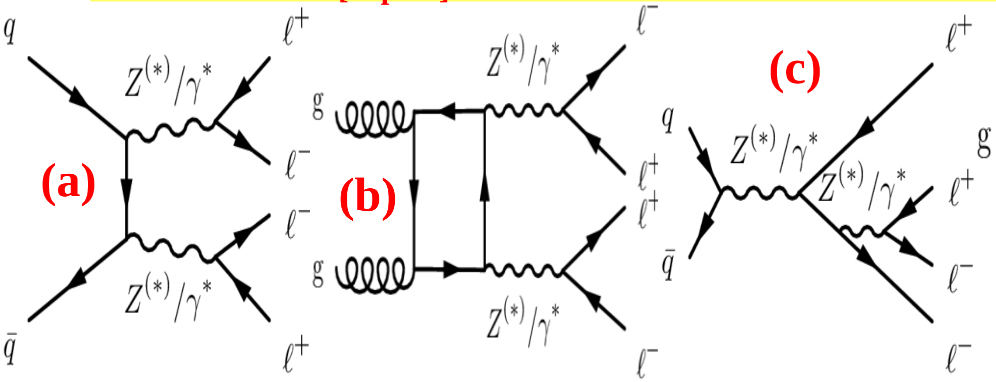

➢ Measurements of ***4l* differential & integrated fiducial** cross-sections in events with **2(e⁺e⁻)** or **2(μ⁺μ⁻)** pairs

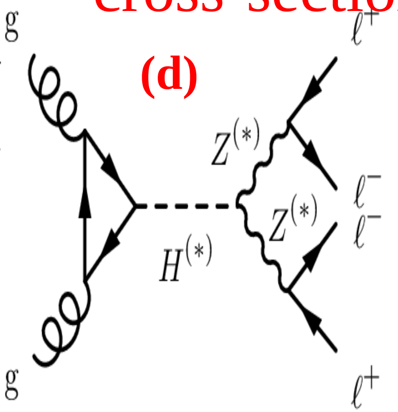

❑ The ***4l* final state** has contributions from interesting **SM** processes: 1. Single **Z** boson production, 2. **Higgs** boson production, 3. On-shell **ZZ** production.

❑ **Sensitive to New Physics / BSM contributions:**

1. Modifications to the couplings of the **Higgs** or **gauge boson**, 2. Possible **4-fermion interactions**, 3. **Models with leptonic decays of Z bosons** or 4. **new particles.**

Contributions to the ***pp→4ℓ (ℓ=e, μ)*** process:

(a) **t-channel** $q\bar{q}\to 2Z^{(*)}/\gamma^{(*)}\to 4\ell$ production,

(b) **gluon-induced** $gg\to 2Z^{(*)}/\gamma^{(*)}\to 4\ell$ production via a quark loop,

(c) **internal conversion in Z boson decays** $q\bar{q}\to Z^{(*)}/\gamma^{(*)}\to 2\ell+Z^{(*)}/\gamma^{(*)}\to 2\ell$,

(d) **Higgs-boson-mediated s-**channel production $gg\to H^{(*)}\to Z^{(*)}Z^{(*)}\to 4\ell$.

The superscript (*) refers to a particle that can be either on-shell or off-shell, whereas * indicates that it is always off-shell

➢ **Fiducial cross-sections in fb in the full fiducial phase space** and in the **following regions of $m_{4\ell}$:**

1. **$Z\to 4\ell$ (60<$m_{4\ell}$<100 GeV)**
2. **$H\to 4\ell$ (120<$m_{4\ell}$<130 GeV)**
3. **off-shell *ZZ*** (20<$m_{4\ell}$<60 GeV;100<$m_{4\ell}$<120 GeV;130<$m_{4\ell}$<180 GeV)
4. **on-shell *ZZ*** (180<$m_{4\ell}$ <2000 GeV)

Agreement

	Region				
	Full	$Z\to 4\ell$	$H\to 4\ell$	Off-shell ZZ	On-shell ZZ
Measured fiducial cross-section [fb]	88.9 ±1.1 (stat.) ±2.3 (syst.) ±1.5 (lumi.) ±3.0 (total)	22.1 ±0.7 (stat.) ±1.1 (syst.) ±0.4 (lumi.) ±1.3 (total)	4.76 ±0.29 (stat.) ±0.18 (syst.) ±0.08 (lumi.) ±0.35 (total)	12.4 ±0.5 (stat.) ±0.6 (syst.) ±0.2 (lumi.) ±0.8 (total)	49.3 ±0.8 (stat.) ±0.8 (syst.) ±0.8 (lumi.) ±1.3 (total)
Sherpa	86±5	23.6±1.5	4.57±0.21	11.5±0.7	46.0±2.9
Powheg + Pythia8	83±5	21.2±1.3	4.38±0.20	10.7±0.7	46.4±3.0

➢ Two predictions are shown for the $q\bar{q}\to 4\ell$ process simulated with **Sherpa** & **Powheg+Pythia8**

1. Cross section of $pp \to 4$ leptons+X at 13 TeV #2

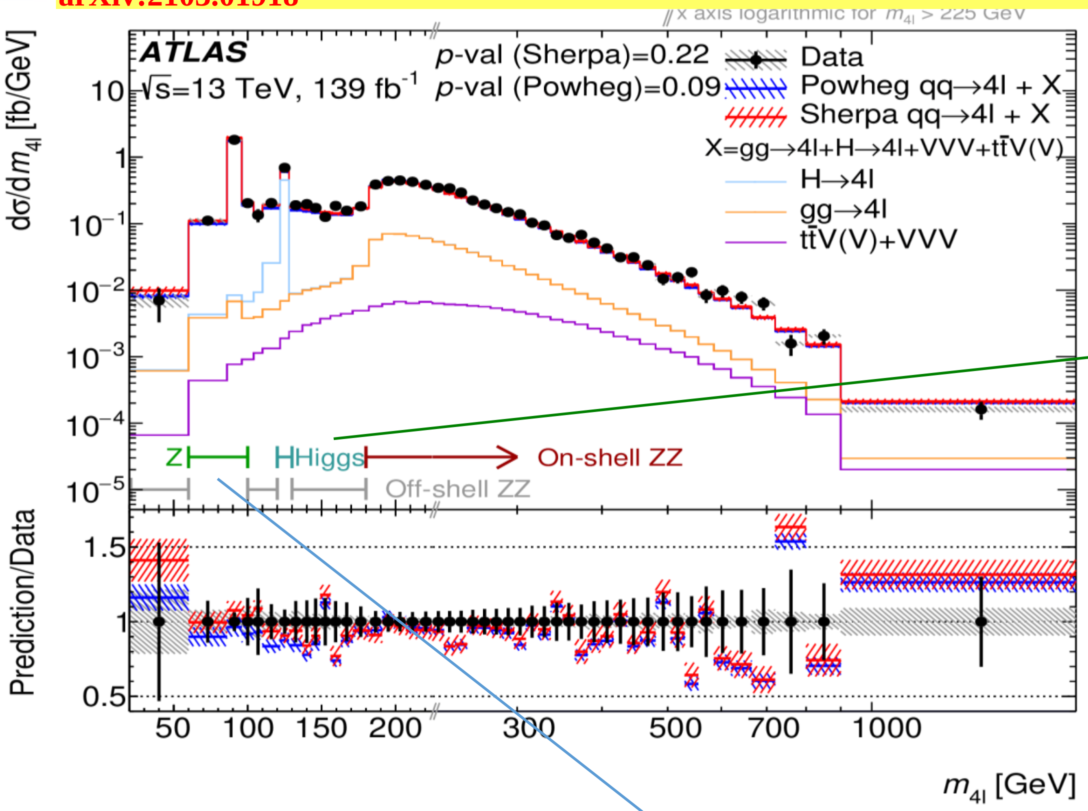

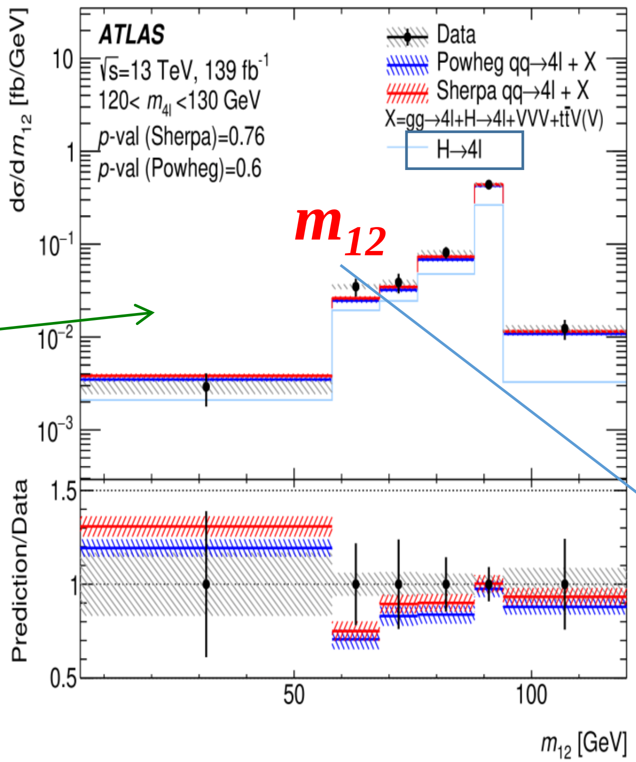

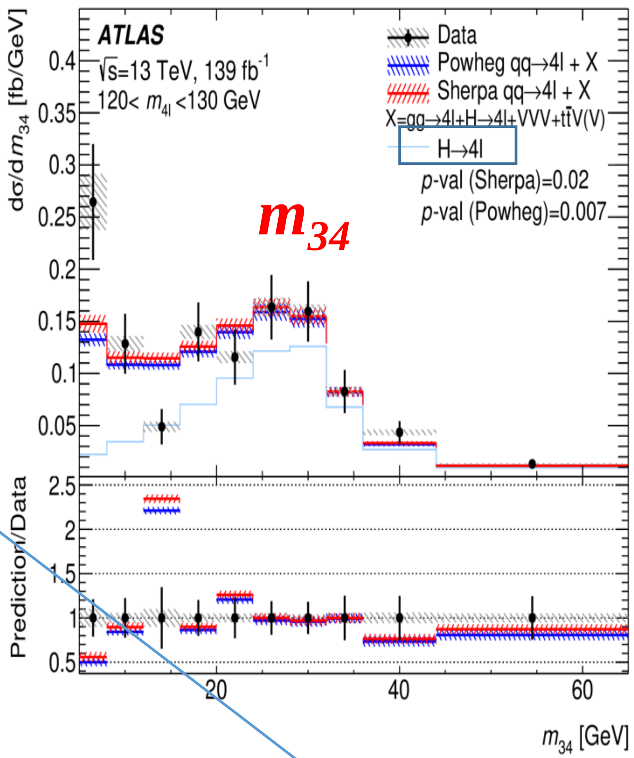

Differential cross-section as a function of $m_{4\ell}$

- The **measured data** are compared with the **SM** prediction using ***Sherpa*** (red) or ***Powheg+PYTHIA*** (blue) models of the ***$q\bar{q} \to 4\ell$*** contribution
- The ***p*-value** is the probability for the χ^2, with k degrees of freedom.

> **The SM predictions agree well within uncertainties over $m_{4\ell}$ spectrum**

- Differential cross-section as a function of m_{12}&m_{34} in the four $m_{4\ell}$ regions:: **for the contribution from Higgs production**.

The same-flavour, opposite-charge pair with an invariant mass **closest to m_Z** is selected as the primary pair in the event with m_{12}.

- The region dominated by $Z \to 4\ell$ production is used to extract the **most precise measurement** of the **$Z \to 4\ell$ branching fraction** to date,

$B_{Z\to 4\ell}$ = [4.41±0.13 (stat)±0.23 (syst)±0.09 (theory)±0.12(lumi)]×10^{-6}

This is **consistent** with previous exp. and with the **Powheg** prediction

$B_{Z\to 4\ell}$ = [4.50 ± 0.01]×10^{-6}

Phys. Lett. B 816 (2021) 136190
arXiv:2010.04019 [hep-ex]

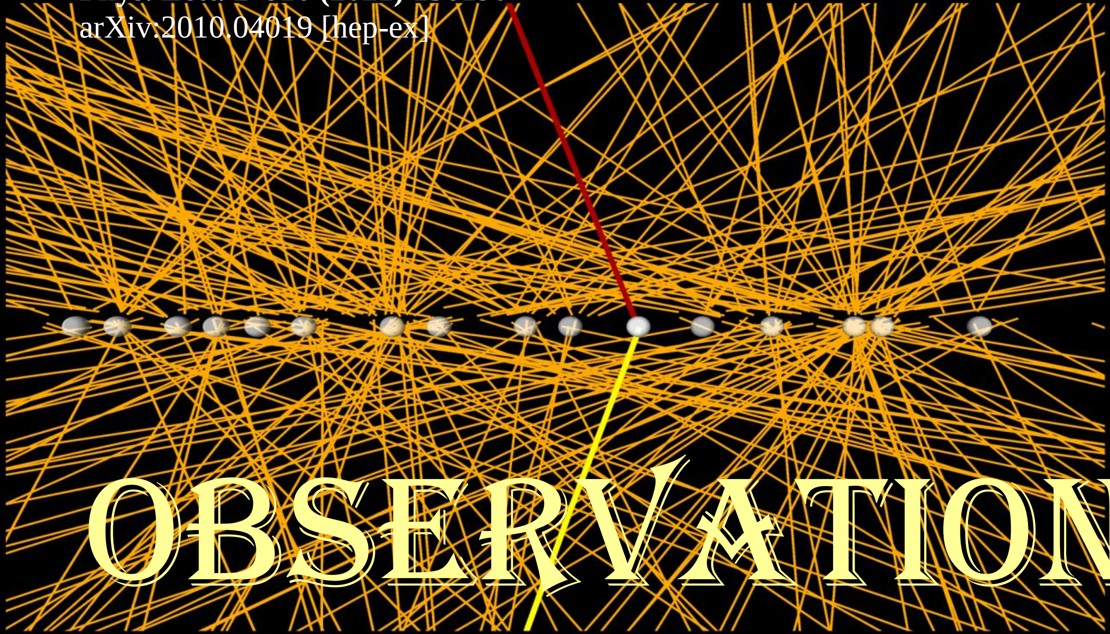

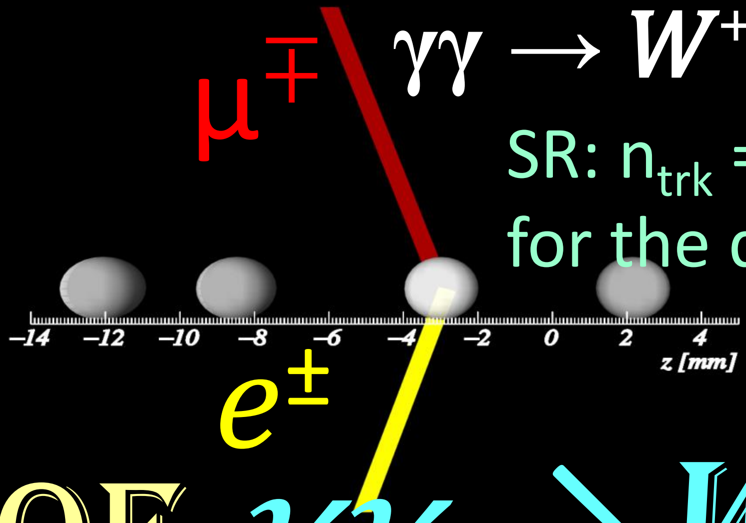

$\gamma\gamma \to W^+W^- \to e^\pm\nu\ \mu^\mp\nu$

SR: n_{trk} =0 & $p_T^{e\mu}$ >30 GeV
for the dilepton system

OBSERVATION OF $\gamma\gamma \to W^+W^-$ & W^+W^- + ≥1 JETS PRODUCTIONS

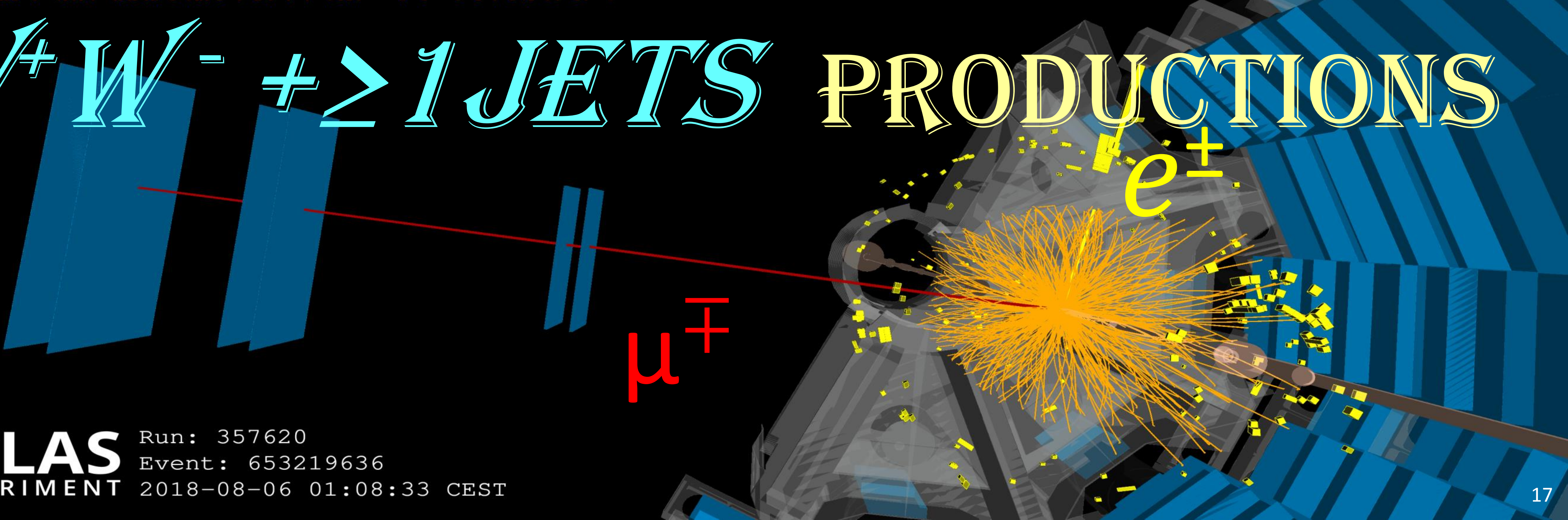

ATLAS EXPERIMENT

2. CROSS-SECTION $PP(\gamma\gamma) \rightarrow P^{(*)} W^+W^- P^{(*)}$, $W^+W^- \rightarrow e^{\pm}\nu\ \mu^{\mp}\nu$ #1

➢ The observation of **photon-induced production of W-boson pairs**, $\gamma\gamma \rightarrow W^+W^- \rightarrow e^{\pm}\nu\,\mu^{\mp}\nu$

❑ **This is unique process**: it only involves diagrams with **self-couplings** of the **EW** gauge bosons

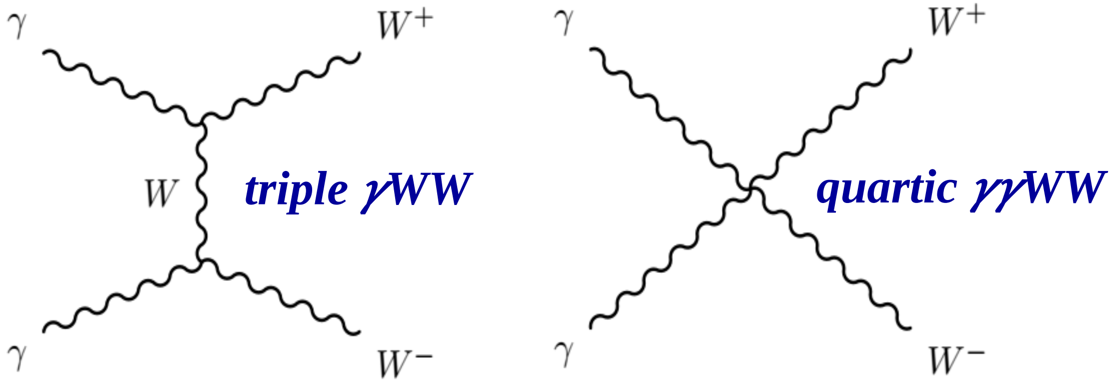

$p^{(*)}$ final-state proton stays intact or fragments emitting a γ

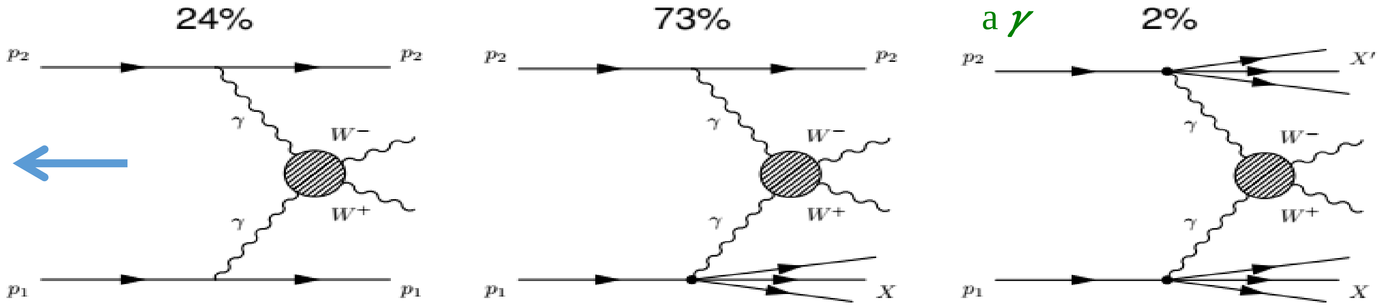

Diagrams for the exclusive $\gamma\gamma \rightarrow W^+W^-$ production representing the

I. **elastic process**

II. **single-dissociation** where one initial proton dissociates (SD)

III. **double-dissociation** where both protons fragment (DD)

❖ Test of the **EW** sector of the **SM**

❖ Direct access to **triple γWW** and **quartic $\gamma\gamma WW$** interactions, $O(a_{EM}^2)$

	Signal region	Control regions		
n_{trk}	SR $n_{trk} = 0$	CR $n_{trk} = 0$	CR $1 \leq n_{trk} \leq 4$	CR $1 \leq n_{trk} \leq 4$
$p_T^{e\mu}$	> 30 GeV	< 30 GeV	> 30 GeV	< 30 GeV
$\gamma\gamma \rightarrow WW$	174 ± 20	45 ± 6	95 ± 19	24 ± 5
$\gamma\gamma \rightarrow \ell\ell$	5.5 ± 0.3	39.6 ± 1.9	5.6 ± 1.2	32 ± 7
Drell–Yan	4.5 ± 0.9	280 ± 40	106 ± 19	4700 ± 400
$qq \rightarrow WW$ (incl. gg and VBS)	101 ± 17	55 ± 10	1700 ± 270	970 ± 150
Non-prompt	14 ± 14	36 ± 35	220 ± 220	500 ± 400
Other backgrounds	7.1 ± 1.7	1.9 ± 0.4	311 ± 76	81 ± 15
Total	305 ± 18	459 ± 19	2460 ± 60	6320 ± 130
Data	307	449	2458	6332

Agreement

Run 1 **evidence** of this process has turned into **observation** in Run2 at 8 TeV

✓ ATLAS: Phys. Rev. D 94 (2016) 032011

✓ CMS: JHEP 08 (2016) 119

Summary of the data event yields, the predicted signal and **BG** event yields in the **Signal Region (SR)** and **Control Regions (CR)** as obtained after the fit

Phys. Lett. B 816 (2021) 136190
arXiv:2010.04019 [hep-ex]

2. CROSS-SECTION $pp(\gamma\gamma)\rightarrow p^{(*)}W^{+}W^{-}p^{(*)}, W^{+}W^{-}\rightarrow e^{\pm}\nu\mu^{\mp}\nu$ #2

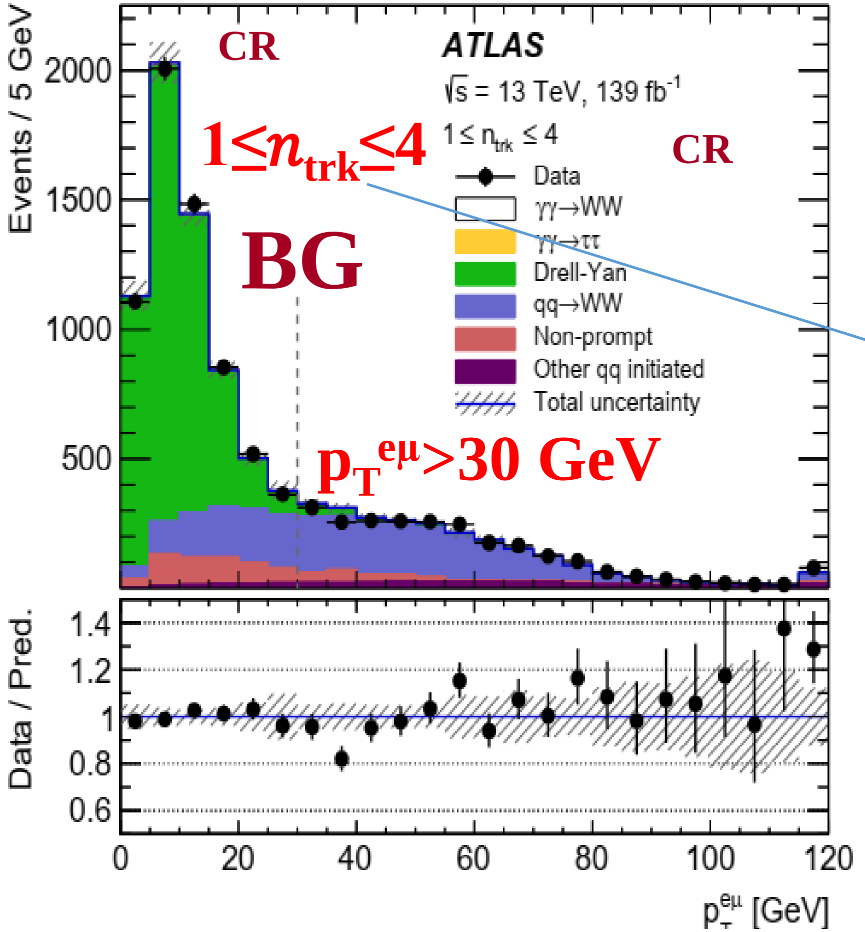

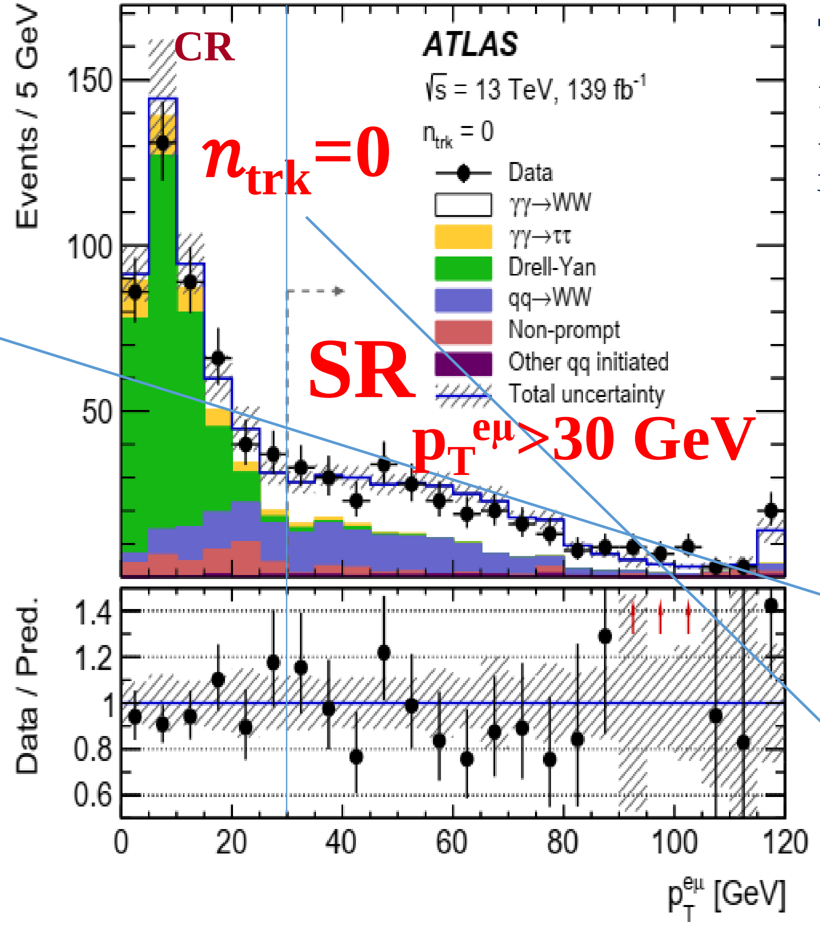

The **interaction vertex** is reconstructed from the **leptons** as the weighted average ***z*-position** of the tracks extrapolated to the beam line:

$$z_{\mathrm{vtx}}^{\ell\ell} = \frac{z_{\ell_1}\sin^2\theta_{\ell_1} + z_{\ell_2}\sin^2\theta_{\ell_2}}{\sin^2\theta_{\ell_1} + \sin^2\theta_{\ell_2}}$$

The weighted mean ***z*-position** of the tracks extrapolated to the beam line. ***n_{trk}*:** number of tracks in a **window $\Delta z=\pm 1$ mm** around **z^{ll}_{vtx} excluding the tracks from leptons**

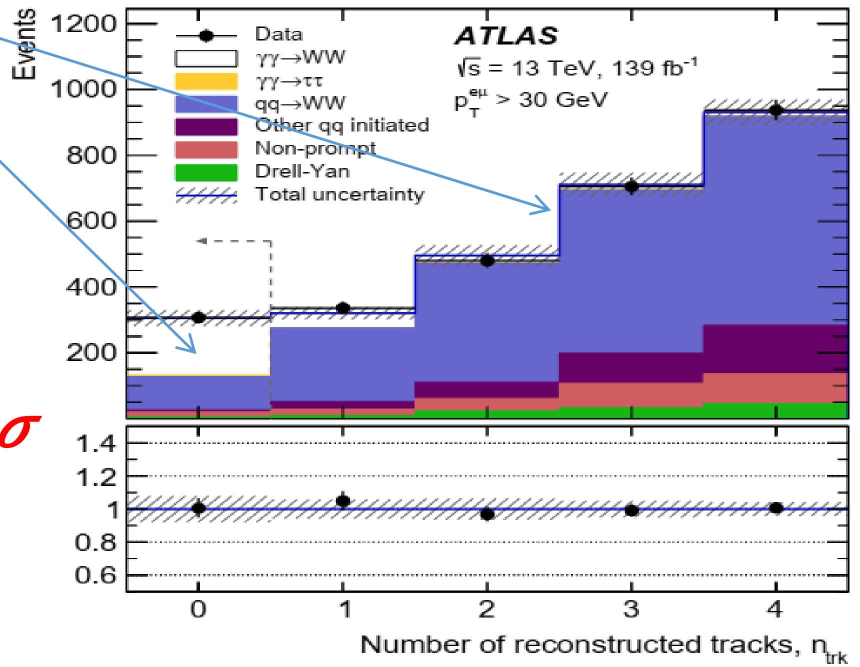

Without additional tracks from hadronic activity and from close-by pileup interactions

The background-only hypothesis is rejected with a significance of 8.4 (5)σ

- ❑ The ***WW* observation** of **photon-induced** production in ***pp*** collisions (**evidence** –previously reported) σ^{fid}=**3.13±0.31(stat)±0.28(syst) fb**

- ✓ The result is in **agreement with the theoretical predictions** σ_{theo}= **4.3±1.0 (scale)± 0.1 (PDF) fb by MG5_aMC@NLO+Pythia8**

- **Fiducial & differential cross-section measurements of W^+W^- production with ≥1 jets**
- It is **sensitive** to the properties of **EW-boson self-interactions**; provide a test of **pQCD & EW theory**

❑ **Events are selected** with **one $e^\pm\mu^\mp$ pair & ≥1 jets** with p_T^{jet}>30 GeV and $|y^{jet}| < 4.5$

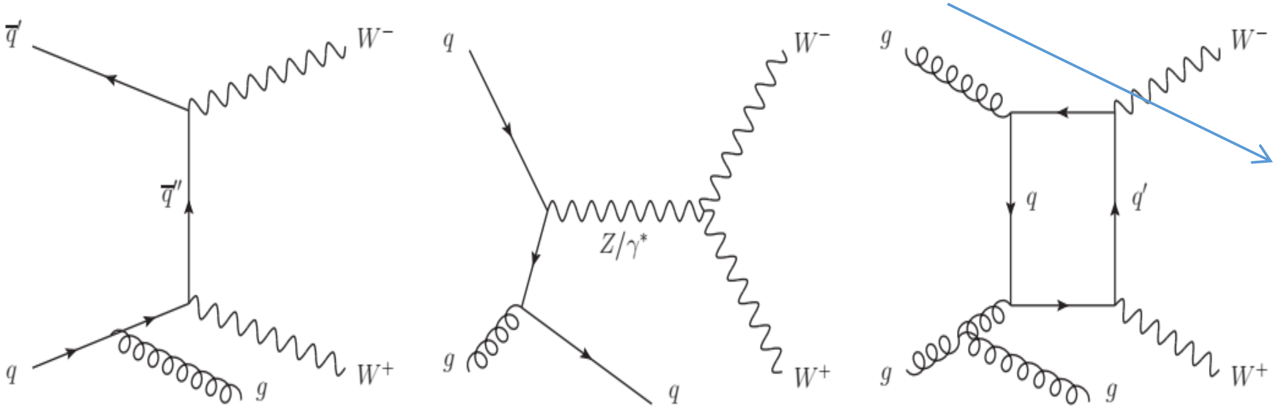

Fiducial selection requirements		
p_T^ℓ	>	27 GeV
$\lvert\eta^\ell\rvert$	<	2.5
$m_{e\mu}$	>	85 GeV
p_T^j	>	30 GeV
$\lvert y^j\rvert$	<	4.5

leptons

jets

❑ Feynman diagrams: W^+W^- boson pair in association with a jet

- The measured fiducial cross-section of $W^+W^- \to e^\pm\nu\mu^\mp\nu + \geq 1$ jets+X

$$\sigma^{fid} = 258 \pm 4\ (stat) \pm 25\ (syst)\ fb$$

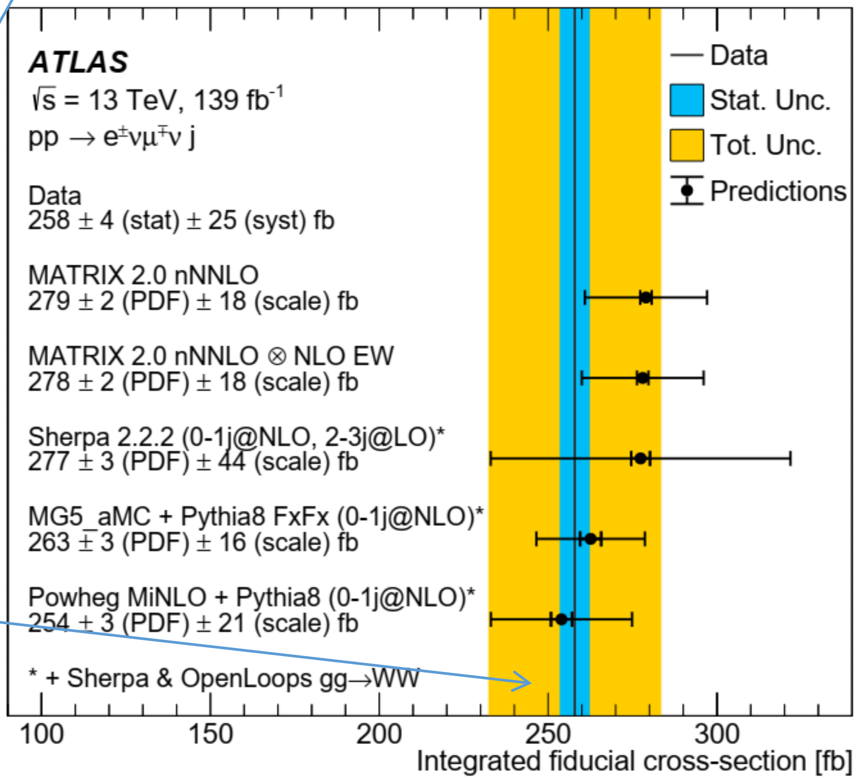

Comparison of the measured fiducial WW + jets cross-section with various theoretical predictions

The result is compared with

- ❑ fixed-order parton-level prediction from **MATRIX 2.0** that is accurate to **NNLO (NLO)** for $q\bar{q} \to WW$ ($Wgg \to W$) product
- ❑ prediction that additionally accounts for **EW** corrections to **WW+jet** production: calculated with **Sherpa 2.2.2+OpenLoops**
- ❑ predictions from **Sherpa 2.2.2, MadGraph5_aMC@NLO+Pythia8** with **FxFx** merging, and **Powheg MiNLO+Pythia8**, which are all supplemented by a **Sherpa 2.2.2+OpenLoops $gg \to WW$** LO+PS prediction

- **The data agree well with all MC predictions**

3. Cross-section $pp \to W^{+}W^{-}$ + ≥1 jets + X #2

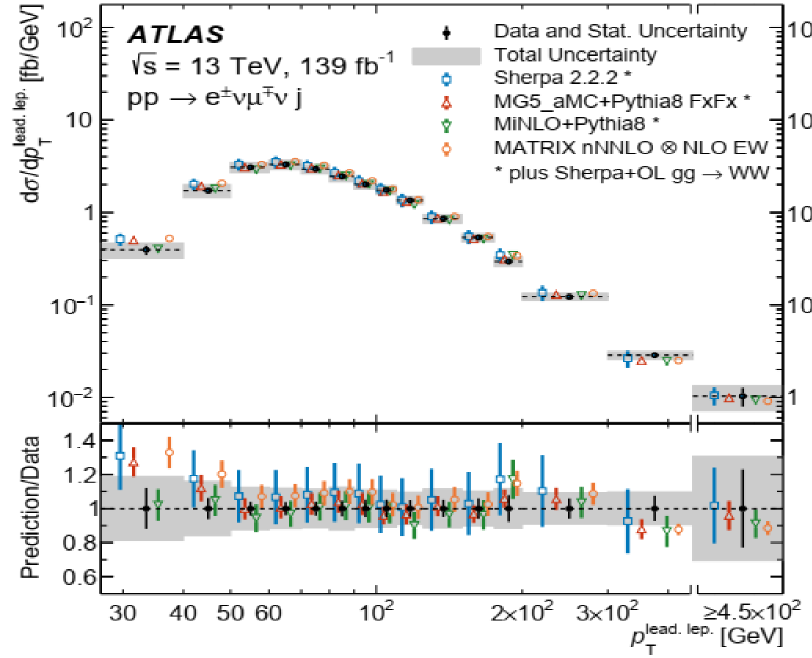

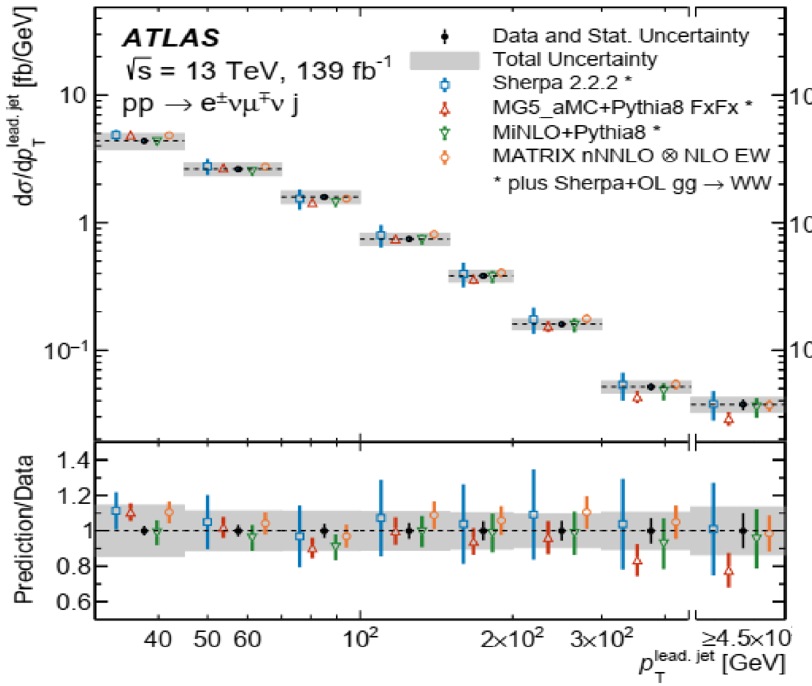

➢ Measured fiducial cross-sections of ***WW*+jets** for: $p_T^{\text{lead.lep.}}$, $p_T^{\text{sub-lead.lep.}}$, $p_T^{\text{lead.Jet}}$, H_T

- All predictions give an **excellent description** of the observed data
- For the nominal **Sherpa 2.2.2** prediction values of χ^2/ndf are below **one**, except for the $m_{e\mu}$ distribution measured for $p_T^{\text{lead.Jet}}$ **>200 GeV**, for which the value is **1.4**
- Comparisons of the remaining predictions with the data yield similar χ^2 values, except for the jet multiplicity, H_T & S_T distributions, where, for **the highest multiplicities and energies**, small discrepancies exist: data / predictions

➢ The **data agree well** with predictions in **all differential distributions**, up to the highest $\mathbf{p_T}$ and for **≤5 jets**

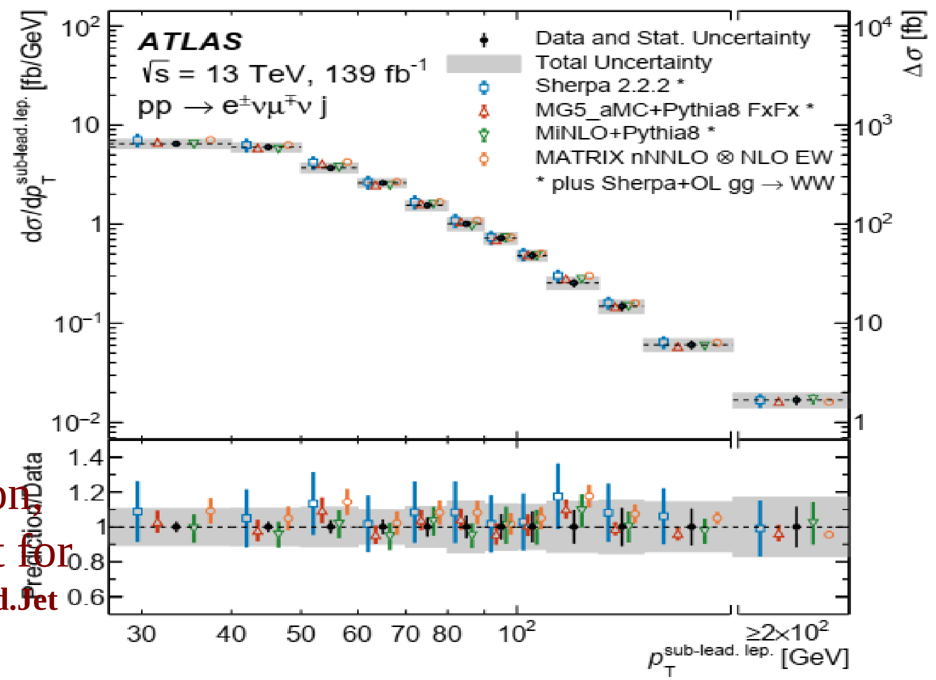

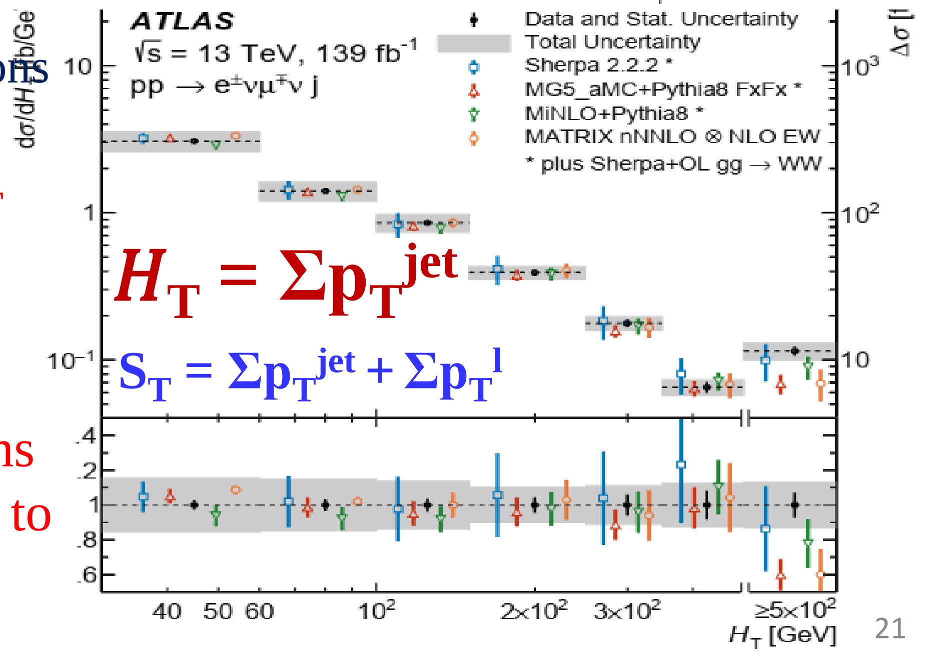

$H_T = \Sigma p_T^{\text{jet}}$

$S_T = \Sigma p_T^{\text{jet}} + \Sigma p_T^{l}$

RAREST ELECTROWEAK $Z(\to \ell\ell)\gamma jj$ & $Z(\to \nu\nu)\gamma jj$ PRODUCTION

$Z(\to\nu\nu)\gamma jj$ candidate event:

- p_T^{γ} = 64 GeV,
- E_T^{miss} = 264 GeV
- m_{jj} = 2.6 TeV

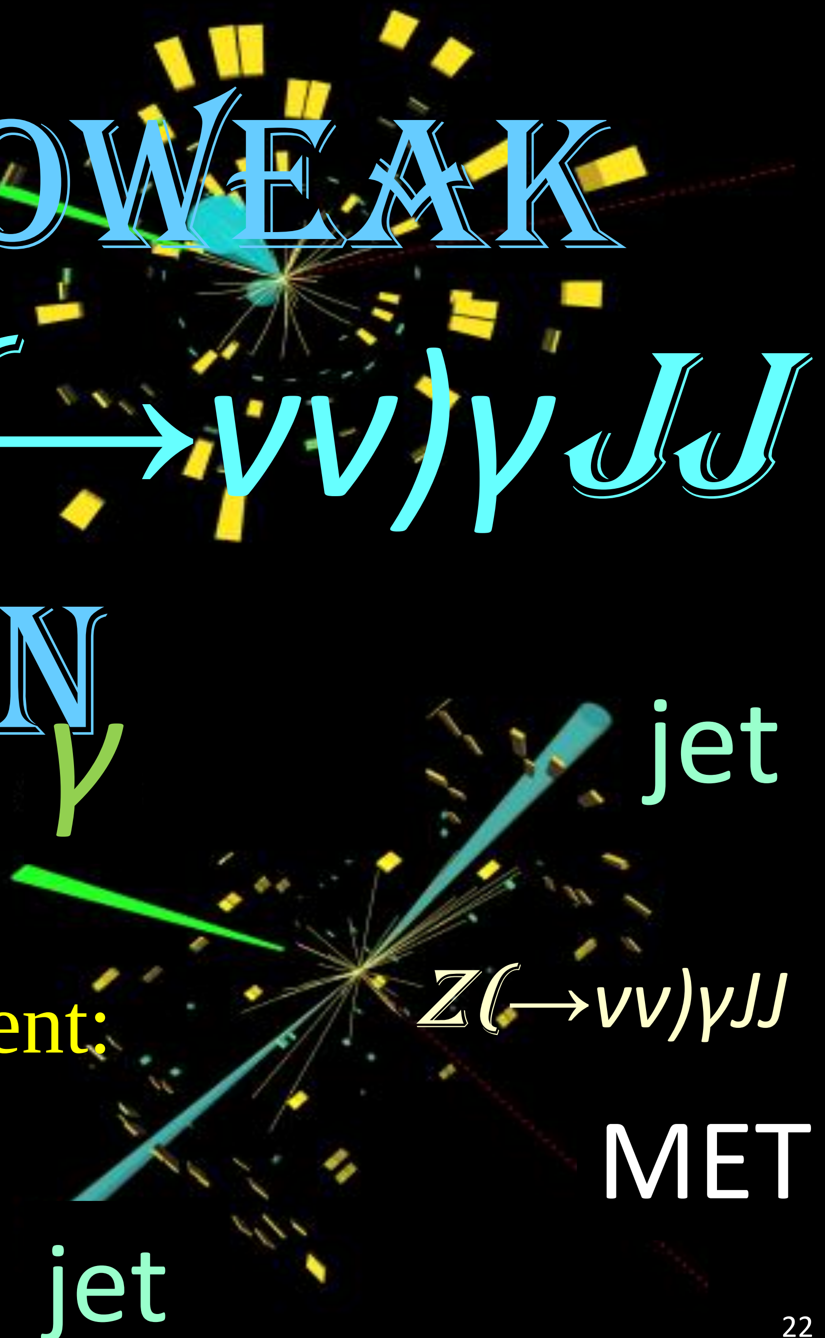

CMS: ELECTROWEAK CROSS SECTION MEASUREMENTS

https://twiki.cern.ch/twiki/bin/view/CMSPublic/PhysicsResultsCombined

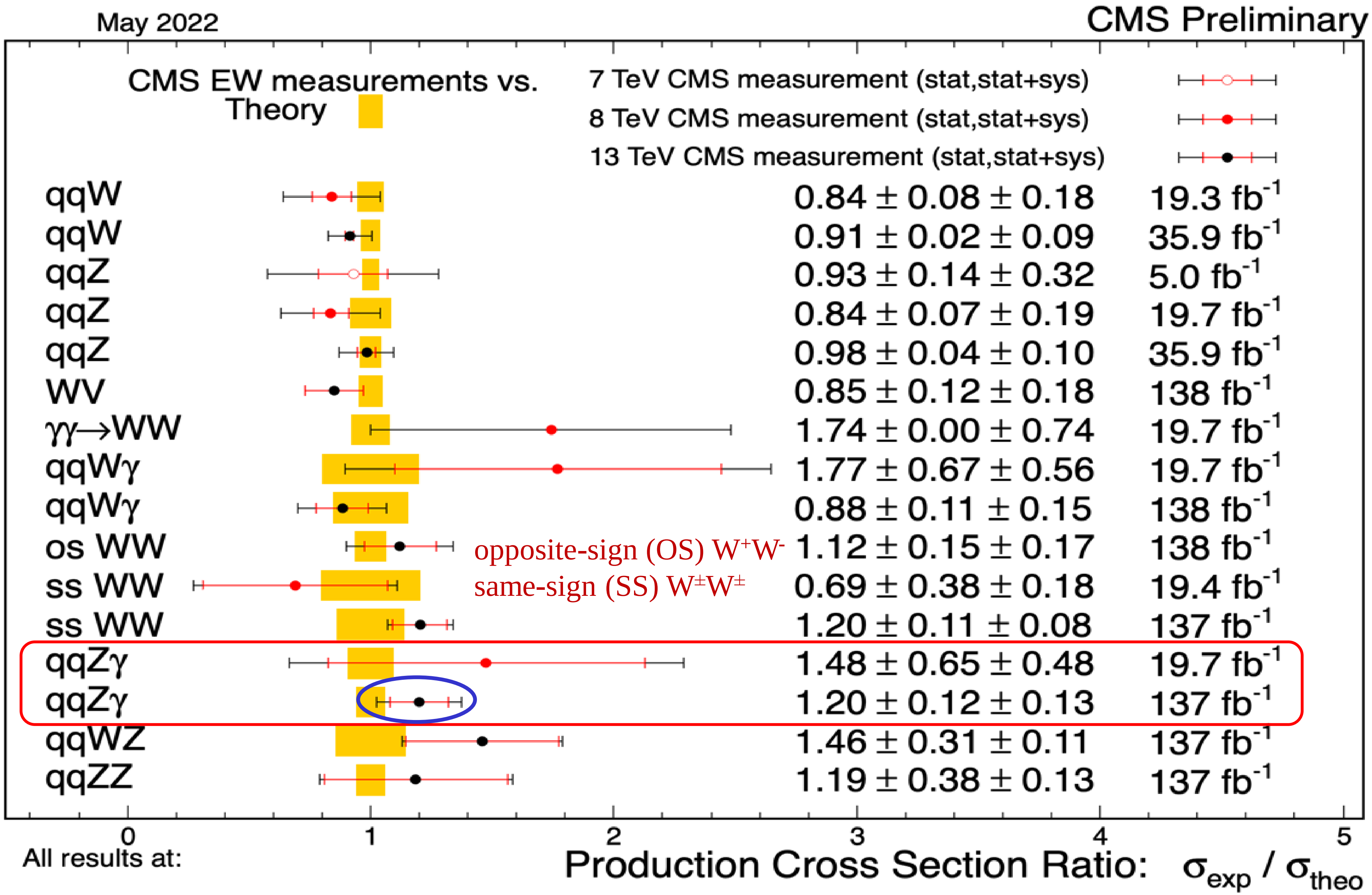

Summary of the cross sections of pure Electroweak (EW) interactions among the gauge bosons presented as a ratio compared to theory

JHEP 06 (2020) 076
Eur. Phys. J. C 82 (2021) 105

List of publication: https://twiki.cern.ch/twiki/bin/view/CMSPublic/PhysicsResultsSMP

ELECTROWEAK $pp \to Z(\to ll)\gamma\ jj + X$ & $pp \to Z(\to \nu\nu)\gamma\ jj + X$ PRODUCTION #1

- **Vector boson scattering** (VBS) processes **(VV→VV with V = W/Z/γ)**
- **Quartic EW coupling experimentally accessible in electroweak production of *VVjj***

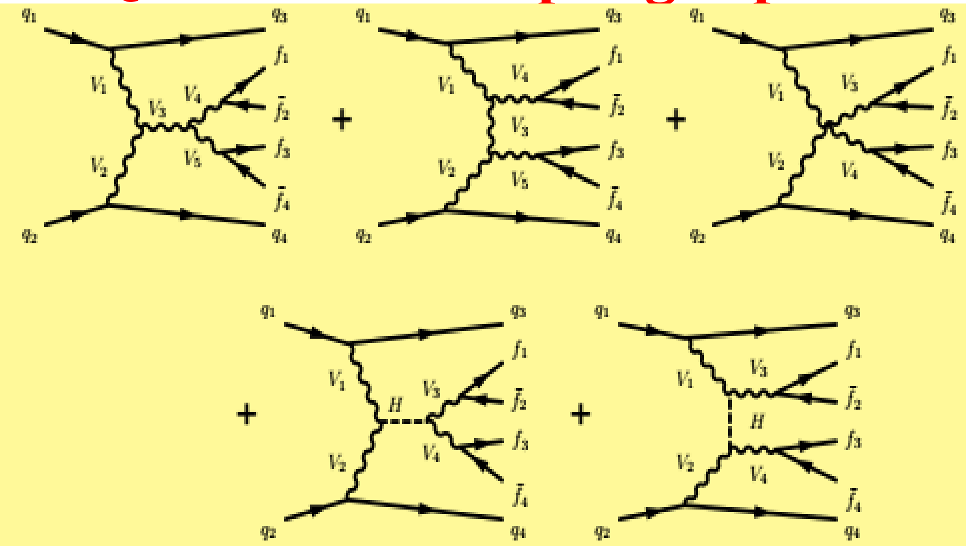

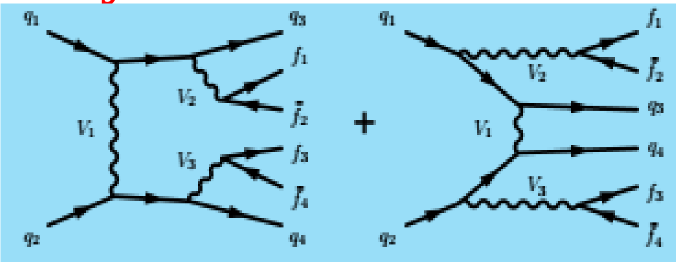

- **Purely EW interactions without self interactions**

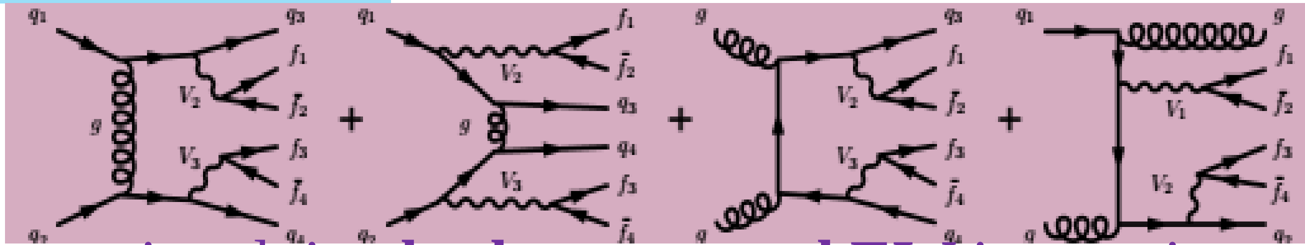

- Processes involving **both strong and EW interactions**

- **Purely EW interactions** involving only **cubic and quartic self interactions**

Zγ production

The *Z→ll* & *Z→νν* decays are studied

Z→ll large contributions from **FSR** off of leptons

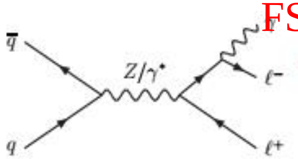

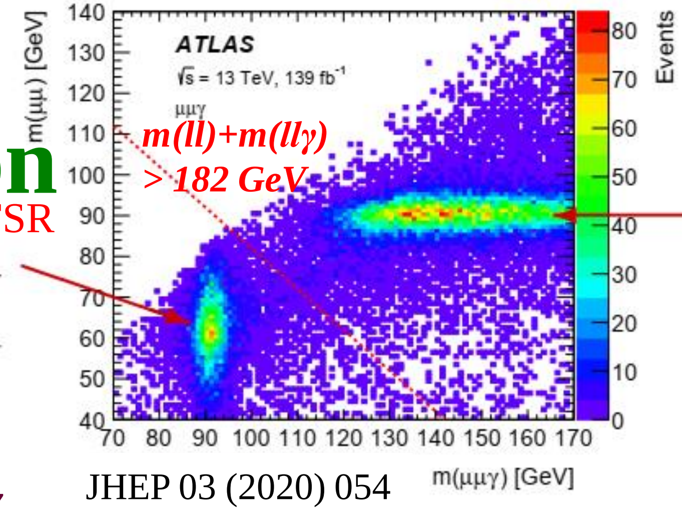

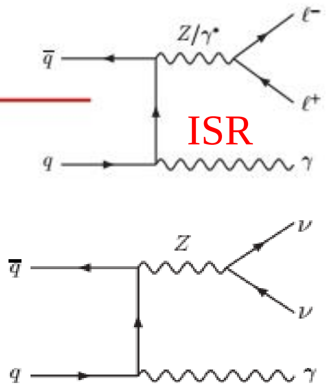

JHEP 03 (2020) 054

Two-dimensional distribution of ***m(ll)*** and ***m(llγ)*** for events satisfying all $\mu^+\mu^-\gamma$ selection criteria except that on the sum of ***m(ll)*** and ***m(llγ)***. *The* photon is emitted from an initial-state quark

- Increase sensitivity to **EW** couplings, by removing **FSR** events
  - Selection on the masses of the ***ll*** and ***llγ*** systems: $\mathbf{m_{ll}+m_{ll\gamma}>2m_Z}$
  - Using ***Z→νν*** decays

ATLAS-CONF-2021-038

ELECTROWEAK $pp \to Z(\to e^+e^-, \mu^+\mu^-)\gamma\ jj+X$ PRODUCTION #1

- ➢ The cross-section of the **EW production:** sensitivity to the **gauge boson self-interactions**
- ❑ Improved constraints probe scales of **new physics** in the **multi-TeV range** and provide a way to look for **signals of new physics** in a **model-independent way**

Selection criteria applied at particle level

Lepton	$p_T^{\ell} > 20, 30$(leading) GeV, $\lvert\eta_\ell\rvert < 2.47$ $N_\ell \geq 2$
Photon	$E_T^{\gamma} > 25$ GeV, $\lvert\eta_\gamma\rvert < 2.37$ $E_T^{cone20} < 0.07 E_T^{\gamma}$ $\Delta R(\ell,\gamma) > 0.4$
Jet	$p_T^{jet} > 50$ GeV, $\lvert y_{jet}\rvert < 4.4$ $\lvert\Delta y\rvert > 1.0$ $m_{jj} > 150$ GeV remove jets if $\Delta R(\gamma, j) < 0.4$ or if $\Delta R(\ell, j) < 0.3$
Event	$m_{\ell\ell} > 40$ GeV $m_{\ell\ell} + m_{\ell\ell\gamma} > 182$ GeV $\zeta(\ell\ell\gamma) < 0.4$ $N^{gap}_{jets} = 0$

VBS **signature** ($\lvert\Delta y\rvert > 1.0$, $m_{jj} > 150$ GeV)

Strong QCD-$Z\gamma jj$ separation ($\zeta(\ell\ell\gamma) < 0.4$, $N^{gap}_{jets} = 0$)

$$\zeta(\ell\ell\gamma) = \left| \frac{y_{\ell\ell\gamma} - (y_{j_1} + y_{j_2})/2}{y_{j_1} - y_{j_2}} \right|$$

The **centrality** of the $l^+l^-\gamma$ system relative to the tagging jets (j_1, j_2)

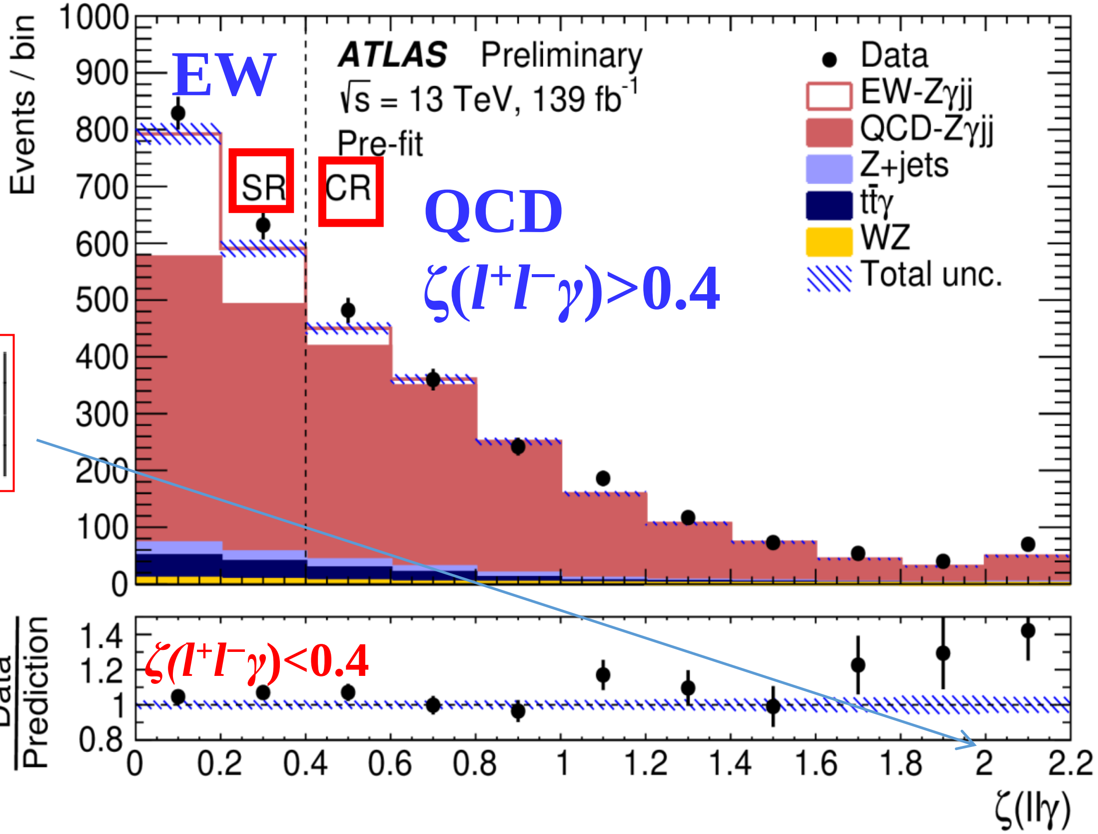

Centrality distributions, $\zeta(l^+l^-\gamma)$, in **Signal Region**, $\zeta(l^+l^-\gamma)<0.4$, and **Control Region**, $\zeta(l^+l^-\gamma)>0.4$, before the fit to extract the **EW-Zγjj** component is performed. **The sum of the signal and the various backgrounds is shown.**

- ❑ Events selected with high $\mathbf{m_{jj}}$ and **high** $|\Delta y_{jj}|$
- ❑ **Centrality** used to **control background** from Strong QCD - ***Zγjj*** production
- ❑ Background from **misidentified photons** estimated in data, background from **ttγ** validated in data

Post-fit m_{jj} distributions in **Signal Region** (SR) & **Control Region** (CR)

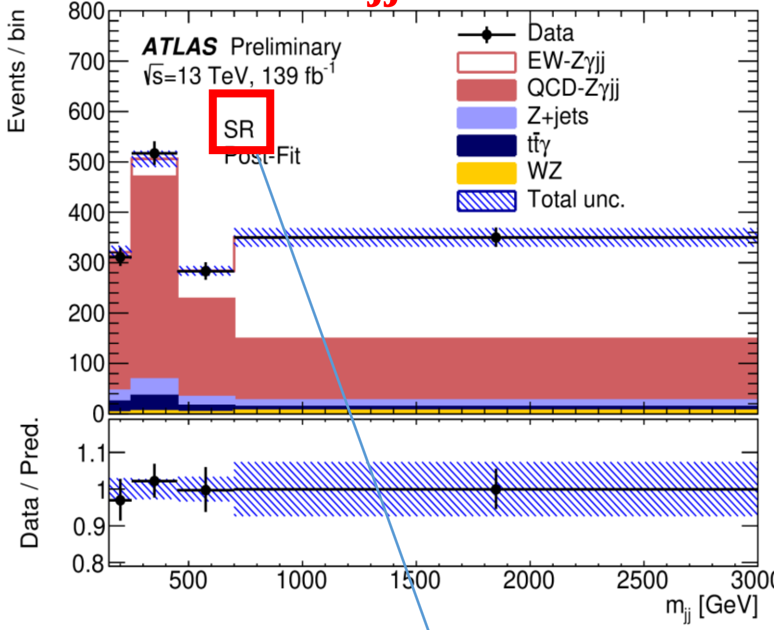

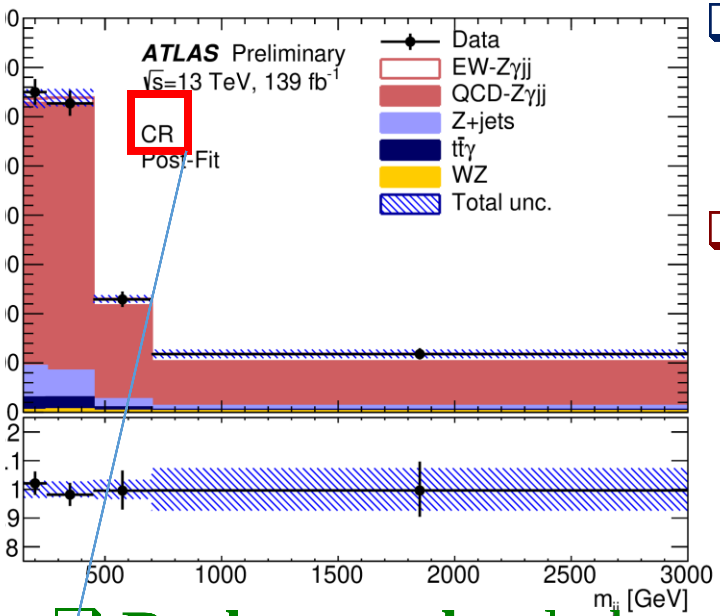

- To minimise dependence on theory modelling, the **high-$\zeta_{ll\gamma}$** is only used to **constrain** the **m_{jj}** distribution
- The normalisation parameters of the ***QCD-Zγjj*** background, **constrained** by data in the **SR & CR** are

$$\beta_{Z\gamma\text{-strong, CR}} = 1.00^{+0.18}_{-0.16}$$

$$\beta_{Z\gamma\text{-strong, SR}} = 1.06^{+0.17}_{-0.16}$$

Summary of the observed number of events in data, **N_{obs}**, background (**N_{Z+jets}, $N_{t\bar{t}\gamma}$, N_{WZjj}**), **EW-Zγjj** signal (**$N_{EW-Z\gamma jj}$**) and **QCD Zγjj** (**$N_{QCD-Z\gamma jj}$**) after the fit.

Sample	SR	CR
$N_{EW-Z\gamma jj}$	300 ± 36	55 ± 7
$N_{QCD-Z\gamma jj}$	987 ± 55	1352 ± 60
$N_{t\bar{t}\gamma}$	72 ± 11	59 ± 9
N_{WZ}	17 ± 3	14 ± 3
N_{Z+jets}	85 ± 30	143 ± 43
Total	1461 ± 38	1624 ± 40
N_{obs}	1461	1624

agreement

- **Background**-only hypothesis rejected with **10σ (11σ)**
- Measured and theoretical **Zγ-EW** cross sections:

σ_{EW}^{exp} =4.49±0.40 (stat)±0.42 (syst) fb

σ_{EW}^{theor} =4.73±0.01 (stat)±0.15 (PDF)$^{+0.23}_{-0.22}$ (scale) fb

(from **MG5_aMC@NLO+Pythia8 at LO**)

Agreement

- Measured and theoretical **Zγ-EW+QCD** cross sections:

σ_{EW+QCD}^{exp} =20.6±0.6 (stat)$^{+1.2}_{-1.1}$ (syst) fb

σ_{EW+QCD}^{theor} =20.4±0.1 (stat)±0.2 (PDF)±2.2 (scale) fb

(from **MG5_aMC@NLO+Pythia8**)

Agreement

Electroweak $pp \to Z(\to \nu\nu)\gamma JJ + X$ production: $15 > P_T^{\gamma} > 110$ GeV #1

EW $Z(\to\nu\nu)\gamma jj$ selection

Observable	Requirements
N_{jet} with $p_T > 25$ GeV	≥ 2
$\lvert\eta(j_{1,2})\rvert$	< 4.5
$p_T(j_1)$ [GeV]	> 60
$p_T(j_2)$ [GeV]	> 50
$\Delta R(j, \ell)$	> 0.4
$\lvert\Delta\eta_{jj}\rvert$	> 3.0
C_3	< 0.7
m_{jj} [TeV]	> 0.5
truth-E_T^{miss} [GeV]	> 150
$\Delta\phi(\text{truth-}\vec{E}_T^{miss}, j_i)$	> 1.0
$p_T(\gamma)$ [GeV]	$> 15, < 110$
$\lvert\eta(\gamma)\rvert$	< 2.37
$E_T^{cone20}/E_T^{\gamma}$	< 0.07
$\Delta R(\gamma, \text{jet-or-}\ell)$	> 0.4
C_γ	> 0.4
$\Delta\phi(\text{truth-}\vec{E}_T^{miss}, \gamma)$	> 1.8
N_ℓ with $p_T > 4$ GeV and $\lvert\eta\rvert < 2.47$	0

=2, 3 reco

Vector boson scattering (VBS) signature

strong-$Z\gamma jj$ separation

reject $W\gamma jj$

- ➢ **Using the E_T^{miss} to trigger $Z(\to\nu\nu)\gamma$ events**
  - ❑ This usually doesn't impact sensitivity to **BSM** effects, as these are expected at high energy

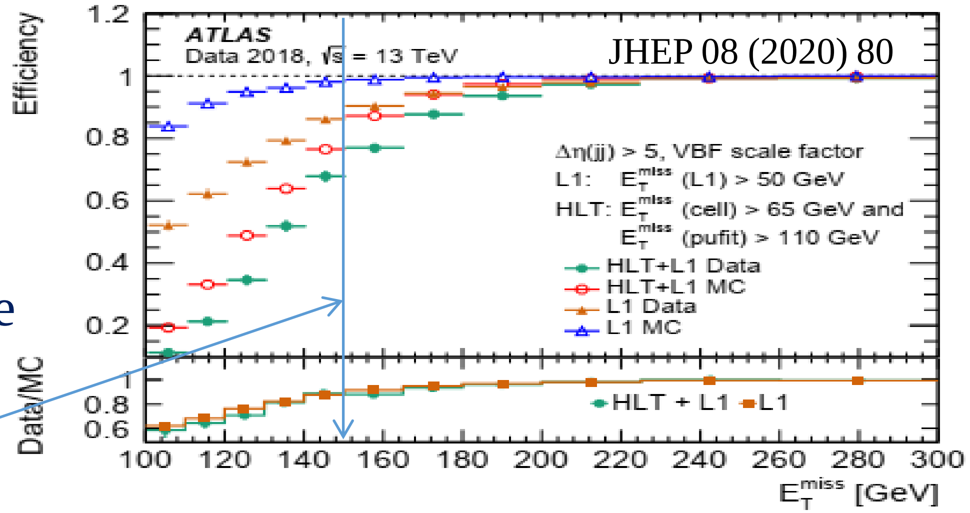

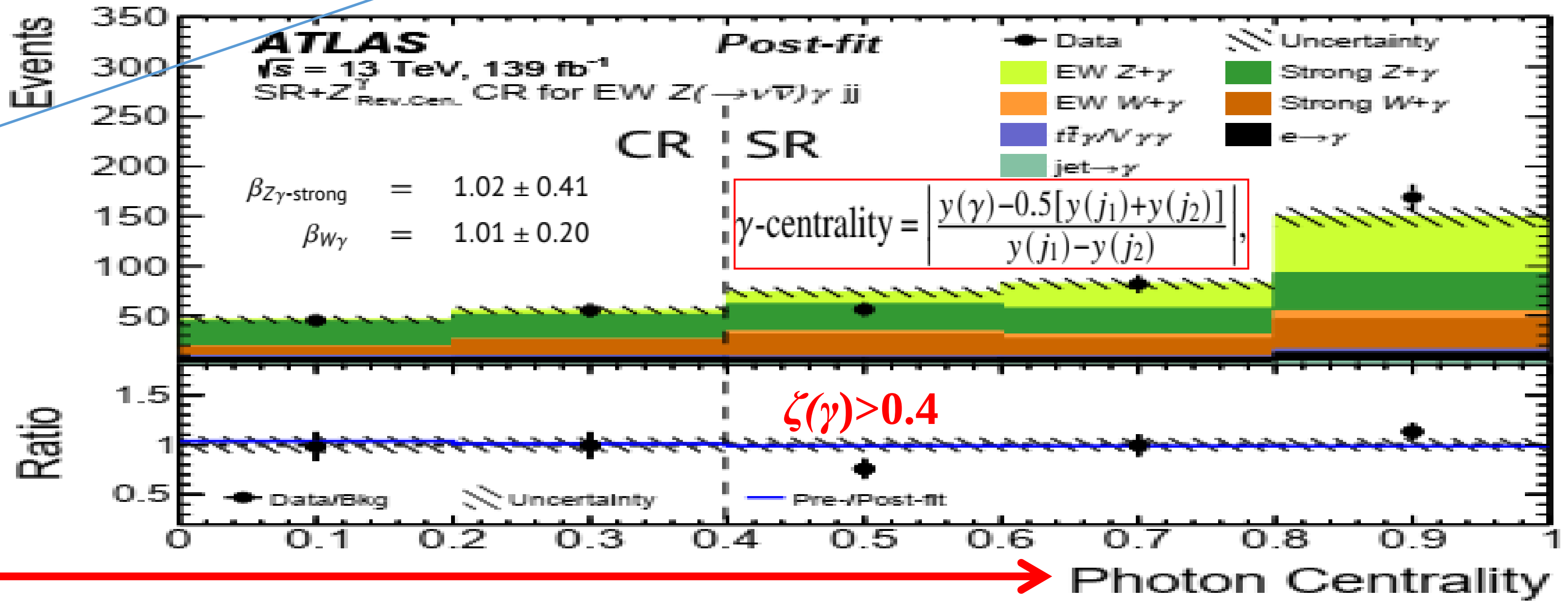

Similar strategy to select **VBS** events; control strong **Zγjj** production

Additional BGs, mainly **Wγjj**, compared to **Z(→ll)γ** in data

ELECTROWEAK $pp \rightarrow Z(\rightarrow \nu\nu)\gamma jj + X$ PRODUCTION: $15 > P_T^{\gamma} > 110$ GEV #2

➢ EW $Z(\rightarrow \nu\nu)\gamma jj$ is observed in this final state with a ***significance of*** 5.2 (5.1)σ

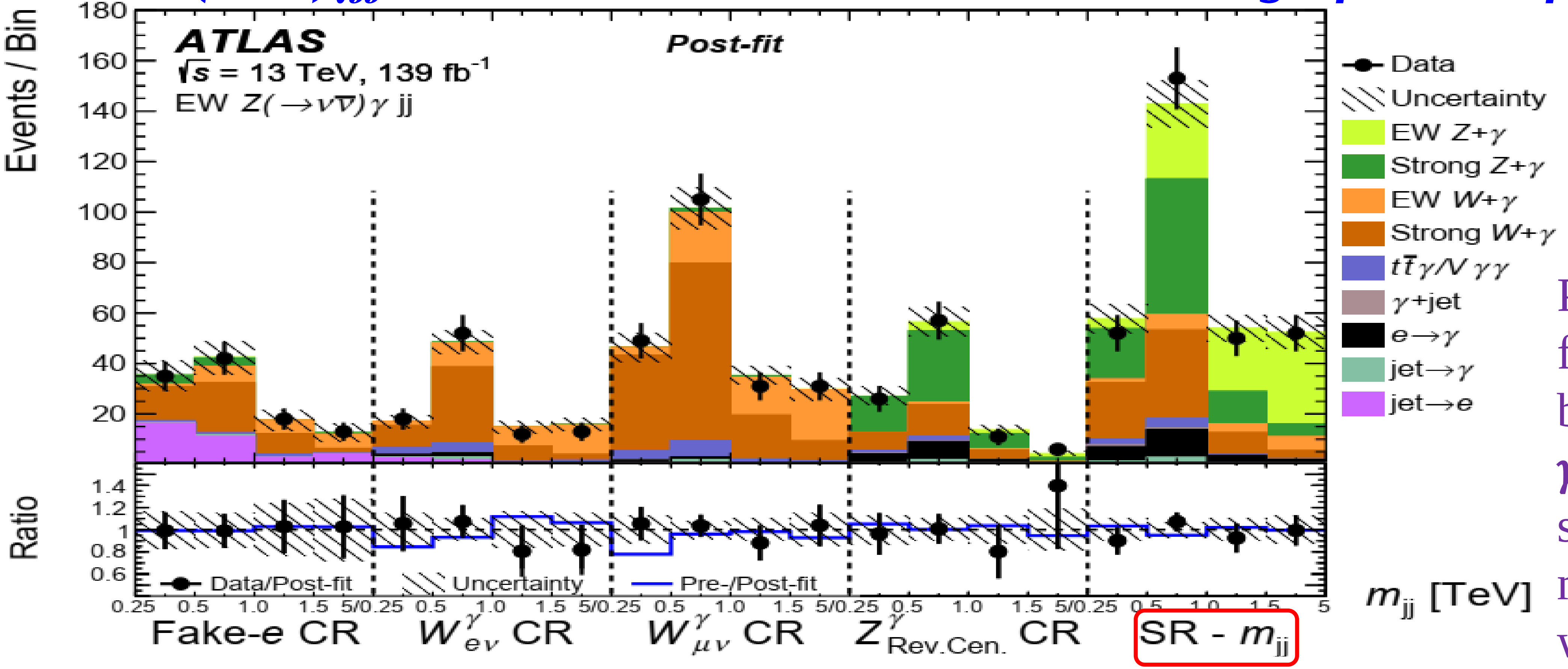

Post-fit results for m_{jj} **SR** & **CR** bins in the **EW *Z*** ***γ*+jets** cross-section measurement with the $\mu_{Z\gamma EW}$ signal normalization floating

❑ Measured and theoretical ***Zγ-EW*** cross sections:

$\sigma_{EW}^{meas.} = 1.31 \pm 0.20$ (stat) ± 0.20 (syst) fb

$\sigma_{EW}^{theo.} = 1.27 \pm 0.01$ (stat) ± 0.17 (scale) ± 0.03 (PDF) fb

Agreement

(from **MG5_aMC@NLO+Pythia8 at LO,** rescaled by 0.3% to VBFNLO)

➢ ***Largest sources of uncertainties*** in ***jet energy*** scale/resolution is ***7.6%*** and in ***Vγ+jets*** modelling is ***6.7%***.

ELECTROWEAK $pp \to Z(\to \nu\nu)\gamma jj + X$ PRODUCTION: E_T^{γ}>150 GEV #1

- The **EW** production of $Z(\to \nu\nu)\gamma jj$ with a γ (E_T>150 GeV), is a **Probe** of the **EW** symmetry **breaking** mechanism in SM & is sensitive to **quartic gauge boson couplings (QGS)** via **vector-boson scattering (VBS)**

Z boson branching ratio $Z\to\nu\nu$ is larger than the branching ratio $Z\to ll$; the background is under better control than in the hadronic decay channel

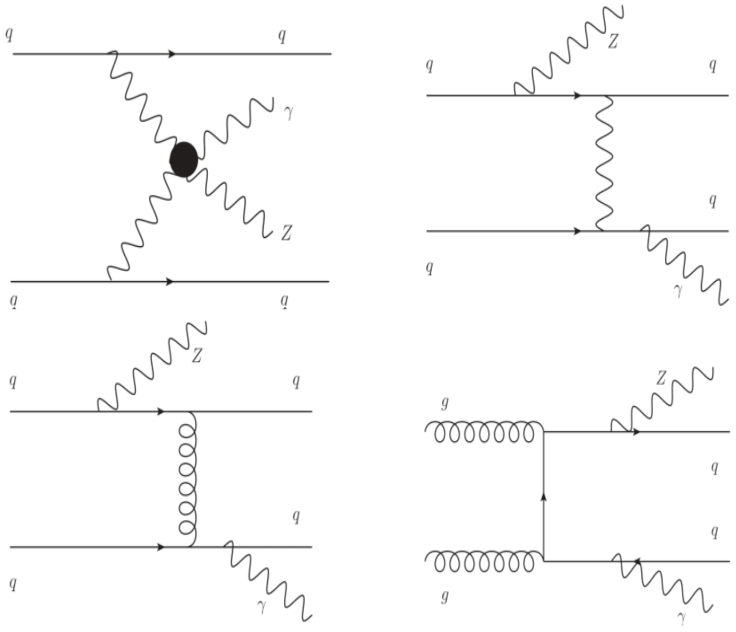

Feynman diagrams of electroweak

- $Z\gamma jj$ production involving the ***VBS*** subprocess (top left) or
- **non-VBS** subprocesses (top right)
- Of **QCD** $Z\gamma jj$ production with gluon exchange (bottom left) or
- the **s-channel** $gg\text{–}qq$ process (bottom right)

Photon centrality relative to the **two jets** with the **highest** p_T values in the event is defined as

$$\gamma\text{-centrality} = \left|\frac{y(\gamma)-0.5[y(j_1)+y(j_2)]}{y(j_1)-y(j_2)}\right|,$$

Were $y = 0.5\times\ln[(E+p_z)/(E-p_z)]$ is the rapidity of the objects (p_z is the z-component of the momentum of a particle)

Fiducial region definition

Selections	Cut value
E_T^{miss}	> 120 GeV
E_T^{γ}	> 150 GeV
Number of isolated photons	$N_\gamma = 1$
Photon isolation	$E_T^{cone40} < 0.022 p_T + 2.45$ GeV, $p_T^{cone20}/p_T < 0.05$
Number of jets	$N_{jets} \geq 2$ with $p_T > 50$ GeV
Overlap removal	$\Delta R(\gamma, jet) > 0.3$
Lepton veto	$N_e = 0, N_\mu = 0$
$\lvert\Delta\phi(\gamma, \vec{p}_T^{miss})\rvert$	> 0.4
$\lvert\Delta\phi(j_1, \vec{p}_T^{miss})\rvert$	> 0.3
$\lvert\Delta\phi(j_2, \vec{p}_T^{miss})\rvert$	> 0.3
m_{jj}	> 300 GeV
γ-centrality	< 0.6

Definition of the $Z\gamma$ subregions

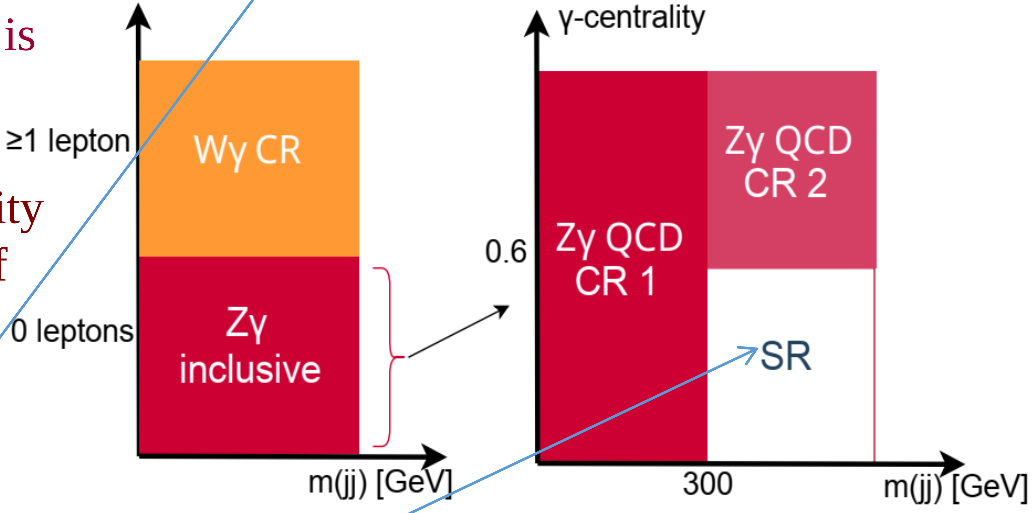

- The **signal region** (SR) is required to have m_{jj}>300 GeV and **γ-centrality < 0.6**, where m_{jj} is defined as the invariant mass of the **2jets** with the highest values of p_T
- The ***Zγ QCD CR 1*** requires events with m_{jj}<300 GeV; it is used to estimate the $Z(\nu\nu)\gamma jj$ *QCD* background yield
- The ***Zγ QCD CR 2*** has the same selection criteria as the ***SR*** but requires events with ***γ-centrality > 0.6***; it is used to check for possible m_{jj} mismodelling. The values of the requirements are chosen to maximise the number of events and the purity of the targeted process in each region

ELECTROWEAK $pp \to Z(\to \nu\nu)\gamma jj + X$ PRODUCTION: $E_T^{\gamma} > 150$ GEV #2

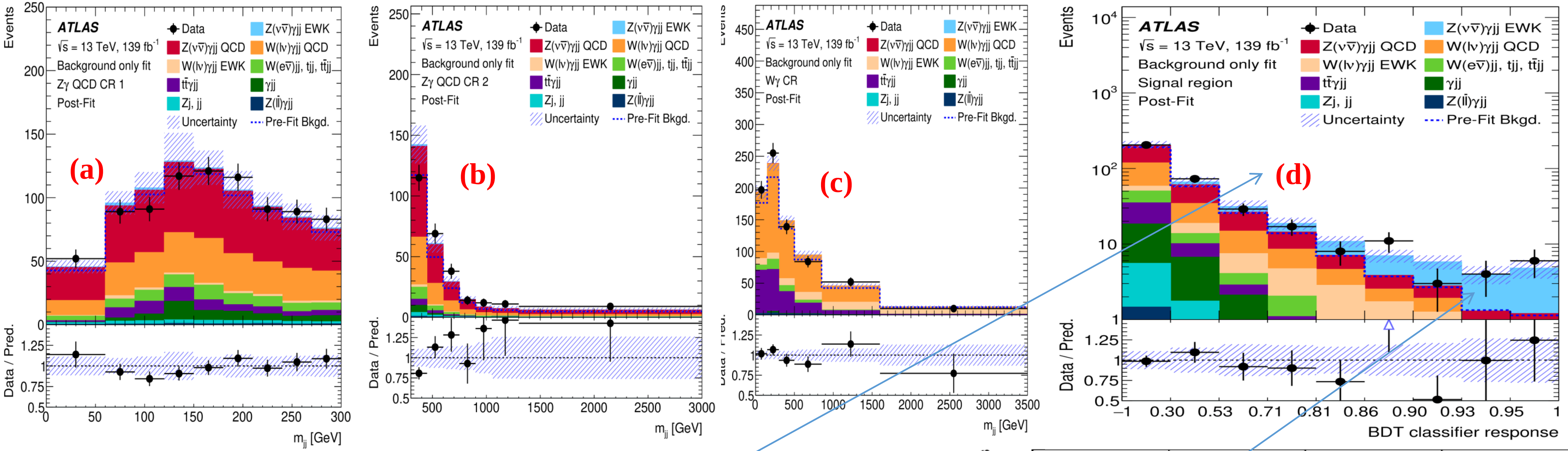

Summary of the yield for processes in all regions, after the fit. The dashed line shows the **total background** distribution before the fit.

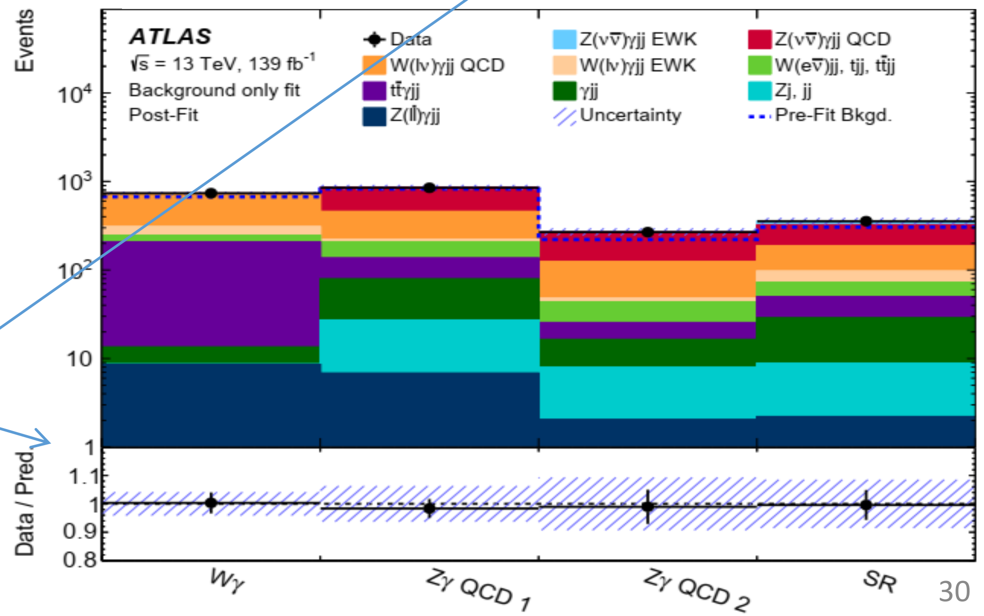

- The m_{jj} distributions for the
  - **(a) CR 1: *Zγ QCD*,**
  - **(b) CR 2: *Zγ QCD*,**
  - **(c) CR: *Wγ*,** and the ***BDT*** classifier response distribution for the
  - **(d) SR: after the fit in all regions**
- The **boosted decision tree (BDT) classifier response** was remapped into equal-width bins for better representation. The dashed line shows the total background distribution before the fit.
- **The signal selection uses a boosted decision tree (BDT)**

➢ **The observed fiducial cross section**

$$\sigma_{Z\gamma \mathrm{EWK}} = 0.77^{+0.34}_{-0.30}\ \mathrm{fb}$$

ATL-PHYS-PUB-2022-009

SM PRODUCTION CROSS SECTION MEASUREMENTS

Experimental Status

	ATLAS		CMS	
VBS $W^\pm W^\pm$	36 fb^{-1}, 6.5σ	PRL 123 (2019) 161801	137 fb^{-1}, $\gg 5\sigma$	PLB 809 (2020) 135710
VBS $W^\pm Z$	36 fb^{-1}, 5.3σ	PLB 793 (2019) 469	137 fb^{-1}, 6.8σ	PLB 809 (2020) 135710
VBS ZZ	139 fb^{-1}, 5.5σ	arXiv:2004.10612	137 fb^{-1}, 4.0σ	PLB 812 (2020) 135992
VBS $W\gamma$	–		(137+20) fb^{-1}, 5.3σ	PLB 811 (2020) 135988
VBS $Z\gamma$	139 fb^{-1}, > 10σ	ATLAS-CONF-2021-038 arXiv:2208.12741	137 fb^{-1}, 9.4σ	arXiv:2106.11082
$\gamma\gamma \to W^+W^-$	139 fb^{-1}, 8.4σ	PLB 816 (2021) 136190	–	
VBS W^+W^-	–		–	
VBS VV	36 fb^{-1}, 2.7σ	PRD 100 (2019) 032007	137 fb^{-1}, 4.4σ	CMS-PAS-SMP-20-013

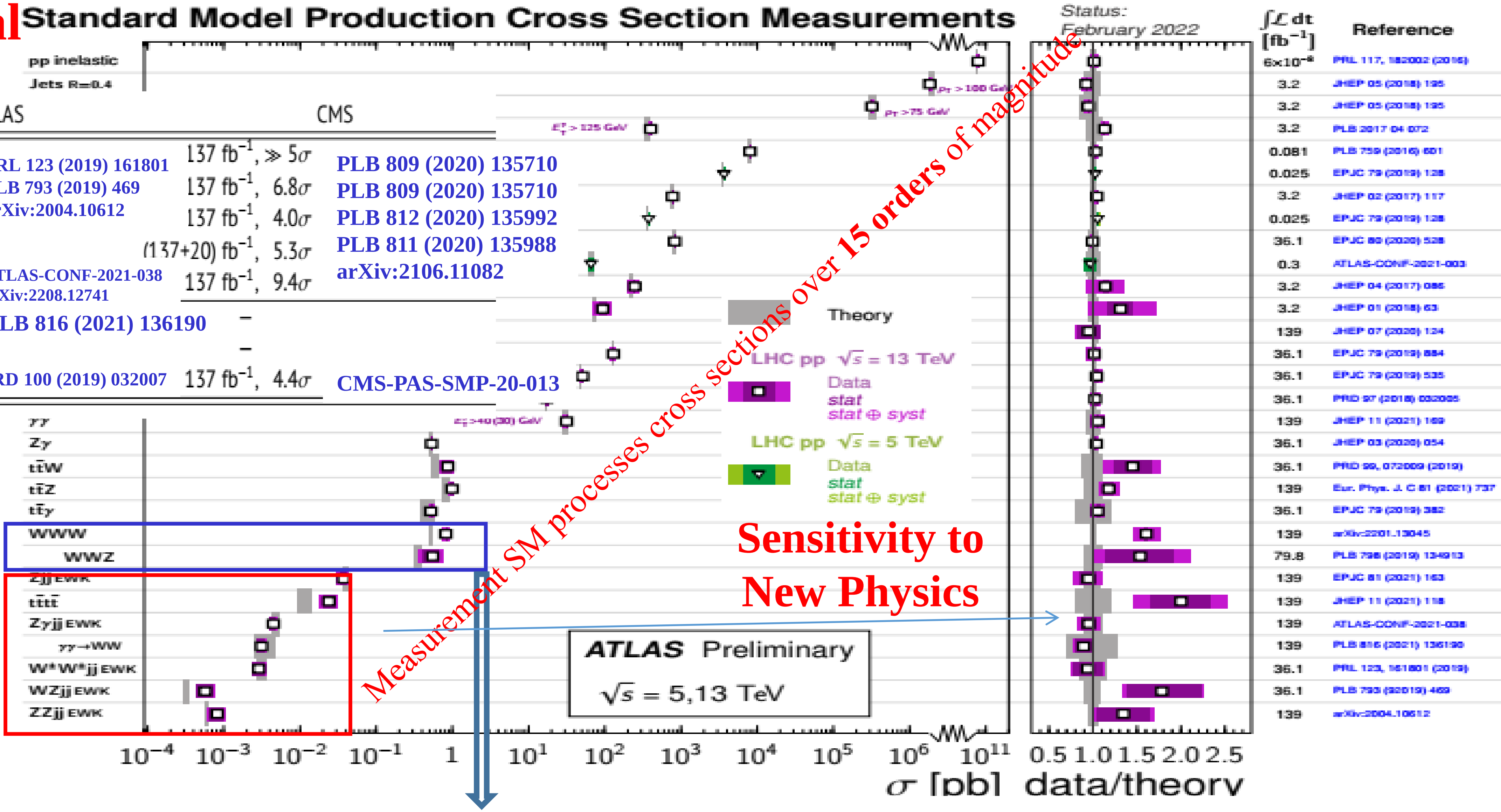

- **Electroweak *VVjj*** production has been observed in all major channels
  - ✓ They are amongst the **rarest processes** currently experimentally accessible

OBSERVATION OF WWW PRODUCTION

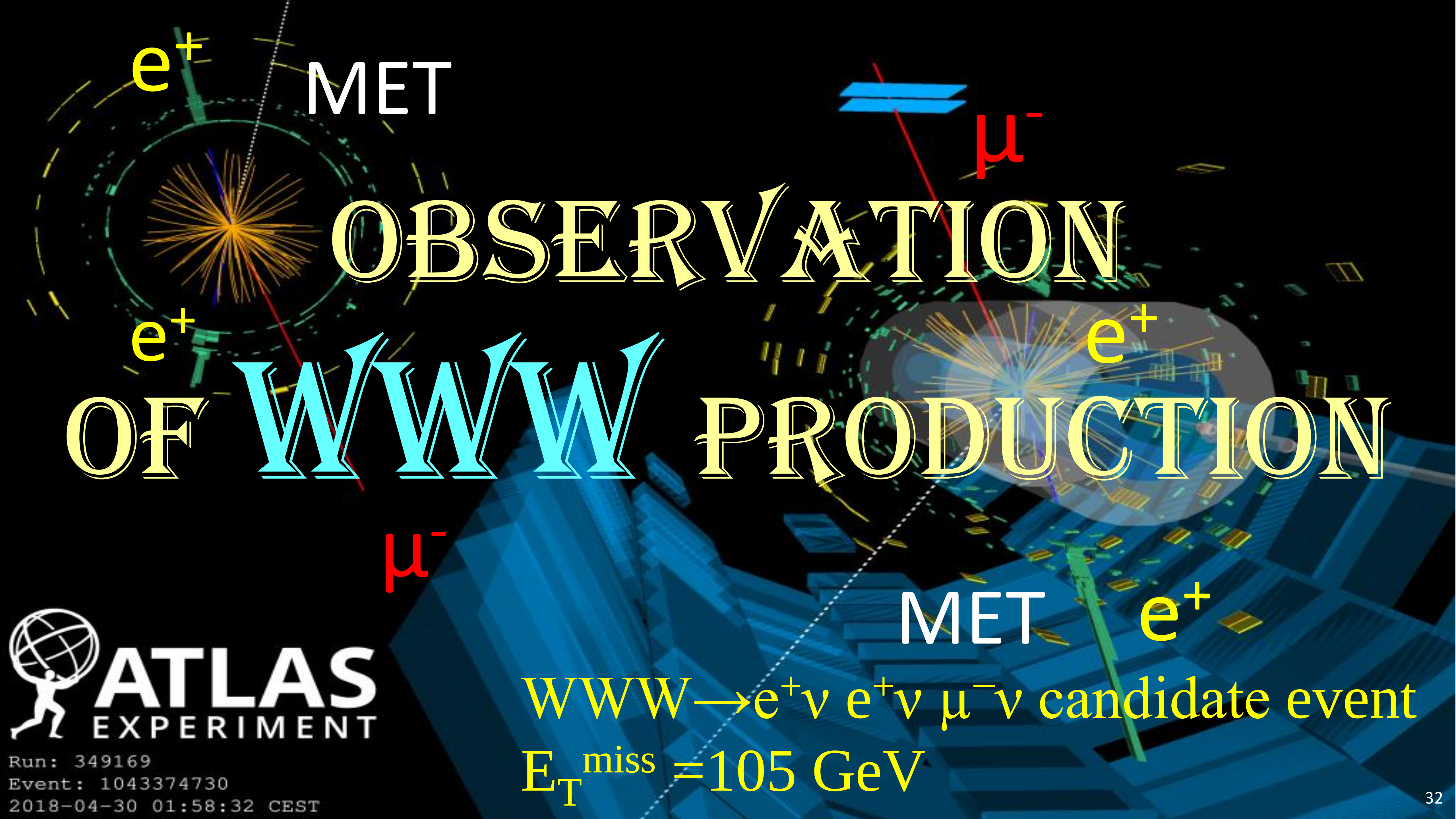

$WWW \rightarrow e^{+}\nu\ e^{+}\nu\ \mu^{-}\nu$ candidate event

$E_T^{miss} = 105$ GeV

VBF, VBS & TRIBOSON CROSS SECTION MEASUREMENTS

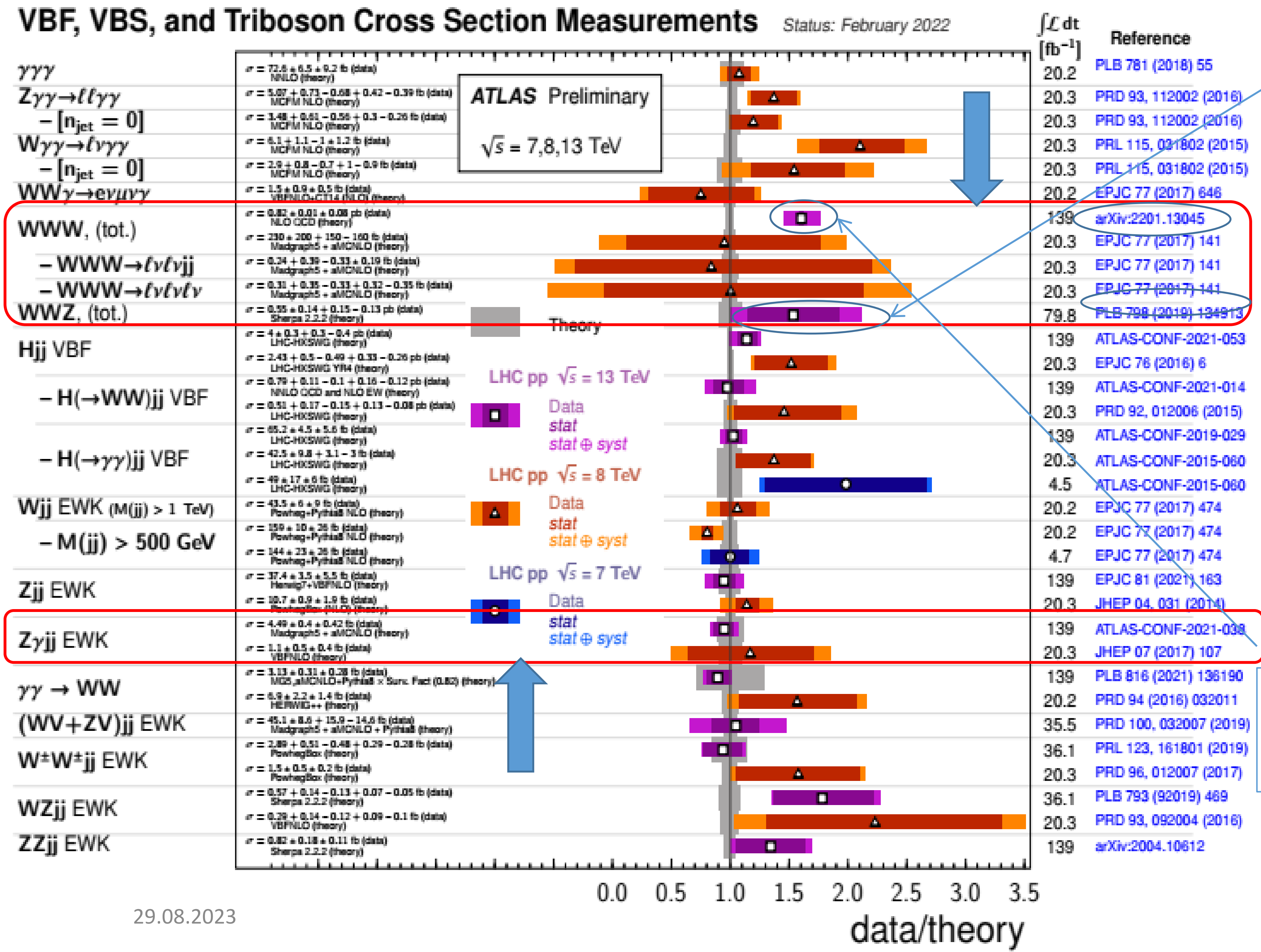

Experimental Status

1. **Evidence for *WVV* from ATLAS**

- ❑ *WWW → lν lν qq (l=e,μ)*
- ❑ *WWW → lν lν l ν*
- ❑ *WWZ →lν qq ll*
- ❑ *WWZ →l ν lν ll*
- ❑ *WZZ →qq ll ll*

in **80 fb^{-1}** (2015-2017 data)

- ❑ **Evidence 4.1σ (WVV) and 3.2σ (WWW) PLB 798 (2019) 134913**

New ATLAS result focuses on WWW in ***$l^{\pm}\nu\ l^{\pm}\nu\ jj$ and $l^{\pm}\nu\ l^{\mp}\nu\ l^{\pm}\nu$;*** Phys.Rev.Lett.129 (2022) 6, 061803; ArXiv 2201.13045

- ❑ *$e^{\pm}e^{\pm}$ + jj,*
- ❑ *$e^{\pm}\mu^{\pm}$ + jj,*
- ❑ *$\mu^{\pm}\mu^{\pm}$ + jj*
- ❑ *3l + E_T^{miss}* with no same-flavour opposite-charge lepton pair

→ strong suppression of ***VV + jets***

The **σ_{WWW+X}=820±100 (stat)±80 (syst) fb** it is **2.6σ of** predicted **σ_{WWW+X}=511±18 fb (NLO QCD and LO EW)**

Observation of VVV from CMS in **137 fb^{-1}** (2015-2018 data)

- ❑ **5.7σ (VVV), 3.3σ (WWW)**

PRL 125 (2020) 151802

Phys. Rev. Lett. 129 (2022) 6, 061803
arXiv:2201.13045, ATLAS-CONF-2021-039

OBSERVATION OF $pp \to WWW+X$ PRODUCTION #1

- ➢ The combined observed (expected) significance ***pp→WWW+X*** is found to be **8.0(5.4)σ**
- ❑ The inclusive cross section is **820±100 (stat)±80 (syst) fb**: **2.6σ** from the **predicted** of **511±18 fb** (**NLO QCD, LO EW** accuracy)

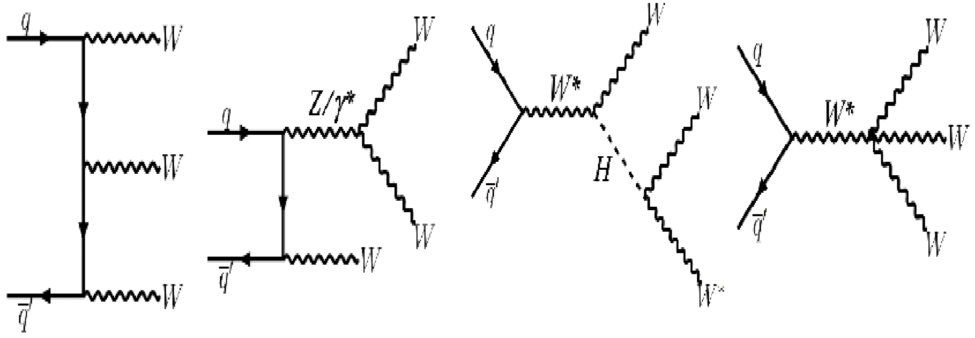

Feynman diagrams at LO for the production of ***WWW*** bosons, including diagrams sensitive to **triple & quartic gauge couplings**

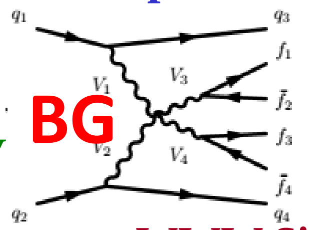

WWW→l±ν l±ν jj is distinguished from **VBS** signatures by requiring at least **2 central jets** with ***m_{jj}<160 GeV*** & ***$\Delta\eta_{jj}$<1.5***

WWW Simulation

- ❑ on-shell ***WWW*** simulated with **Sherpa 2.2.2 at NLO**
- ❑ ***WH →WWW**** simulated with **Powheg+Pythia8 at NLO**
- ❑ spin correlations accounted for in *W* decays
- ❑ **t-** and **u-**channel production at **O(α⁶)** as background

Signal is measured in a fit to a ***boosted-decision-tree* (*BDT*)** discriminant

12 BDT training variables

2ℓ
$\lvert m_{jj} - m_W \rvert$
p_T (forward jet)
E_T^{miss} significance
$p_T(j_2)$
minimum $m(\ell, j)$
$m(\ell_2, j_1)$
N(jets)
p_T (ℓ_2)
$m_{\ell\ell}$
$\lvert\eta(\ell_1)\rvert$
N(leptons in jets)
$m(\ell_1, j_1)$

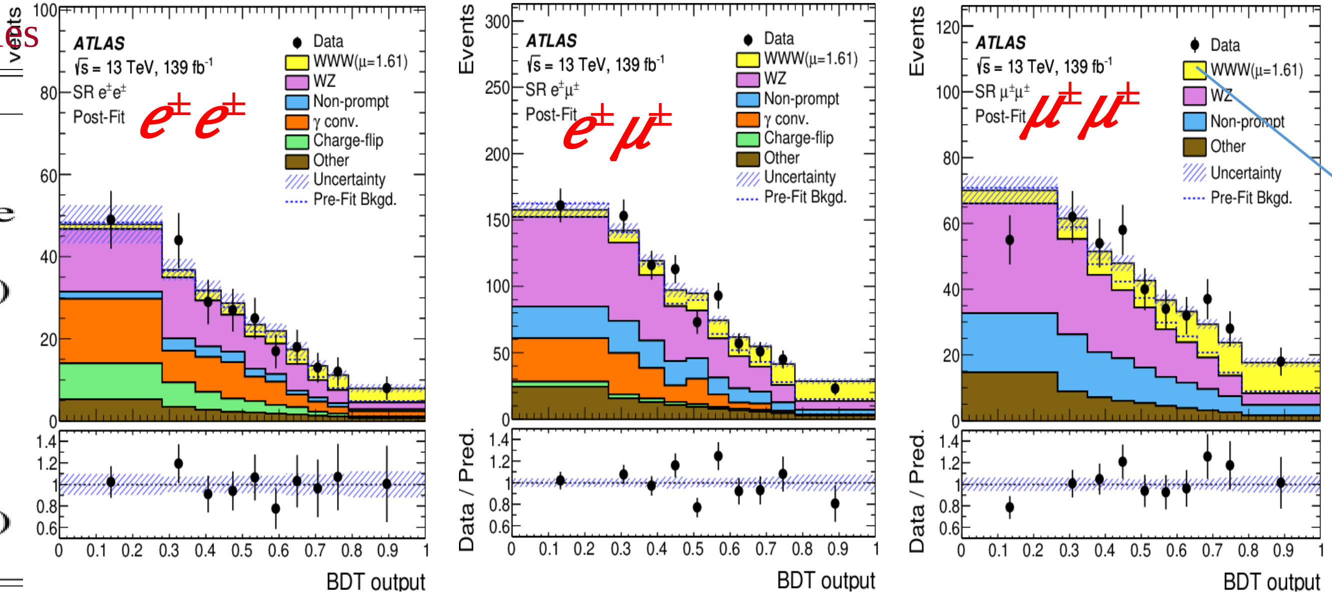

Number of events for postfit signal, **BG** & data observed in the *2ℓ & 3ℓ SRs*

	$e^\pm e^\pm$	$e^\pm\mu^\pm$	$\mu^\pm\mu^\pm$	3ℓ
WWW signal	28.4 ± 4.3	124 ± 19	82 ± 12	34.8 ± 5.2
WZ	81.1 ± 5.7	346 ± 22	170 ± 10	16.4 ± 1.5
Charge-flip	31.1 ± 7.3	19 ± 5	...	1.7 ± 0.4
γ conversions	60.8 ± 8.5	139 ± 15	...	1.5 ± 0.1
Nonprompt	17.0 ± 4.0	145 ± 23	104 ± 21	26.6 ± 2.9
Other	22.3 ± 2.4	100 ± 10	58 ± 6	8.0 ± 0.9
Total predicted	241 ± 11	873 ± 22	415 ± 17	89.0 ± 5.4
Data	242	885	418	79

Agreement

- ➢ Postfit *BDT* output distribution in the ***e±e±, e±μ±, μ±μ± & 3ℓ*** channels for *improving the separation between signal and background*

OBSERVATION OF $pp \rightarrow WWW+X$ PRODUCTION #2

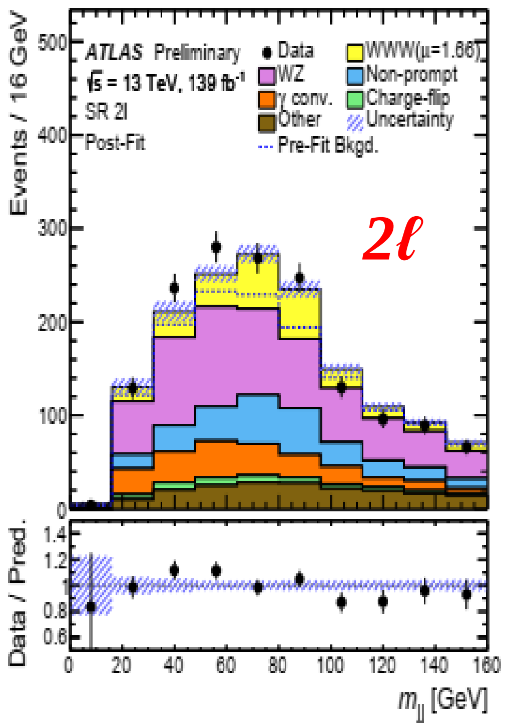

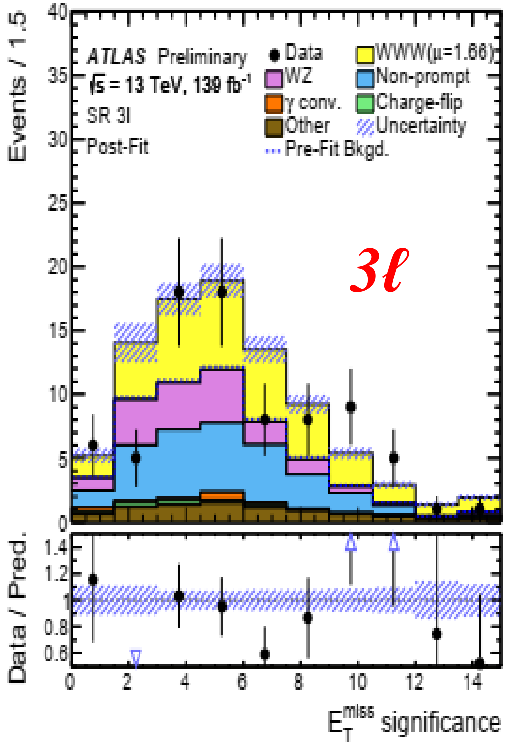

11 BDT training variables

3ℓ
E_T^{miss} significance ×10/E_T^{miss}
$p_T(\ell_2)$
N(jets)
same flavor $m_{\ell\ell}$
$m_T(\ell\ell\ell, E_T^{miss})$
$m(\ell_2, \ell_3)$
$\Delta\phi(\ell\ell\ell, E_T^{miss})$
minimum $\Delta R(\ell, \ell)$
$p_T(\ell_3)$
$m_T(\ell_2, E_T^{miss})$
E_T^{miss} significance

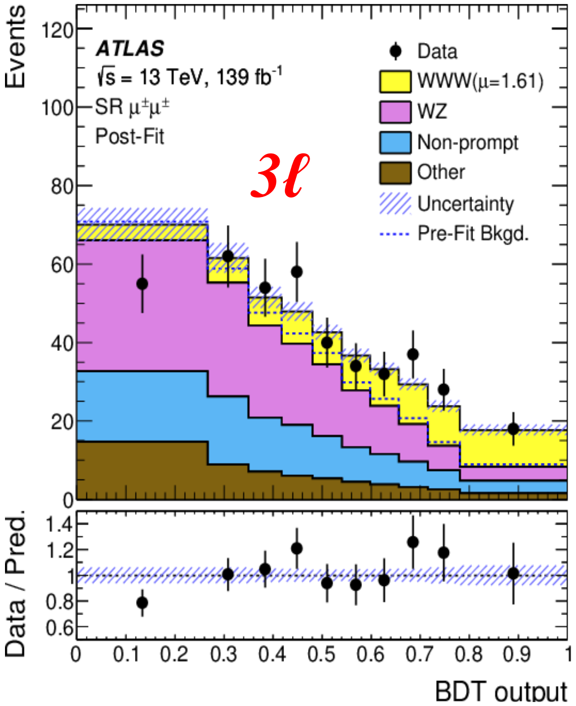

Backgrounds and Background Estimation

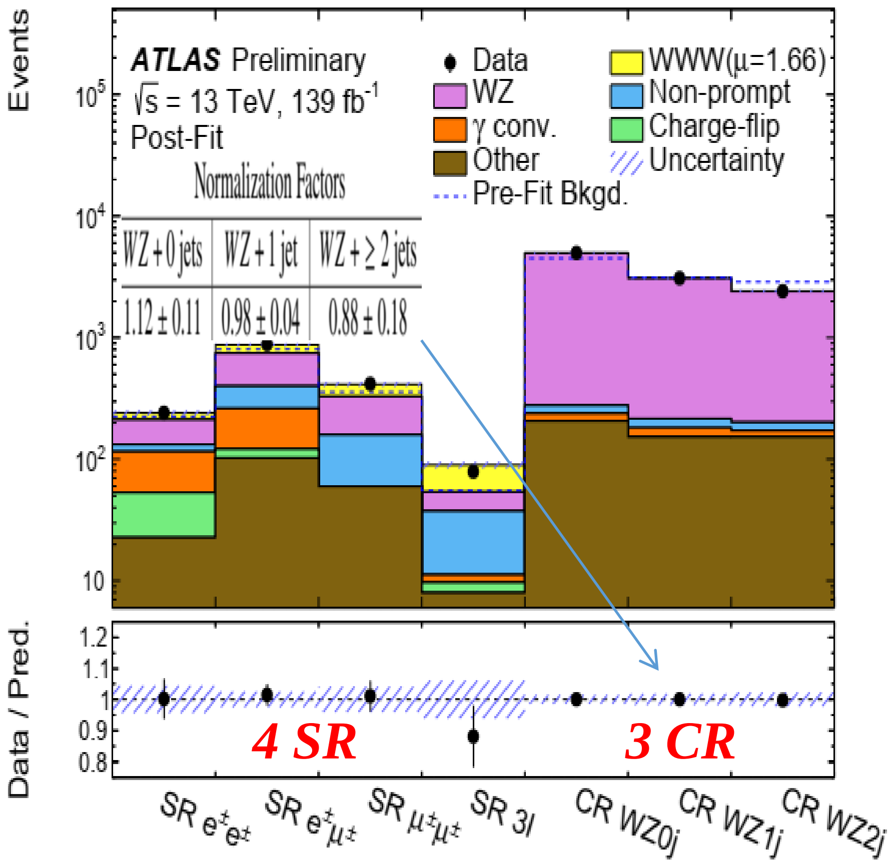

- ➢ Higher signal purity in ***3l*** events compared to $l^\pm l^\pm jj$
- ❑ Separate **boosted decision tree** (BDT) training to extract signal: Kinematic and angular variables, combining **leptons** and **E_T^{miss}**
- ❑ Similar validation of BDT modelling as for ***$l^\pm l^\pm jj$***

- ❑ Fit of BDT (**SR**s) and ***m_{3l}*** (**WZ CR**s)
- ❑ Largest **source of background** from **WZ+jets** production, constrained in control regions
- ❑ **Other backgrounds** are instrumental and **estimated in data** (misidentified leptons, **γ** -conversions, electron charge misreconstruction)

- ❑ **The measured cross section**, ***extrapolated to the total phase space***:
- ✓ **σ_{WWW}=820±100 (stat)±80 (syst) fb; σ_{WWW}^{MC}=511±18 fb**

2.6σ from the predicted of calculated at **NLO QCD** and **LO EW** accuracy

Phys.Rev.Lett.125 (2020) 151802
arXiv:2006.11191

- The production of ***VVV*** (***V = W, Z***) bosons in ***pp*** collisions at $\sqrt{s}$=**13 TeV**
- ***5 final states***: $W^{\pm}W^{\pm}W^{\mp} \to \ell^{\pm}\ell^{\pm}2\nu q\bar{q}$, $W^{\pm}W^{\pm}W^{\mp} \to \ell^{\pm}\ell^{\pm}\ell^{\mp}3\nu$, $W^{\pm}W^{\mp}Z \to \ell^{\pm}\ell^{\mp}2\nu\, \ell^{\pm}\ell^{\mp}$, $W^{\pm}ZZ \to \ell^{\pm}\nu 2(\ell^{\pm}\ell^{\mp})$, $ZZZ \to 3(\ell^{\pm}\ell^{\mp})$

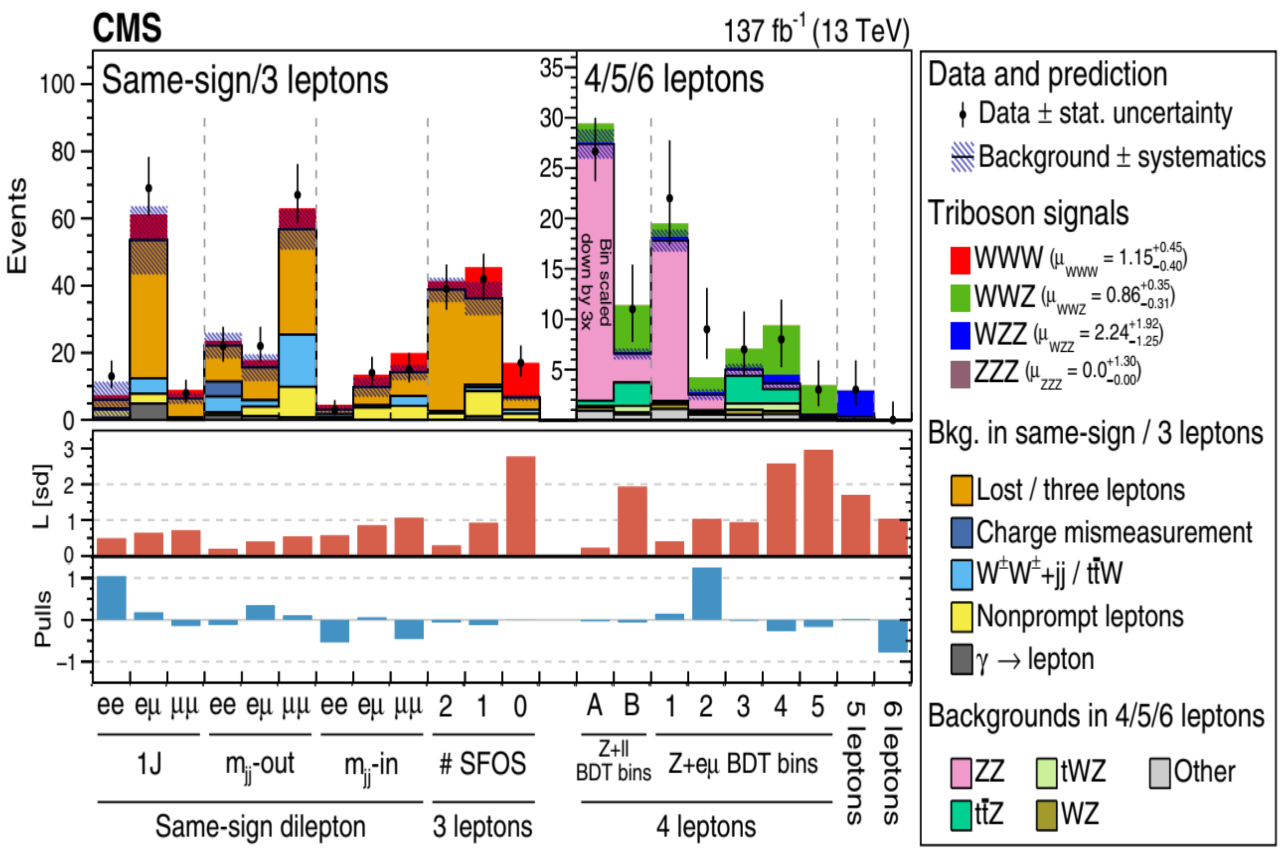

Comparison of the observed numbers of events to the predicted yields after fitting. For the ***WWW & WWZ*** channels, the results from the ***boosted decision trees*** (***BDT)*** based selections are used. Events with two or more jets are categorized as ***"m_{jj}-in" or "m_{jj}-out".*** The expected significance ***L*** in the middle panel represents the number of standard deviations with which the null hypothesis (no signal) is rejected; it is calculated for the fit for μ_{comb}. Pulls are the differences in the numbers of observed and predicted events normalized to the uncertainties in the numbers of predicted events.

- The observed significance of the combined ***VVV*** production signal is ***5.7 (5.9)***
- the corresponding measured cross section relative to SM prediction is $\mathbf{1.02^{+0.26}_{-0.23}}$
- The observed significances for the individual **triboson** production processes:
  - **3.3 (3.1)** ***WWW,***
  - ***3.4 (4.1) WWZ,***
  - ***1.7 (0.7) WZZ,***
  - ***0.0 (0.9) ZZZ.***

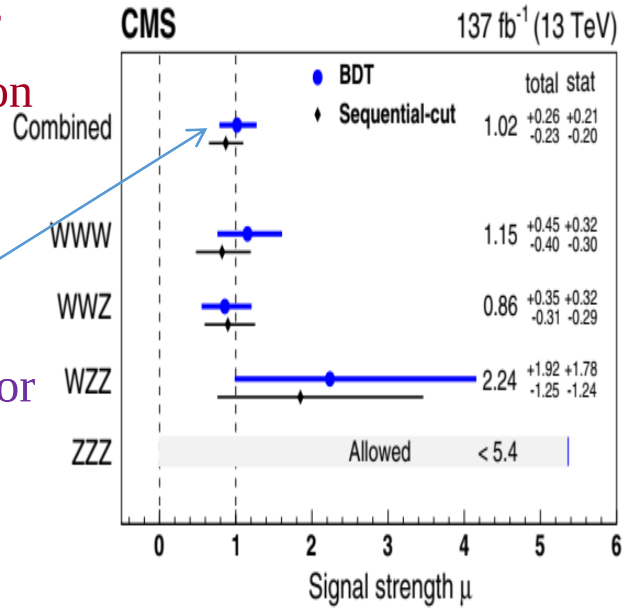

Best fit values of the signal strengths for the BDT-based analyses and the sequential-cut analyses

Process	Cross section (fb), treating Higgs boson contributions as: Signal	Background
VVV	$1010^{+210+150}_{-200-120}$	$370^{+140+80}_{-130-60}$
WWW	$590^{+160+160}_{-150-130}$	$190^{+110+80}_{-100-70}$
WWZ	$300^{+120+50}_{-100-40}$	100^{+80+30}_{-70-30}
WZZ	$200^{+160+70}_{-110-20}$	$110^{+100+30}_{-70-10}$
ZZZ	< 200	< 80

ATL-PHYS-PUB-2022-009

VECTOR BOSON +X CROSS SECTION MEASUREMENTS

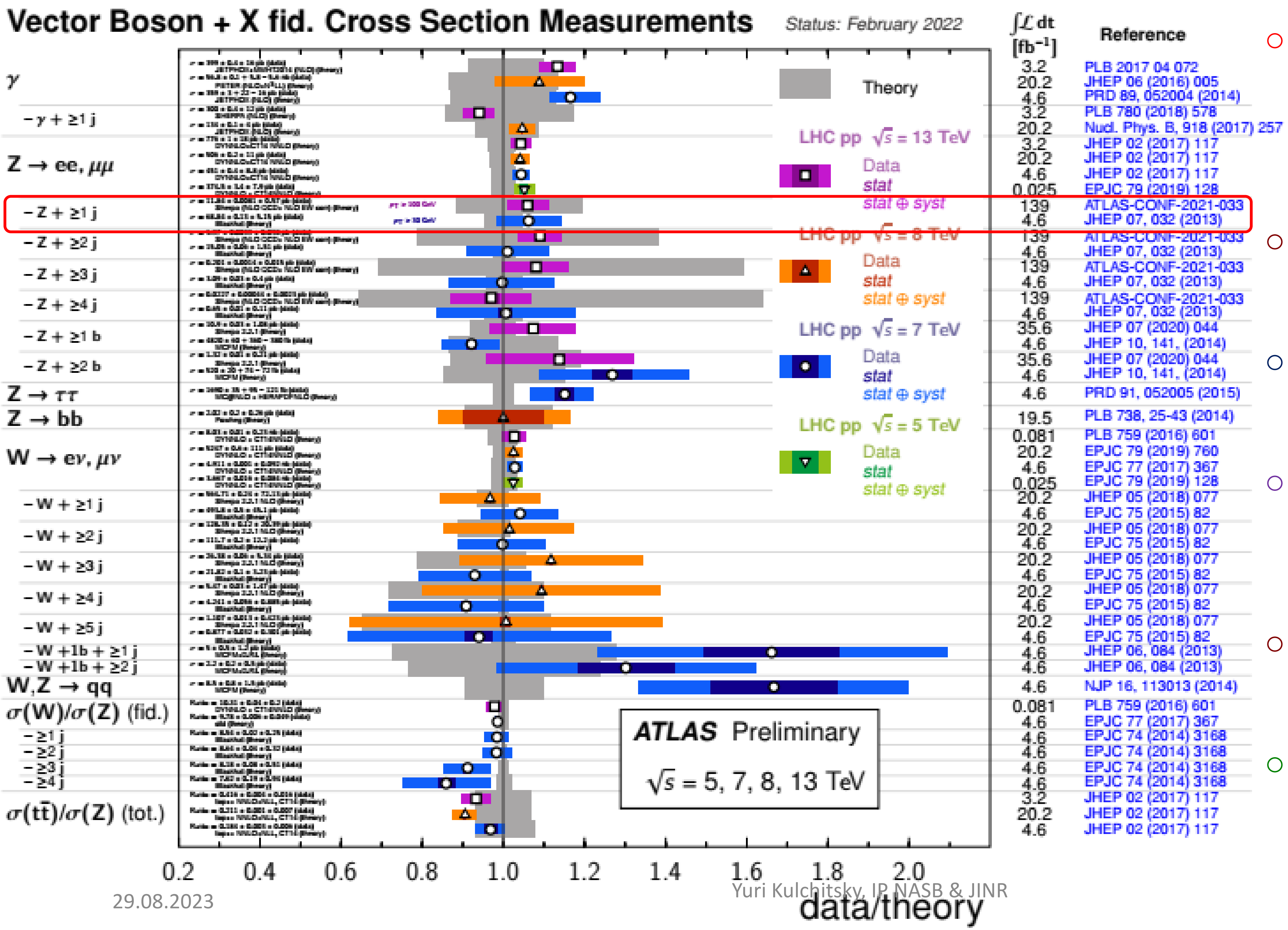

- The **data/theory ratio** for several single-boson fiducial production cross section measurements, corrected for leptonic branching fractions
- All **theoretical expectations** were calculated at **NLO or higher**
- The dark-color error bar represents the statistical uncertainly
- The lighter-color error bar represents the full uncertainty, including systematics and luminosity uncertainties
- The luminosity used and reference for each measurement are also shown
- They were not always evaluated using the same prescriptions for PDFs and scales

Cross-section $pp \to Z(\to e^+e^-, \mu^+\mu^-)$ +≥1jet ($p_{T,J} \geq 100$ GeV) +X #1

- The $pp \to Z$+high-p_T jets+X provides a way to probe the ***interplay** between **QCD & higher-order EW** processes*
- The **angular correlations** between the ***Z* boson** and the ***closest jet*** are performed in events with at ***≥1 jet** with* $p_T \geq$ **500 GeV**

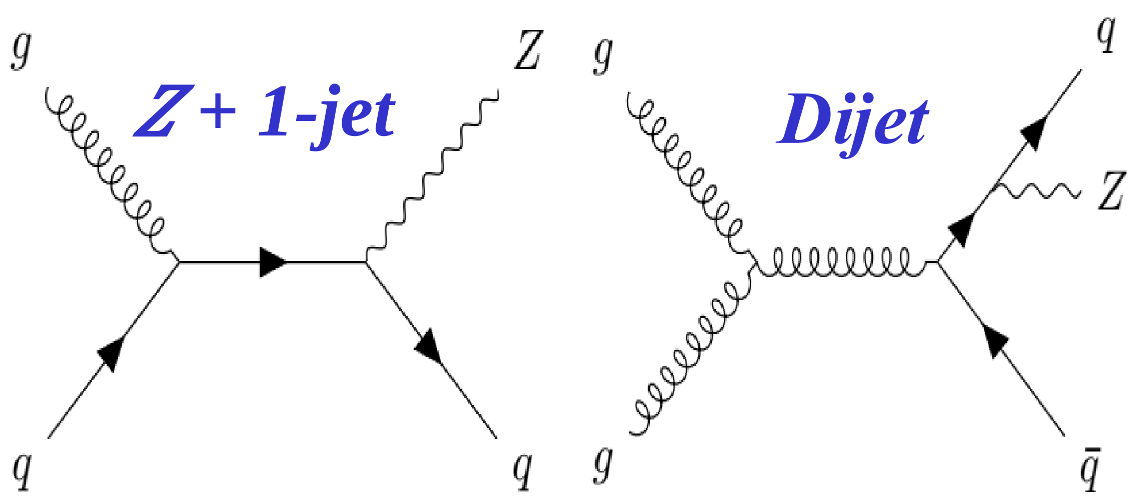

*Feynman diagrams for the production of a Z boson in association with **high-p_T jets***

- The ***Z* + 1-jet** events are expected to populate the **back-to-back** region where the *Z* boson is balanced against a ***single high-p_T jet***
- In ***dijet*** events, the ***Z* boson** is expected to be **radiated** from the quark leg, with kinematics leading *to small values* of the **angular distance** between the ***Z* boson** and the closest ***jet***, $\Delta R_{\min Z,j}$ and, therefore, populating the collinear region

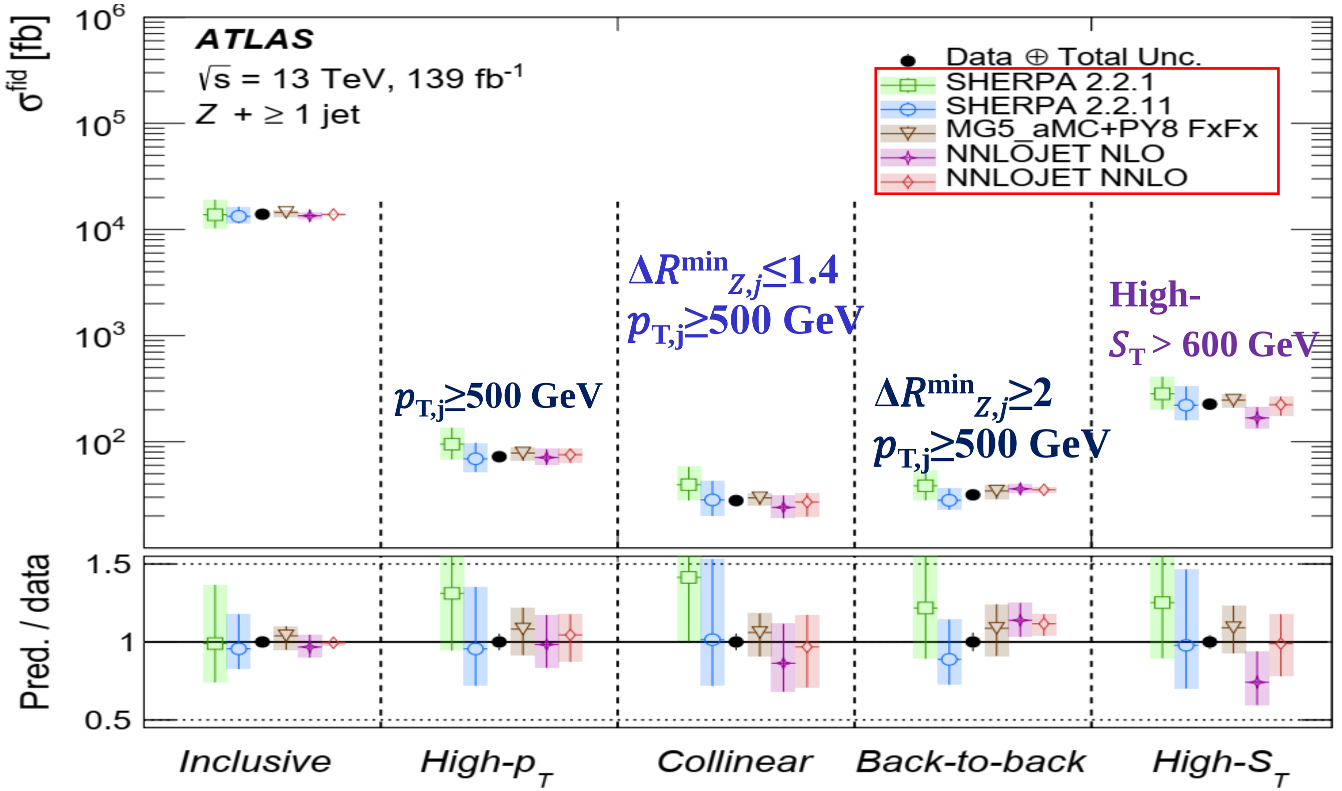

Summary of integrated fiducial cross-section results

- Data are compared with predictions from MC generators
- S_T is the scalar sum of the transverse momentum of all selected jets. ***High-S_T > 600 GeV***
- The ***collinear*** is for $\Delta R^{min}_{Z,j} \leq 1.4$
- The ***back-to-back*** regions is for $\Delta R^{min}_{Z,j} \geq 2.0$

$$S_T = \Sigma p_T^{jet} + \Sigma p_T^{l}$$

CROSS-SECTION $pp \to Z(\to e^+e^-, \mu^+\mu^-) + \geq 1$JET $+X$ #2

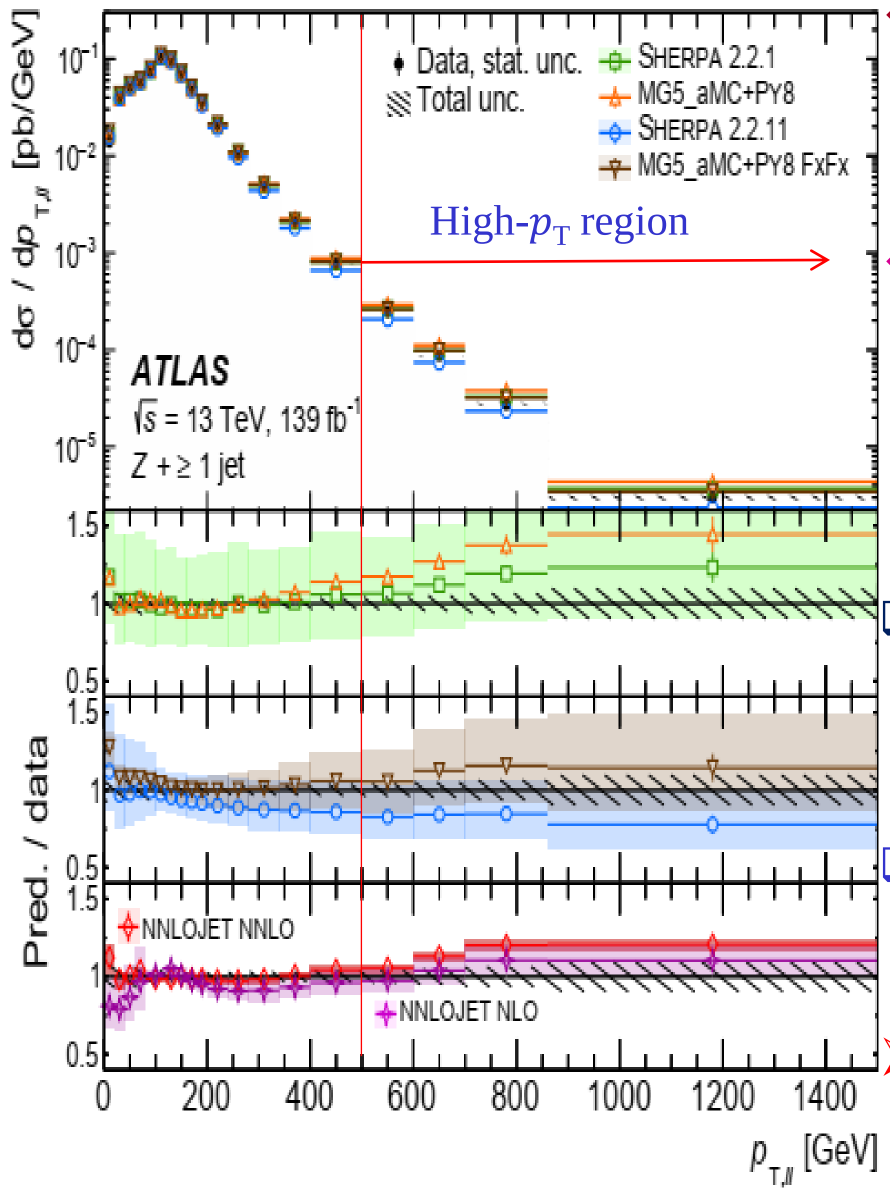

- The ***Z*-boson p_T** and **jet p_T** are observables of the ***Z* + jets process** and probe **perturbative QCD** over a wide range of scales
- Understanding the kinematics of **jets** in events with V-bosons produced in association with several jets is essential for the modelling of backgrounds for other SM processes & **searches beyond the SM**

- The ***high-$p_{T,Z}$*** region is dominated by the **back-to-back topology** and receives significant **negative corrections due to EW effects**
- In contrast, events with a ***high-p_T jet*** typically result in **both back-to-back and collinear topologies**

➢ The **NNLOjet@NNLO** predictions describe the data **very precisely**, except for **large values** of $p_{T,\ell\ell}$ ($p_{T,j1}$)

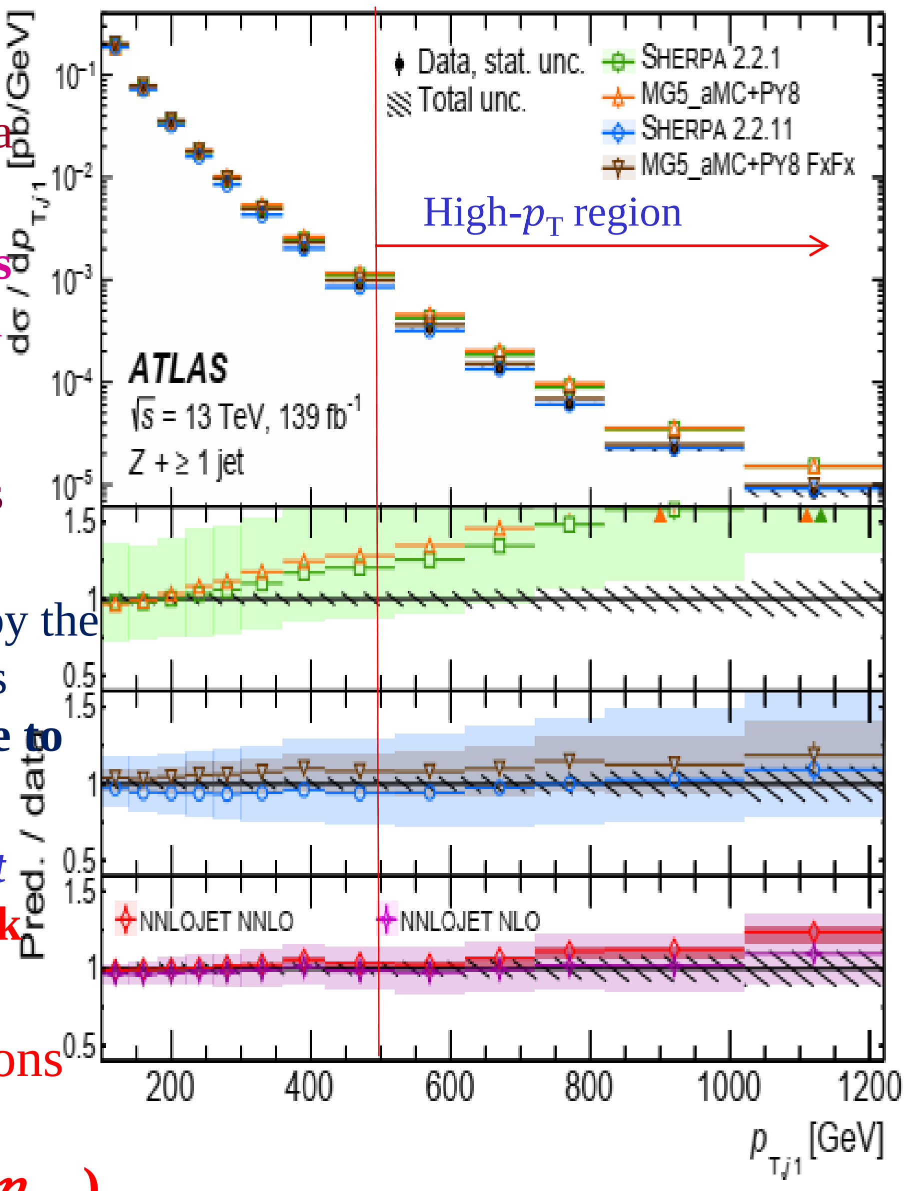

➢ Differential cross section as a function of the $p_{T,Z}$ and for **leading jet ($p_{T,j1}$)** in the inclusive region

Cross-section $pp \to Z(\to e^+e^-, \mu^+\mu^-)$ + large-radius jet + X #1

- **Heavy-flavor** partons in the initial state of a hard-scattering process are understood to **arise from gluon splittings** into $b\bar{b}$, $c\bar{c}$
- A ***high-mass new particle decaying*** into **resonances** naturally ***generates high-momentum merged jets***, and ***the high-momentum regime*** is particularly ***sensitive to modifications to SM*** dynamics by ***new physics***
- A **large-*R*-jet** is required as a proxy for a **high-p, hadronically decaying or splitting object** (high-energy gluon)

	Inclusive		2-tag	
	ee	*μμ*	*ee*	*μμ*
$Z+b\bar{b}$	324 ± 4	305 ± 4	163.8 ± 2.6	157.2 ± 2.5
$Z+c\bar{c}$	536 ± 10	530 ± 9	12.3 ± 1.8	19.3 ± 2.0
$Z+bc$	89 ± 2	81 ± 2	14.6 ± 1.2	12.1 ± 0.9
$Z+b$	2588 ± 13	2423 ± 12	14.8 ± 1.1	12.4 ± 1.3
$Z+c$	5073 ± 32	4862 ± 39	5.5 ± 1.3	6.9 ± 1.7
Z+light	53 808 ± 164	51 206 ± 145	9.4 ± 1.1	11.1 ± 1.5
$t\bar{t}$	5960 ± 46	5204 ± 43	82.7 ± 5.3	75.4 ± 5.6
W+jets	73 ± 4	7 ± 1	0.4 ± 0.1	< 0.1
Diboson	2042 ± 17	1834 ± 16	21.5 ± 1.4	20.7 ± 1.4
MC total	70 493 ± 175	66 452 ± 158	324.9 ± 6.8	315.1 ± 7.2
Data	66 481	65 034	391	384

Reconstruction-level event-selection yields in the *ee* & *μμ* channels from each process's MC sample (with **Sherpa 2.2.1** used for the ***Z*+jets** samples) and from collision data

- The **single-top process** was found to make a negligible contribution to all event selections and has been omitted
- **Multijet backgrounds were estimated to be negligible by a data-driven method**

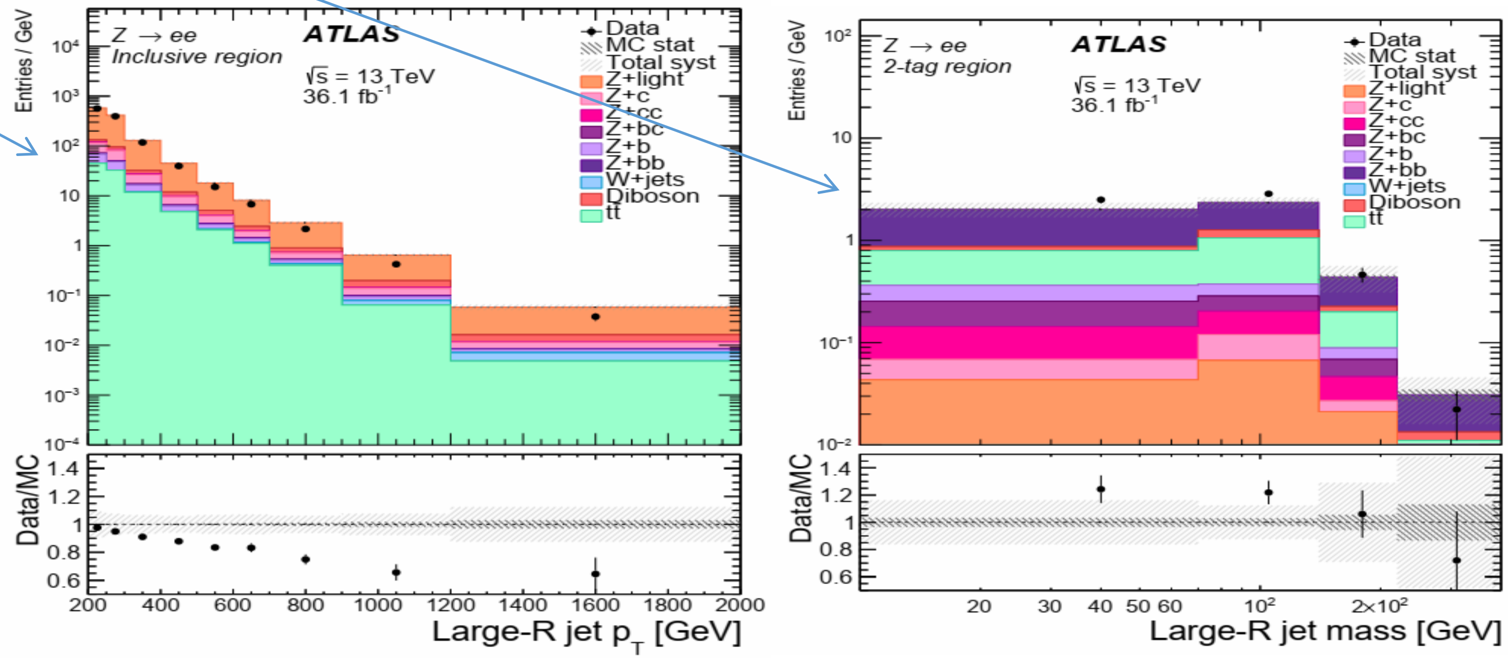

Selected reconstruction-level observables, compared with **pre-fit MC simulation** with **Sherpa 2.2.1** used for the ***Z*+jets** samples: the left shows the inclusive-selection *ee* **large-*R* jet p_T** and the **2-tag** selection ***ee* large-*R* jet mass** distributions

- The **2-tag** region was defined as a subset of **inclusive** with requiring "**the large-*R* jet contains exactly two *b*-tagged** subjets" (**highest-p_T** 2-tag **large-*R* jet** in the 2-tag selection)

Subject separation: the angular separation, $\Delta R(b, \bar{b})$, between 2 *b*-tagged subjets arXiv:2204.12355

CROSS-SECTION $pp \rightarrow Z(\rightarrow e^+e^-, \mu^+\mu^-)$ + LARGE-RADIUS JET+X #2

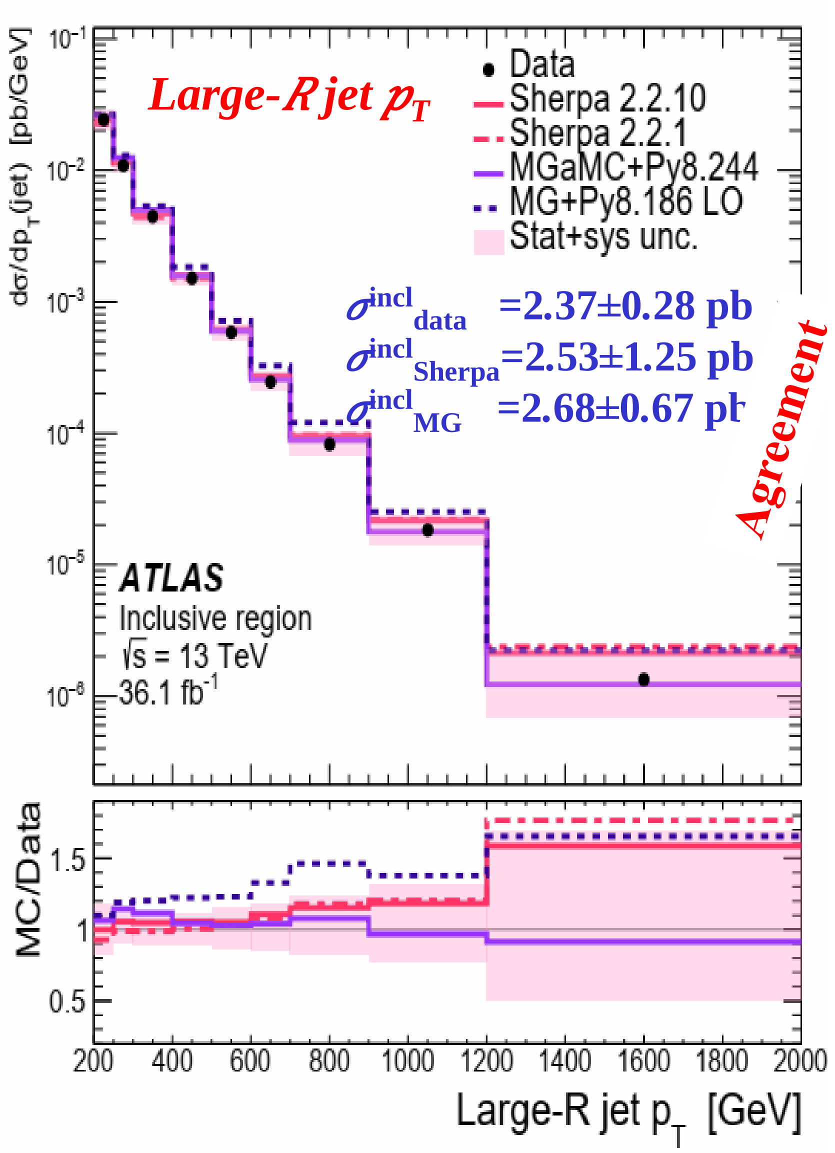

- The differential cross-sections indicate significant **mismodeling of QCD activity** in the **inclusive** event selection by MC models
- The **NLO Sherpa** and **LO MadGraph+ Pythia8** event generators **predicting greater** p_T and azimuthal decorrelation in the ***Z*+J system** than seen in the data. The **large-*R* jet** itself is consequently biased to higher p_T and mass values than in data, although to a lesser extent than the deviations in the ***Z*+J-system** observables
- **The NLO MadGraph5_aMC@NLO + Pythia8 model describes all distribution shapes well,** with only a small overestimate of the inclusive fiducial cross-section.
- All models somewhat overestimate this cross-section, with recent **Sherpa** versions providing the **best description**

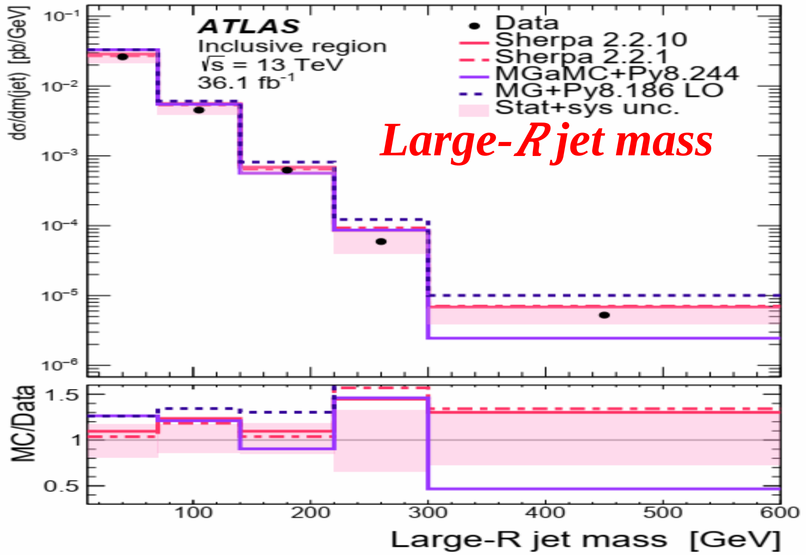

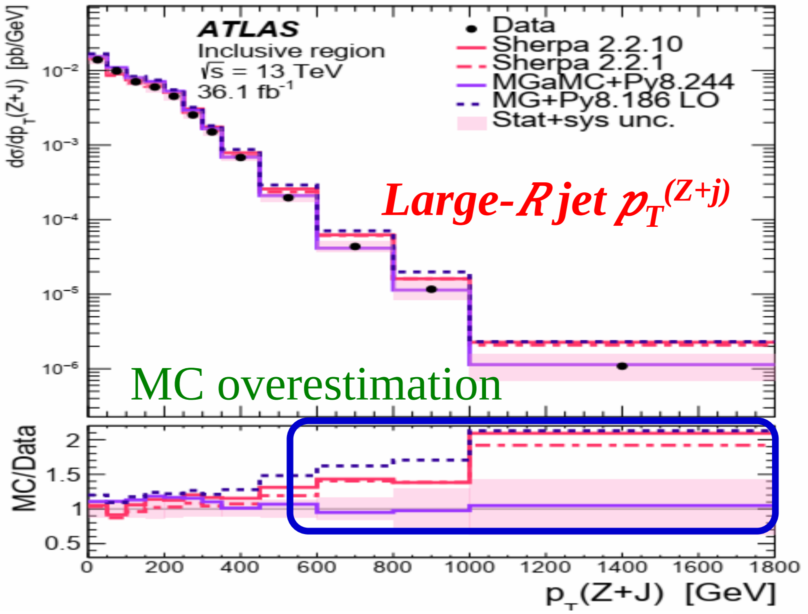

Particle-level differential cross-sections in *the inclusive event selection*. In the legend, **"MGaMC"** refers to **NLO** configurations of the **MadGraph5_aMC@NLO** generator, and **"MG"** to **LO MadGraph**, both run in conjunction with **Pythia 8**. All models are using the **"5FNS"** refer to the flavor-number scheme used. These are a significant background to important Higgs-boson searches.

arXiv:2204.12355

CROSS-SECTION $pp \to Z(\to e^+e^-, \mu^+\mu^-)$ + LARGE-RADIUS JET+X #3

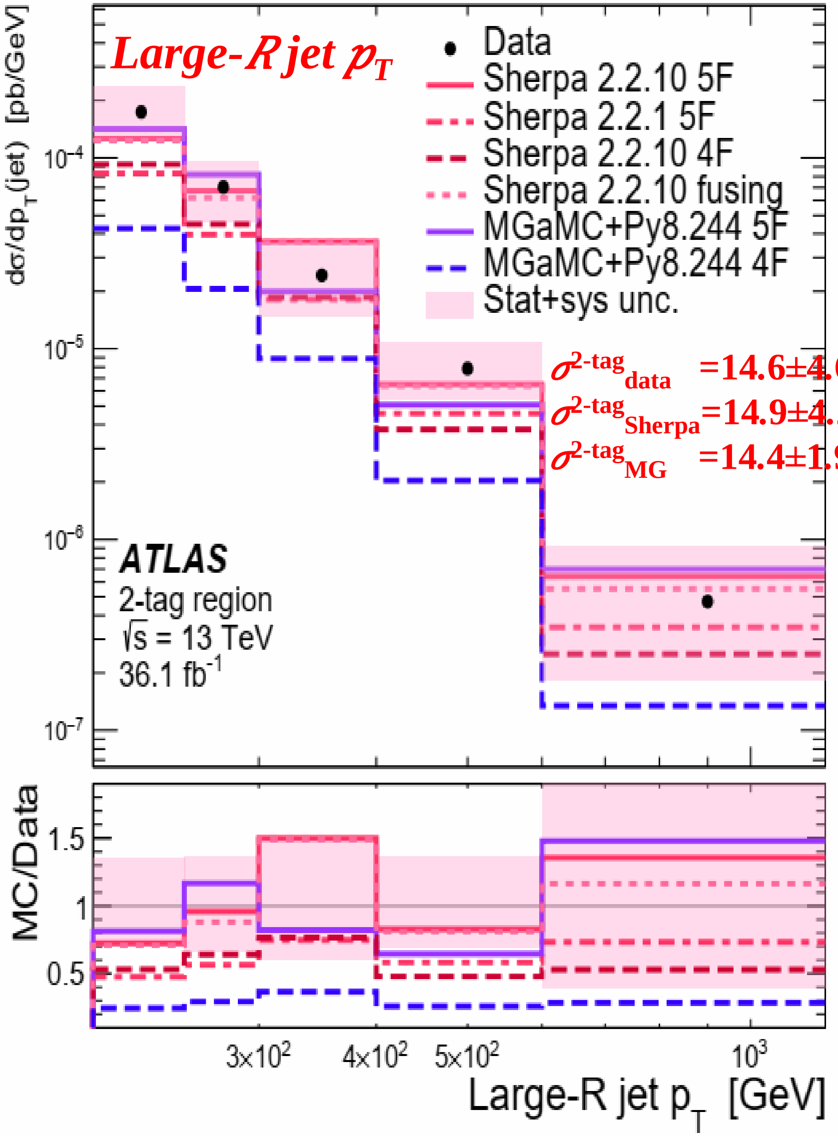

$\sigma^{2\text{-tag}}_{data}$ =14.6±4.6 fb
$\sigma^{2\text{-tag}}_{Sherpa}$ =14.9±4.2 fb
$\sigma^{2\text{-tag}}_{MG}$ =14.4±1.9 fb

- $\sigma^{2\text{-tag}}_{data}/\sigma^{incl}_{data}$=(0.62±0.12)%
  $\sigma^{2\text{-tag}}_{Sher}/\sigma^{incl}_{Sher}$=(0.59±0.39)%
  $\sigma^{2\text{-tag}}_{MG}/\sigma^{incl}_{MG}$=(0.54±0.21)% **Agreement**
- The 2-tag selection: there is good shape **agreement** between the data & MC models
- The strongest feature observed in this event-selection region is in normalization, with models using **four-flavor number scheme** (**4FNS**, **b-absent in PDF**) approach significantly **underestimating** the rate of ***bb̄*** **boosted-jet production**
- **Five-four-flavor number scheme (5FNS, with b)** approaches with modern tools **do much better** (**Sherpa 2.2.10 & MadGraph5_ aMC@NLO**) providing accurate predictions for the **2-tag** cross-section and the **ratio of 2-tag** to inclusive
- This results is important for future use of MC-derived **large-*R* jet** flavor composition in studies of the *VH*(*bb̄*) process

The **2-tag** region was defined as a subset of **inclusive** with requiring "**the large-*R* jet contains exactly two *b*-tagged subjets**"

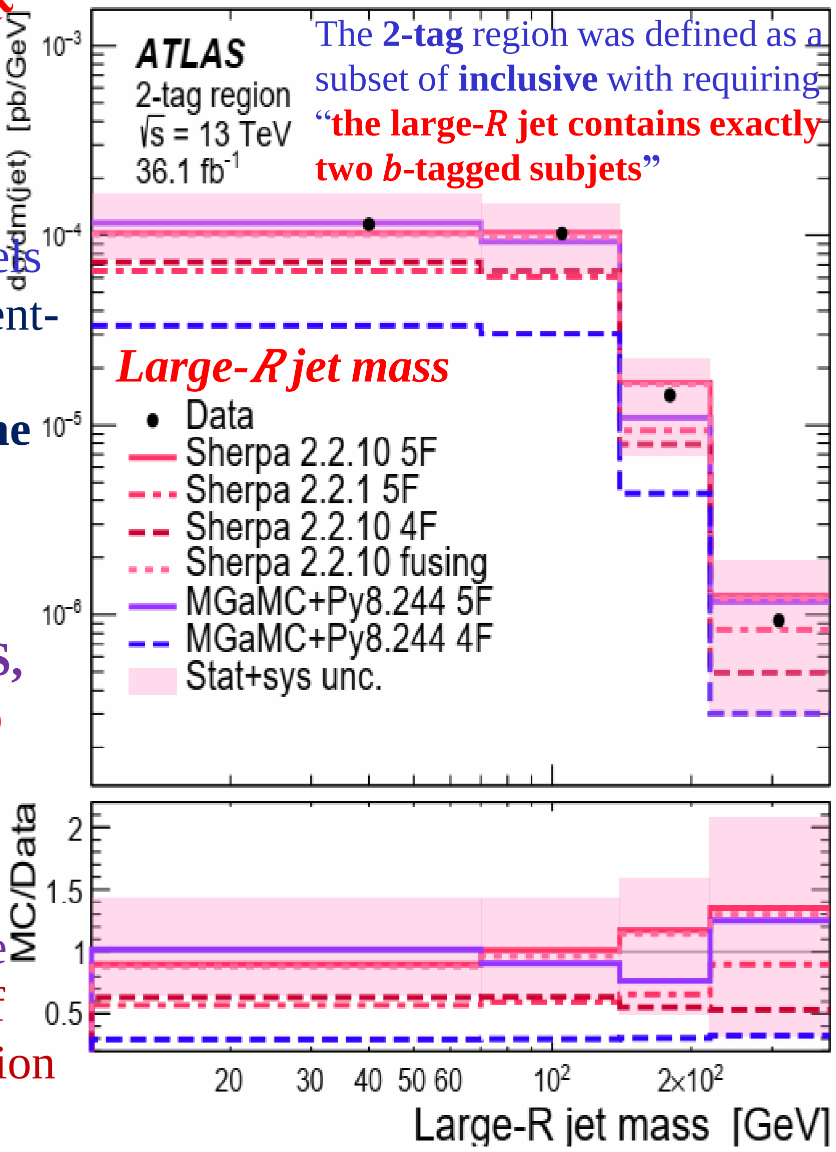

Particle-level differential cross-sections in *the 2-tag event selection*. In the legend, **"MGaMC"** refers to **NLO** configurations of the **MadGraph5_aMC@NLO** generator, and **"MG"** to **LO MadGraph**, both run in conjunction with **Pythia 8**. All models are using the **"4/5FNS"** refer to the flavor-number scheme used.

JHEP 12 (2021) 131
arXiv:2108.11650

B-quark fragmentation properties in jets: in the decay $B^{\pm}\rightarrow J/\psi K^{\pm}\rightarrow\mu^{+}\mu^{-}K^{\pm}$

- The fragmentation of **heavy quarks** is a **crucial** aspect of QCD
- Detailed studies and precision measurements of the heavy-quark fragmentation properties allow a **deeper underst. of QCD**
- **The fragmentation properties of jets containing *b*-hadrons are studied using $B^{\pm}\rightarrow J/\psi K^{\pm}$ in *pp* collisions, with $J/\psi\rightarrow\mu^{+}\mu^{-}$**
- The measurement determines the $\boldsymbol{p_L}$ and $\boldsymbol{p_T}$ profiles of the reconstructed ***B*** hadrons with respect to the axes of the ***jets*** to which they are geometrically associated

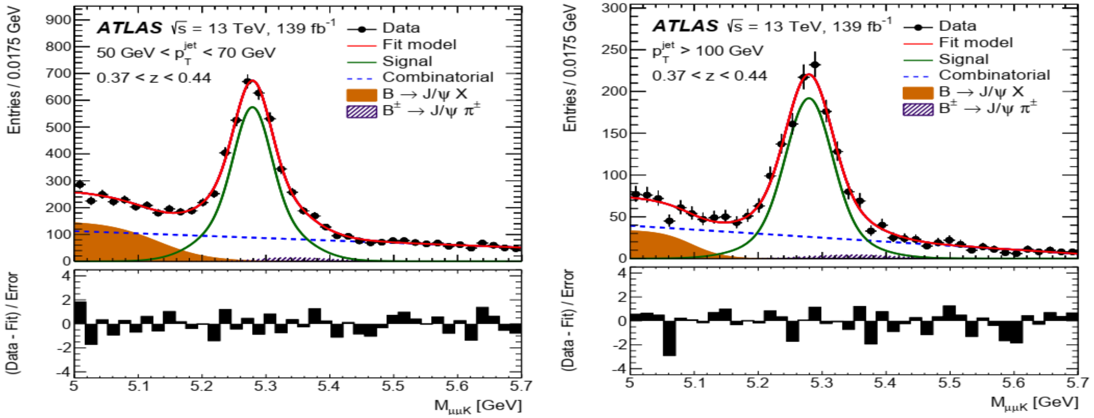

Fits to the invariant mass distributions of $B^{\pm}$ candidates for 0.37<z< 0.44

The provides key measurements which help to **better understand the fragmentation functions of heavy quarks:**

- **Significant differences** among **different MC models** are **observed**, and also **between the models and the data**
- Some of the discrepancies are understood to arise from poor modelling of the $\boldsymbol{g\rightarrow b\bar{b}}$ splittings, **to which the present analysis has substantial sensitivity**
- Including the present measurements in a **future tune** of the MC predictions **may help to improve the description** and **reduce the theoretical uncertainties** of processes where **heavy-flavour** quarks are present **in the final state**, ***such as top quark pair production or Higgs boson decays into heavy quark pairs***

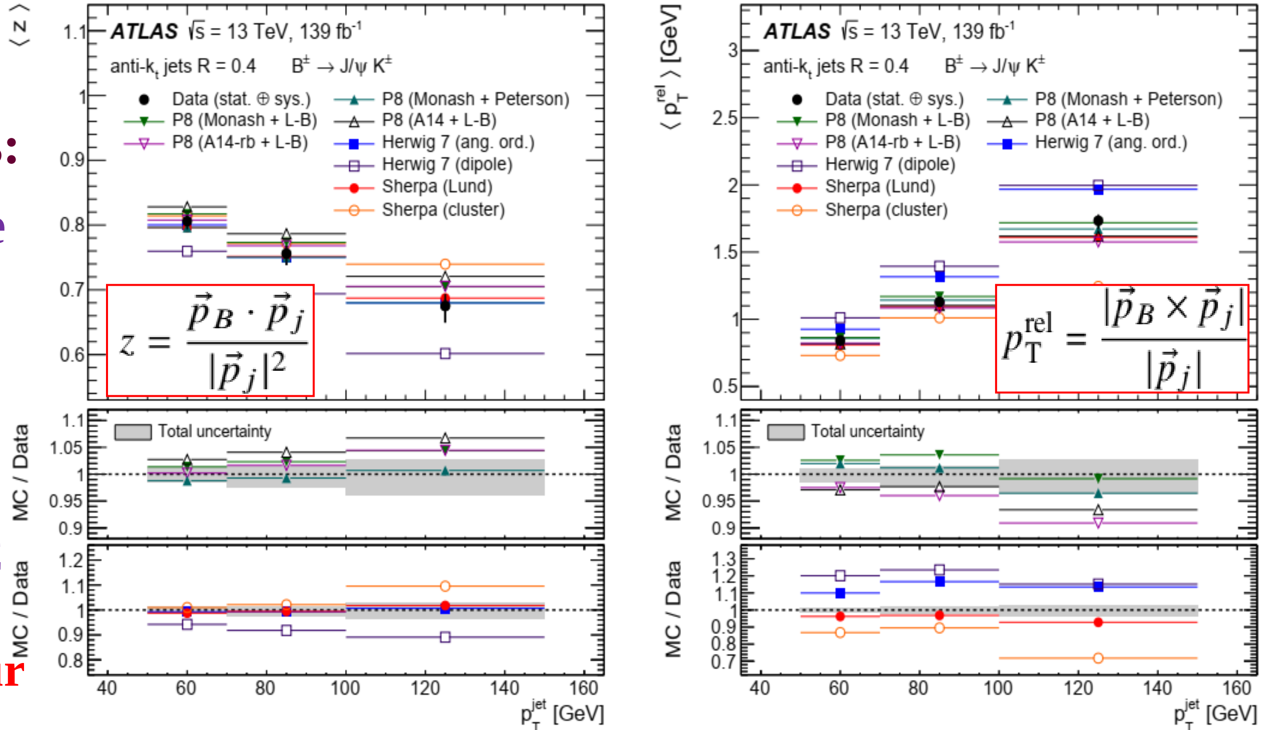

Average values of the longitudinal profile $\langle z\rangle$ and of the transverse profile $\langle p_T^{rel}\rangle$ as a function of the $p_T^{\ jet}$

FORWARD PROTON SCATTERING: $pp \to p(\gamma\gamma \to \ell^+\ell^-)\, p^{(*)}$

- The observation of ***forward p*** scattering with **2 leptons** ($e^+e^-/\mu^+\mu^-$) produced via **photon fusion**
- The scattered **proton** is detected by **Forward Proton Spectrometer** while the $\ell^+\ell^-$ are reconstructed by the **Central Detector**
- The **57 (123)** ***ee*** **(*μμ*)** data event candidates in the **dilepton rapidity** $y_{\ell\ell}$ **vs** $m_{\ell\ell}$ plane satisfying even selection and kinematic matching
- **Proton-tagging techniques are introduced for X-section measurements**

$$\sigma_{ee+p}^{\text{fid}} = 11.0 \pm 2.6\ (\text{stat}) \pm 1.2\ (\text{syst}) \pm 0.3\ (\text{lumi})\ \text{fb}$$
$$\sigma_{\mu\mu+p}^{\text{fid}} = 7.2 \pm 1.6\ (\text{stat}) \pm 0.9\ (\text{syst}) \pm 0.2\ (\text{lumi})\ \text{fb}$$

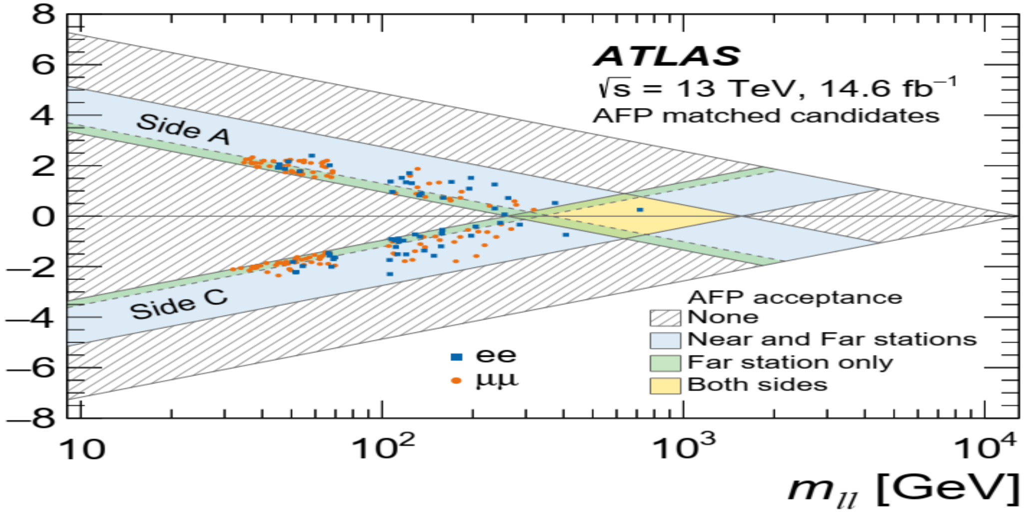

$\sigma_{\text{HERWIG+LPAIR}} \times S_{\text{surv}}$	$\sigma^{\text{fid.}}_{ee+p}$ (fb)	$\sigma^{\text{fid.}}_{\mu\mu+p}$ (fb)
$S_{\text{surv}} = 1$	15.5 ± 1.2	13.5 ± 1.1
S_{surv} using Refs. [33, 34]	10.9 ± 0.8	9.4 ± 0.7
SUPERCHIC 4 [97]	12.2 ± 0.9	10.4 ± 0.7
Measurement	11.0 ± 2.9	7.2 ± 1.8

Agreement

- $pp \to p(\gamma\gamma \to \ell^+\ell^-)\, p^{(*)}$ is observed with a significance exceeding 5σ in both the e^+e^-+p & $\mu^+\mu^-+p$ final states
- These results demonstrate that the **ATLAS Forward Proton** spectrometer performs well in high-luminosity data taking
- Proton tagging is introduced for cross-section measurements of **photon fusion processes** at the electroweak scale

➢ Compares X-sections with the combined **HERWIG+LPAIR** predictions assuming unit **soft-survival factors** $S_{\text{surv}}=1$

➢ Soft-survival effects are included using an $m_{\ell\ell}$**-dependent** reweighting of these predictions to S_{surv} calculated **for exclusive** processes; **LPAIR** predictions are additionally **scaled down by 15%** to account for S_{surv} being lower for single-dissociative processes. **SUPERCHIC4** predictions include **full kinematic dependence** on S_{surv} for exclusive, single-, and double-dissociative processes.

BOSE-EINSTEIN CORRELATION VS. MULTIPLICITY

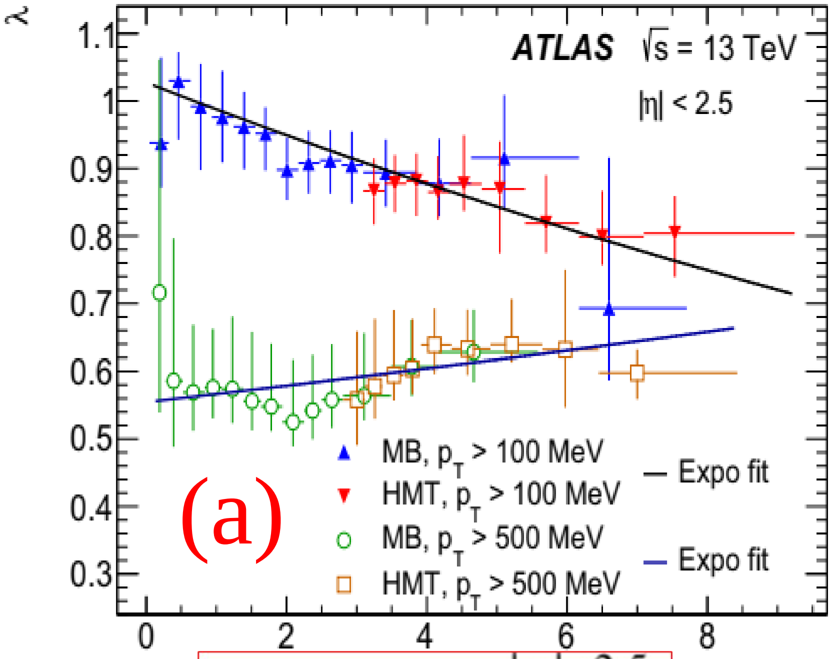

$$m_{ch} \equiv n_{ch} / \langle n_{ch}^{|\eta|<2.5} \rangle$$

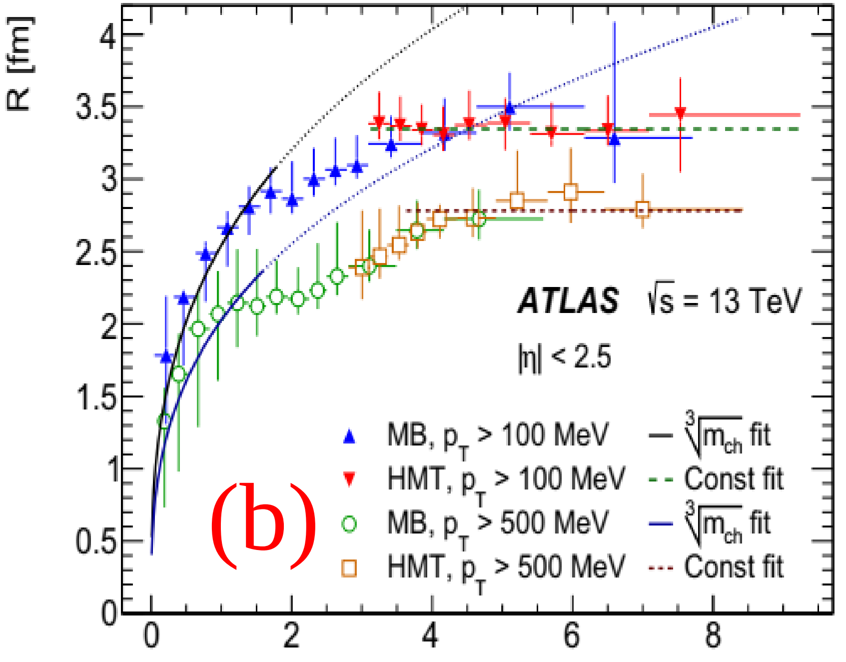

$$\langle n_{ch}^{|\eta|<2.5} \rangle = 5 \langle dn_{ch}/d\eta|_{|\eta|<0.2} \rangle$$

- The dependence of the $\lambda(m_{ch})$ on rescaled multiplicity obtained from the exponential fit of the $R_2(Q)$ correlation functions for tracks with p_T>100 MeV and p_T>500 MeV at $\sqrt{s}$=13 TeV for MB & HMT data.
- The dependence of the $R(m_{ch})$ on m_{ch}. The uncertainties represent the sum in quadrature of the statistical and asymmetric systematic contributions.

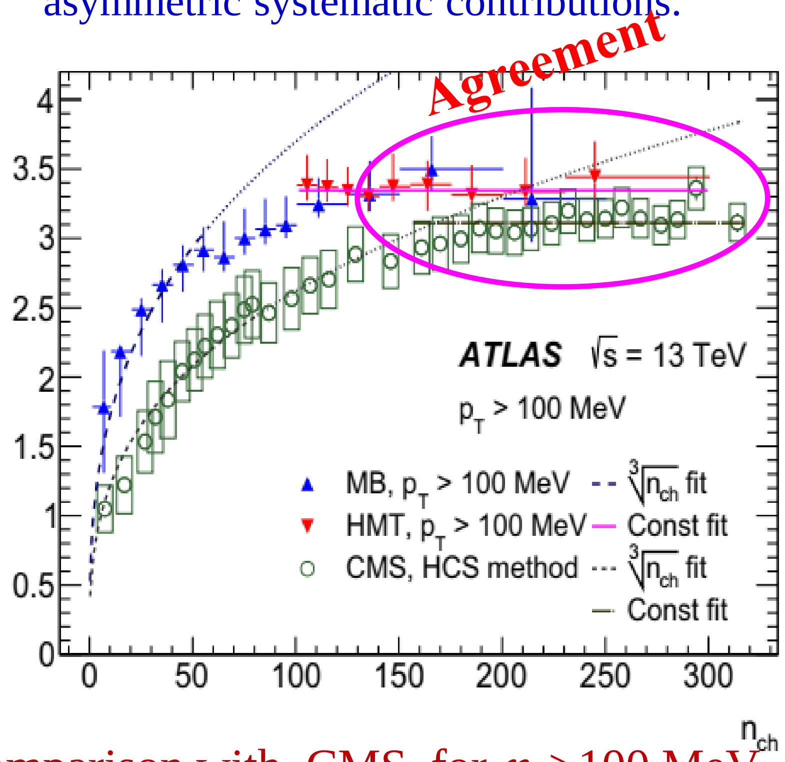

Comparison with CMS for p_T>100 MeV and $|\eta|$ < 2.4.

- The parameter $R(m_{ch})$ is found to increase as $\boldsymbol{a m_{ch}^{0.33}}$ for multiplicity up to $m_{ch}\approx 2$: p_T>100 MeV, $a=2.54^{+0.12}_{-0.22}$ fm
- For $\boldsymbol{m_{ch} \geq 3}$, the source radius R **saturates** at a value $\boldsymbol{R=3.35^{+0.20}_{-0.09}}$ **fm**
- Results indicate a direct dependence of R on the p_T threshold
- The parameter $\lambda(m_{ch})$ decreases with multiplicity for the lower p_T threshold and is lower for the higher p_T threshold but increases slightly with multiplicity
  - The behaviour of R is qualitatively similar.
  - There is a clear difference in the results at **low n_{ch}**.

BEC PARAMETERS VS MULTIPLICITY #3

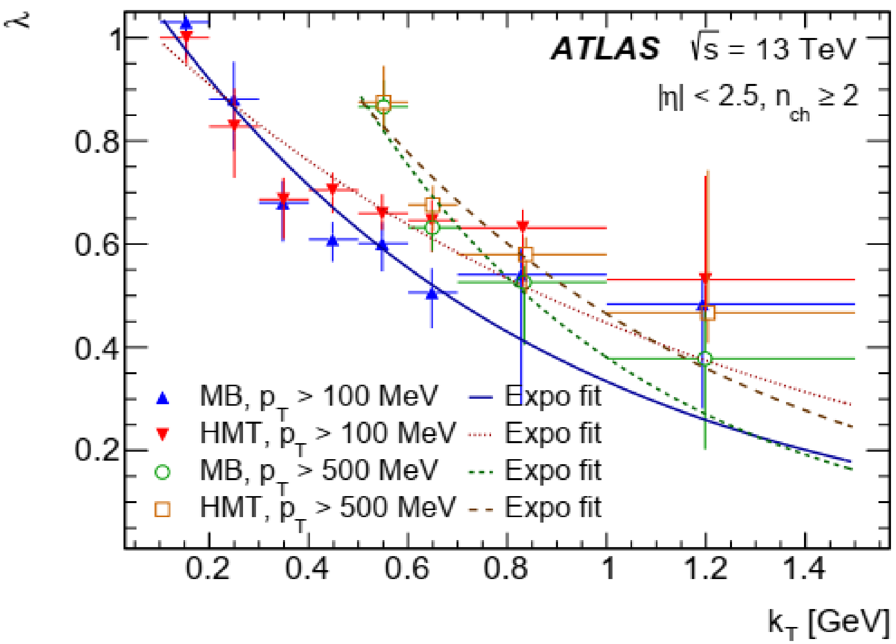

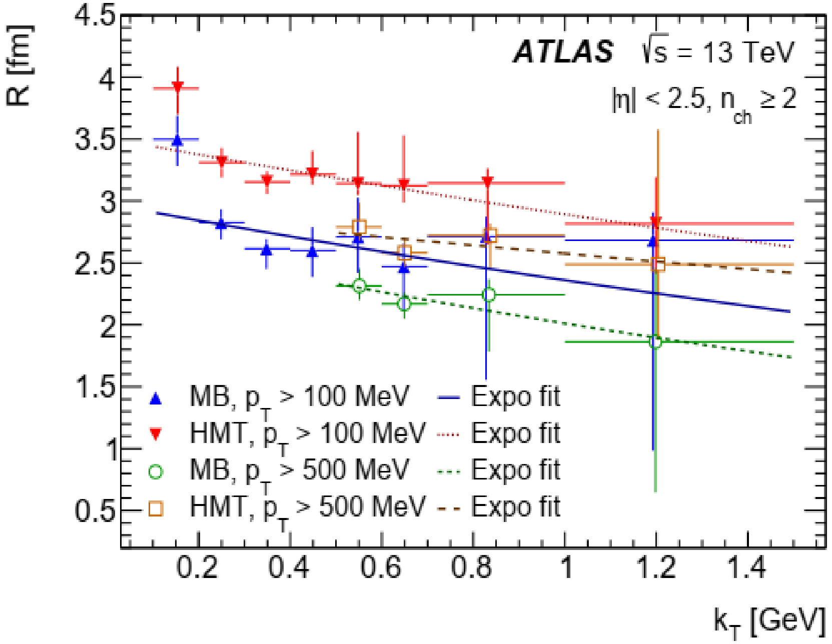

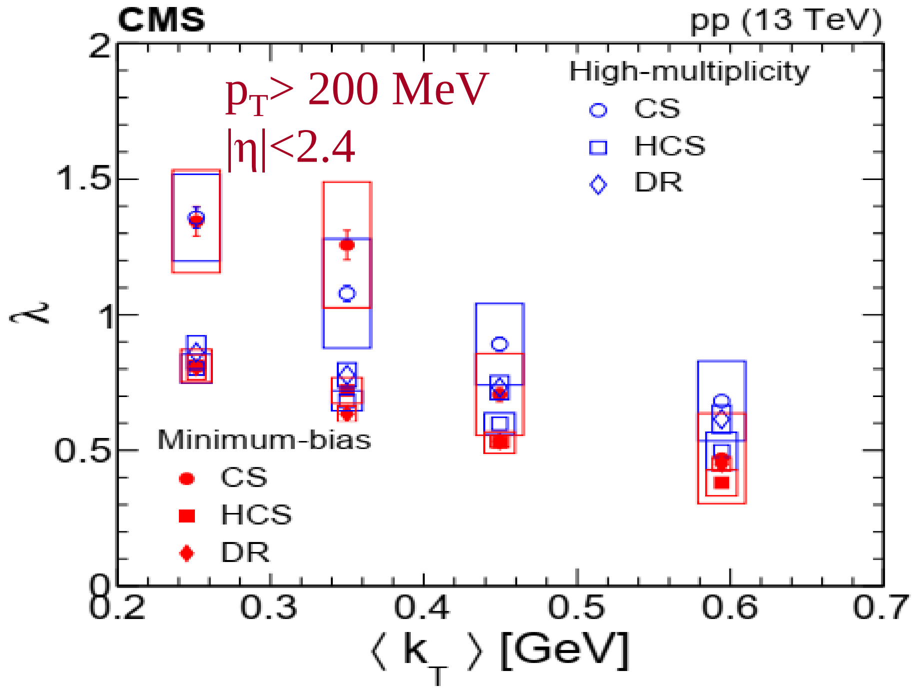

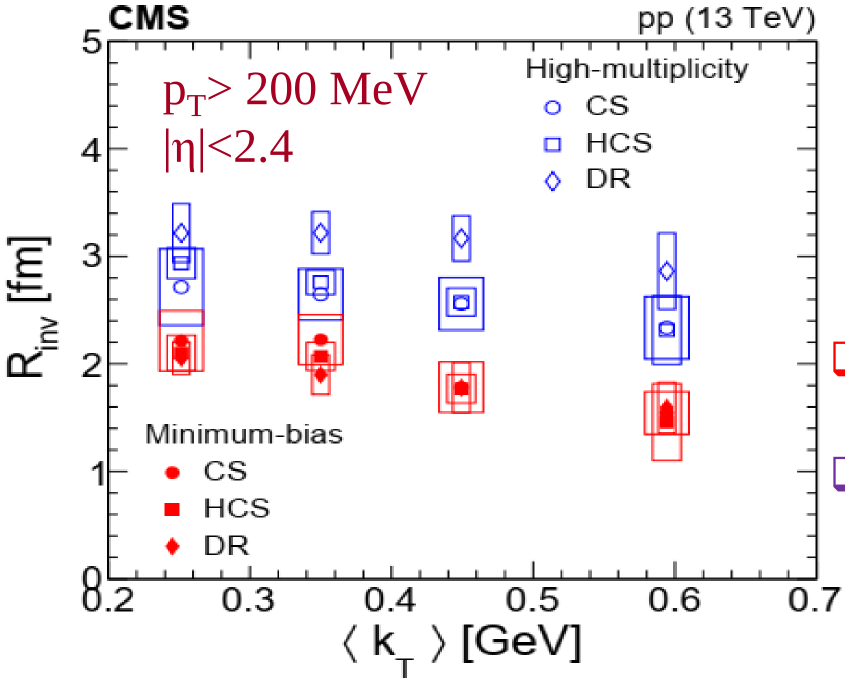

- **ATLAS:** The k_T dependence of the correlation strength, $\lambda(k_T)$, and the source radius, $R(k_T)$, obtained from the exponential fit to the $R_2(Q)$ correlation functions for events with multiplicity $n_{ch} \geq 2$ and transfer momentum of tracks with p_T>100 MeV and p_T>500 MeV at 13 TeV for the minimum-bias (MB) and high-multiplicity track (HMT) events.
- The uncertainties represent the sum in quadrature of the statistical & systematic contributions.
- The curves represent the exponential fits to $\lambda(k_T)$ and $R(k_T)$.

- **CMS**: Results for R_{inv} and λ from the three methods as a function of k_T
- In the lower plots, statistical & systematic uncertainties are shown as error bars and open boxes, respectively

BONUS:: MEASUREMENT OF THE W BOSON MASS: 7σ FROM SM PREDICTION

CDF II Collaboration, High-precision measurement of the W boson mass with the CDF detector. ***PoS* ICHEP2022 (2022) 898**

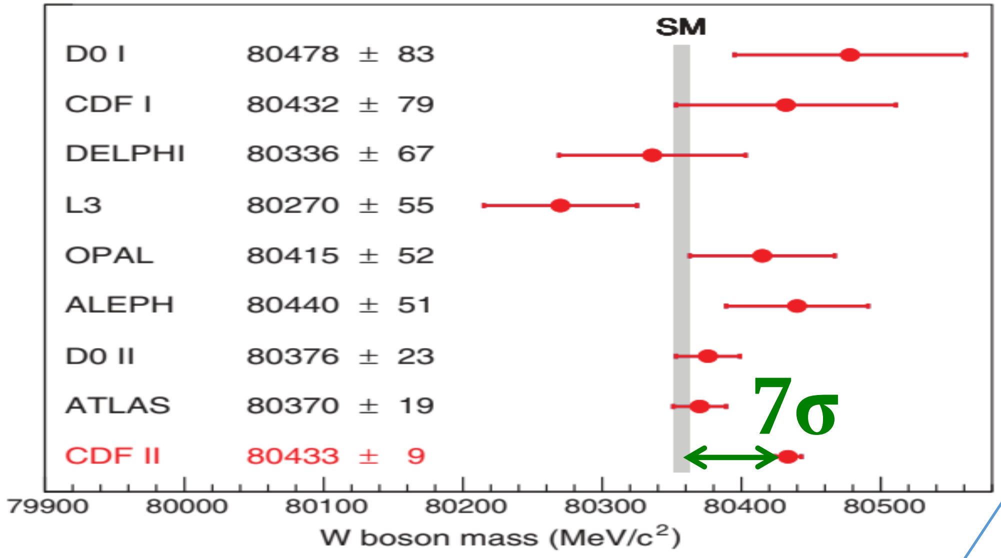

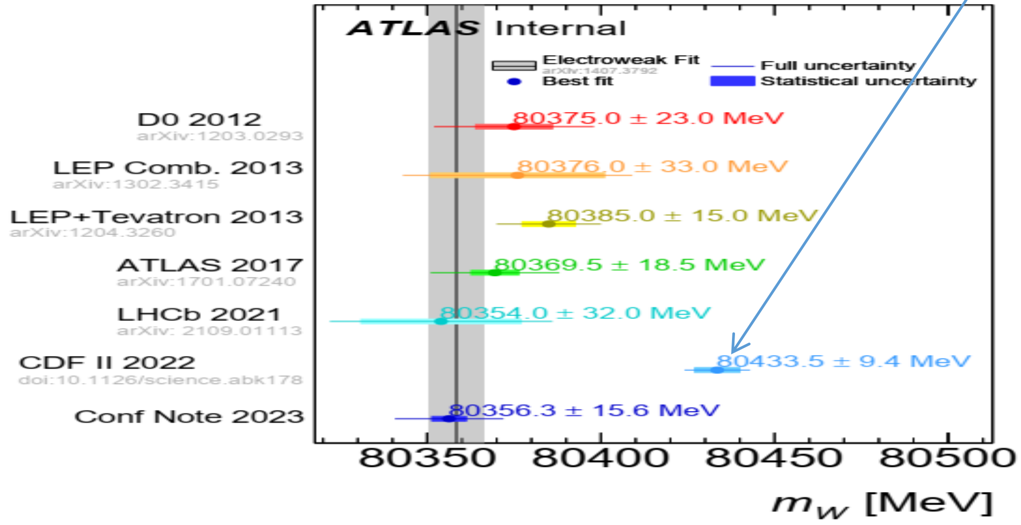

The ATLAS Collaboration has reported a measurement

M_W=80370±7 (stat)±11(syst)±1(mod. syst)=80370±19 MeV

M_W=80356±5 (stat)±15(syst) =80356±16 MeV

- **CDF II** measure the W boson mass, M_W, using data corresponding to **8.8 fb^{-1}** collected in proton-antiproton collisions at a **1.96 TeV** with the CDF II detector at the Fermilab Tevatron collider. A sample of approximately 4x10^6 **W** boson is used to obtain **M_W=80433.5±6.4(stat) ±6.9(syst) =80433.5±9.4 MeV.** The ***W*** bosons are identified using their decays to ***eν*** & ***μν*** and the mass is measured by fitting template distributions of transverse momentum and mass: $m_T = \sqrt{2p_T^{\ell}p_T^{\nu}(1-\cos\Delta\phi)}$
- A comparison with the **SM expectation** of **M_W=80357±6 MeV,** treating the quoted uncertainties as independent, yields a difference with a significance of **7σ.** The suggests are:
  - **the improvements to the SM calculation or**
  - **of extensions to the SM**
- SM result includes the published estimates of the uncertainty (4 MeV) due to missing higher-order quantum corrections and the uncertainty (4 MeV) from other global measurements used as input to the calculation
  - **ATLAS Collaboration**, Measurement of the *W*W-boson mass in pp collisions at √s =7 TeV with the ATLAS detector, **EPJ C 78, 110 (2018), EPJ C 78, 898 (2018), arXiv:1701.07240;** A measurement of the mass of the W boson is presented based on proton–proton collision data recorded in 2011 at a **7 TeV** with the **ATLAS** detector at the LHC, and corresponding to **4.6 fb^{-1}** of integrated luminosity. The selected data sample consists of 7.8×10^6 candidates in the ***W→μν*** channel and 5.9×10^6 candidates in the ***W→eν*** channel.

ATLAS/CMS: Run-2 at 13 TeV **is 139/137 fb^{-1}**

CONCLUSIONS

1. Many new SM results with the latest Run 2 dataset by the ATLAS and the CMS Collaborations were published
2. Measurement SM processes cross sections over 15 orders of magnitude
3. Comparison of the measurement SM processes to theory expectations
4. Evidence or Observation of rare processes
5. The most precise measurement of the total cross section pp-interactions
6. Observation of the BEC radius saturation for very high multiplicity

List of the SM papers:

CMS Collaboration: https://twiki.cern.ch/twiki/bin/view/CMSPublic/PhysicsResultsSMP

ATLAS Collaboration: https://twiki.cern.ch/twiki/bin/view/AtlasPublic/StandardModelPublicResults


Thank You
Very Much
For Attention!

BACKUP SLIDES

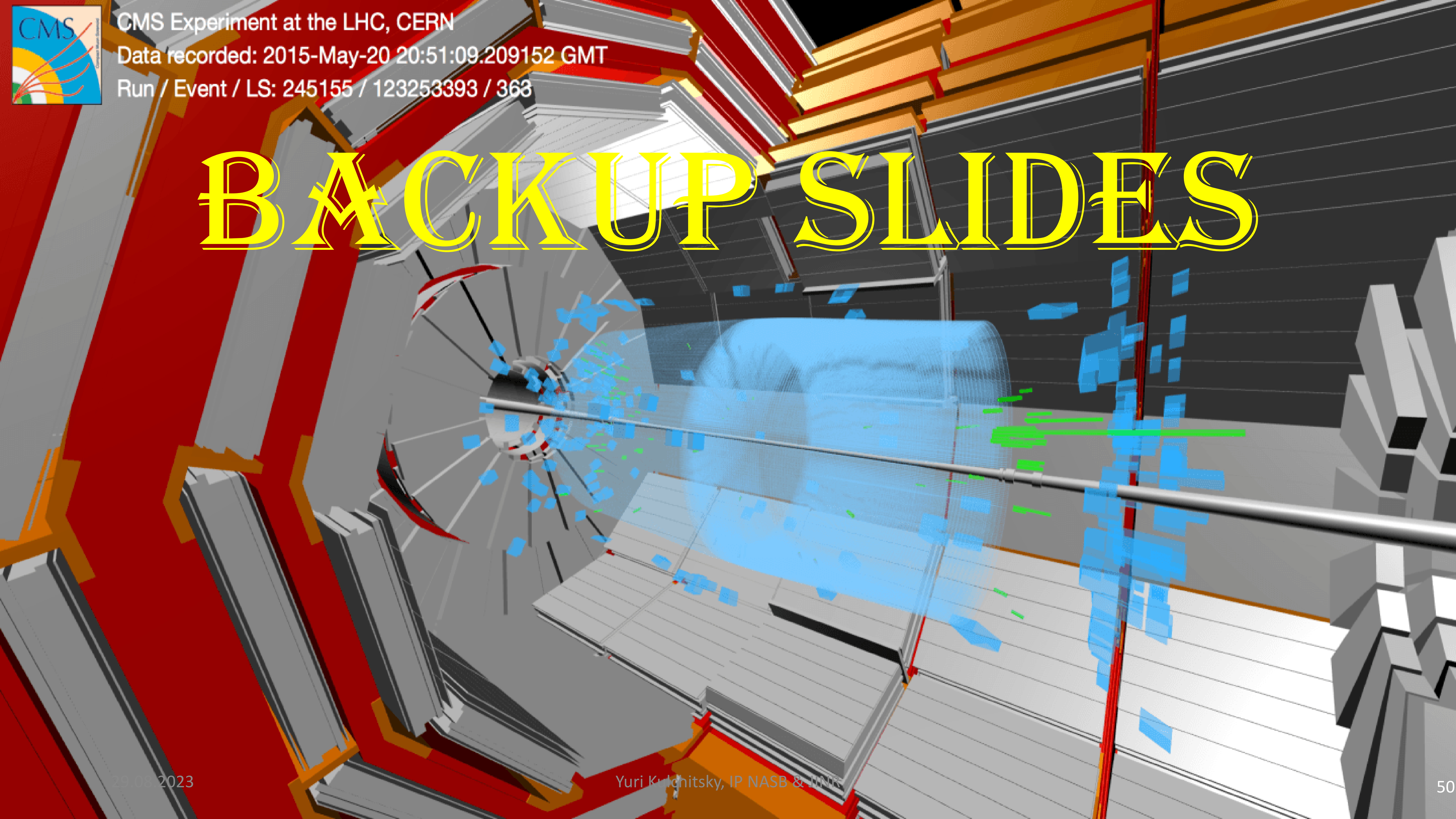

STANDARD MODEL: LAGRANGIAN

- **The Quantum chromodynamics sector** (QCD) sector defines the **interactions between quarks and gluons**, which is a Yang–Mills gauge theory with SU(3) symmetry. Since **leptons do not interact with gluons**, they are not affected by this sector. The Dirac Lagrangian of the quarks coupled to the gluon fields is given by

$$\mathcal{L}_{\rm QCD} = \sum_\psi \bar{\psi}_i \left(i\gamma^\mu (\partial_\mu \delta_{ij} - i g_s G^a_\mu T^a_{ij}) \right) \psi_j - \frac{1}{4} G^a_{\mu\nu} G^{\mu\nu}_a ,$$

ψ_i is the Dirac spinor of the quark field, where i={r, g, b} represents color,
γ_μ are the Dirac matrices,
G^a_μ is the 8-component (a =1,2,…,8) SU(3) gauge field,
T^a_{ij} are the 3×3 Gell-Mann matrices, generators of the SU(3) color group,
$G^a_{\mu\nu}$ represents the gluon field strength tensor,
g_s is the strong coupling constant.

- **The Electroweak sector** is a Yang–Mills gauge theory with the symmetry group U(1) × SU(2)$_L$,

$$\mathcal{L}_{\rm EW} = \sum_\psi \bar{\psi}\gamma^\mu \left(i\partial_\mu - g' \frac{1}{2} Y_{\rm W} B_\mu - g \frac{1}{2} \vec{\tau}_{\rm L} \vec{W}_\mu \right) \psi - \frac{1}{4} W^{\mu\nu}_a W^a_{\mu\nu} - \frac{1}{4} B^{\mu\nu} B_{\mu\nu},$$

B_μ is the U(1) gauge field,
Y_W is the weak hypercharge – the generator of the U(1) group,
W_μ is the 3-component SU(2) gauge field,
τ_L are the Pauli matrices – infinitesimal generators of the SU(2) group – with subscript L to indicate that they only act on left-chiral fermions,
g' and g are the U(1) and SU(2) coupling constants respectively,
$W^a_{\mu\nu}$ (a=1,2,3) and $B^{\mu\nu}$ are the field strength tensors for the weak isospin and weak hypercharge fields.

- **Higgs sector:** In the Standard Model, the Higgs field is a complex scalar of the group SU(2)$_L$:

$$\mathcal{L}_{\rm H} = \left| \left(\partial_\mu + \frac{i}{2} \left(g' Y_{\rm W} B_\mu + g \vec{\tau} \vec{W}_\mu \right) \right) \varphi \right|^2 - \frac{\lambda^2}{4} (\varphi^\dagger \varphi - v^2)^2 .$$

- **Yukawa sector:** The Yukawa interaction terms are

$$\mathcal{L}_{\rm Yukawa} = \overline{U}_{\rm L} G_{\rm u} U_{\rm R} \varphi^0 - \overline{D}_{\rm L} G_{\rm u} U_{\rm R} \varphi^- + \overline{U}_{\rm L} G_{\rm d} D_{\rm R} \varphi^+ + \overline{D}_{\rm L} G_{\rm d} D_{\rm R} \varphi^0 + {\rm h.c.},$$

JET PHYSICS IN PP-COLLISIONS MC MODELS

Jets are crucial for understanding of the SM. *Probing of the QCD → Jets are the result of fragmentation of partons produced in a scattering process*

In High-Energy Particle collisions – *two main phases:*

- ❑ **Perturbative phase**: **partons with *high-transverse momentum* are produced in a hard-scattering process at a scale Q**
- ❑ **Non-perturbative phase**: **partons convert in hadrons *emitting gluons and $q\bar{q}$-pairs* an interplay between *Hadronization Process (HP) and Underlying Event (UE):***

- ➢ **Hadronization Process**: ***transition from partons to hadrons***
- ➢ **Underlying Event**:
  - ❑ ***initial-state radiation (ISR);***
  - ❑ ***final-state radiation (FSR);***
  - ❑ ***multiple-parton interactions;***
  - ❑ ***colour-reconnection effects***

- ❖ ***Effects of HP and UE depend on Jet radius parameter and are most pronounced at low p_T***
- ❖ ***All these aspects of high energy collisions can be Probed in the Jet Physics***

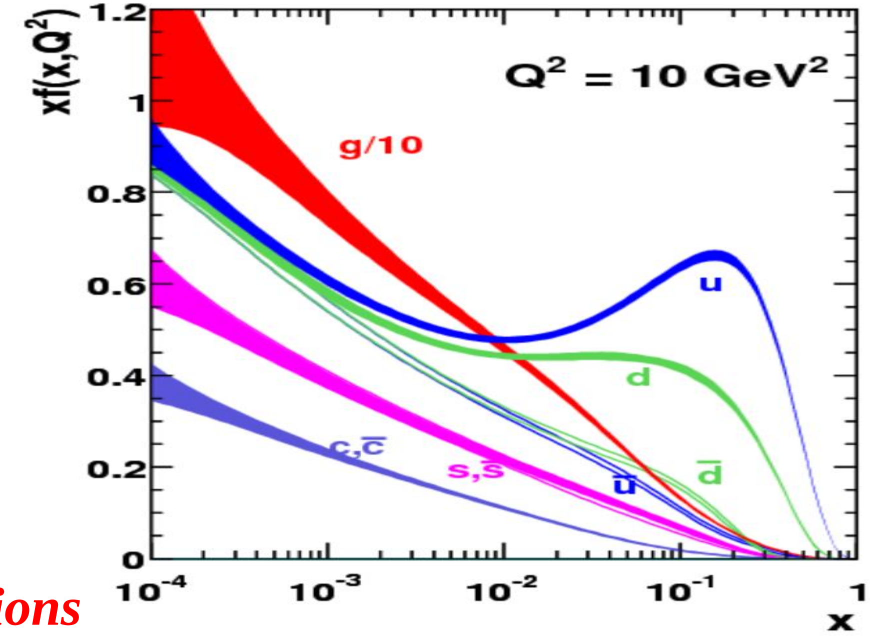

Parton density functions (PDF)

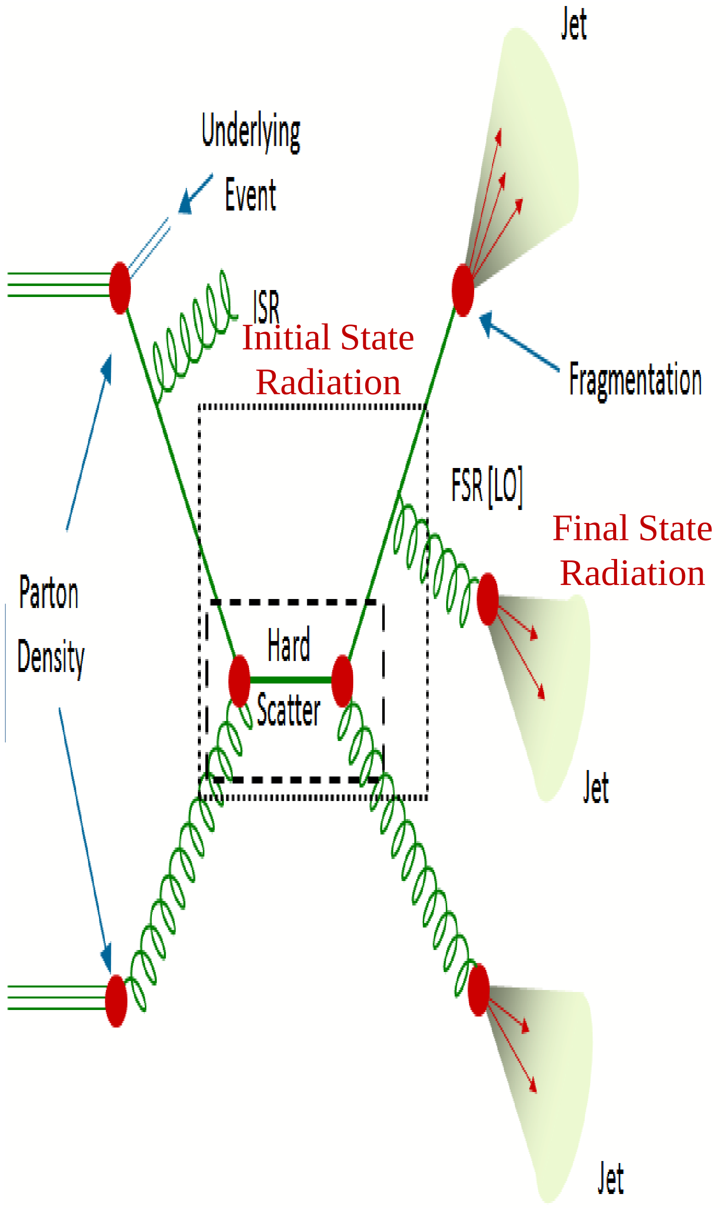

EXAMPLE: JETS MC MODELS

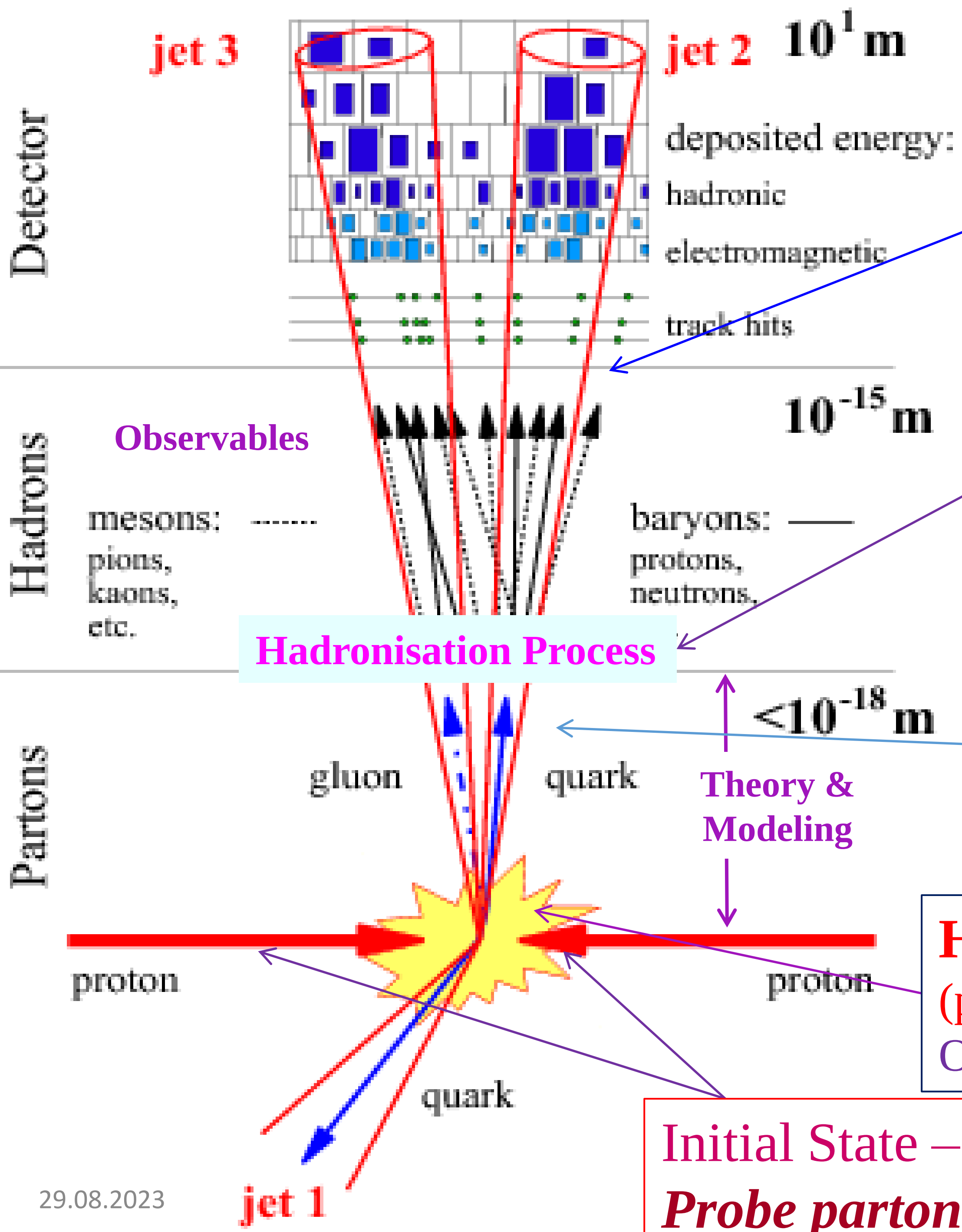

Jets: *narrow collimated clusters of stable particles produced by the fragmentation of a hard parton*

Probe highest p_T → best handles on searches for new physics

Parton fragmentation

- **Phenomenological models (*PYTHIA*, *HERWIG*, ...)**
- Matching to fixed order

Parton shower (PS)

- Soft- and collinear approximations
- Mismatch between kinematics of virtual and real corrections: *soft-gluon resummation*

Hard scattering – perturbative Quantum ChromoDynamics (pQCD) predictions at fixed-orders QCD calculations: Leading Order (LO), Next–to–LO (NLO), Next–to–Next–to–LO (NNLO)

Initial State – **Parton Distribution Functions (PDFs)**

Probe parton substructure → test QCD through wide energy range

INNER DETECTORS (ID)

ATLAS tracking detectors:
Pixels, SCT & TRT

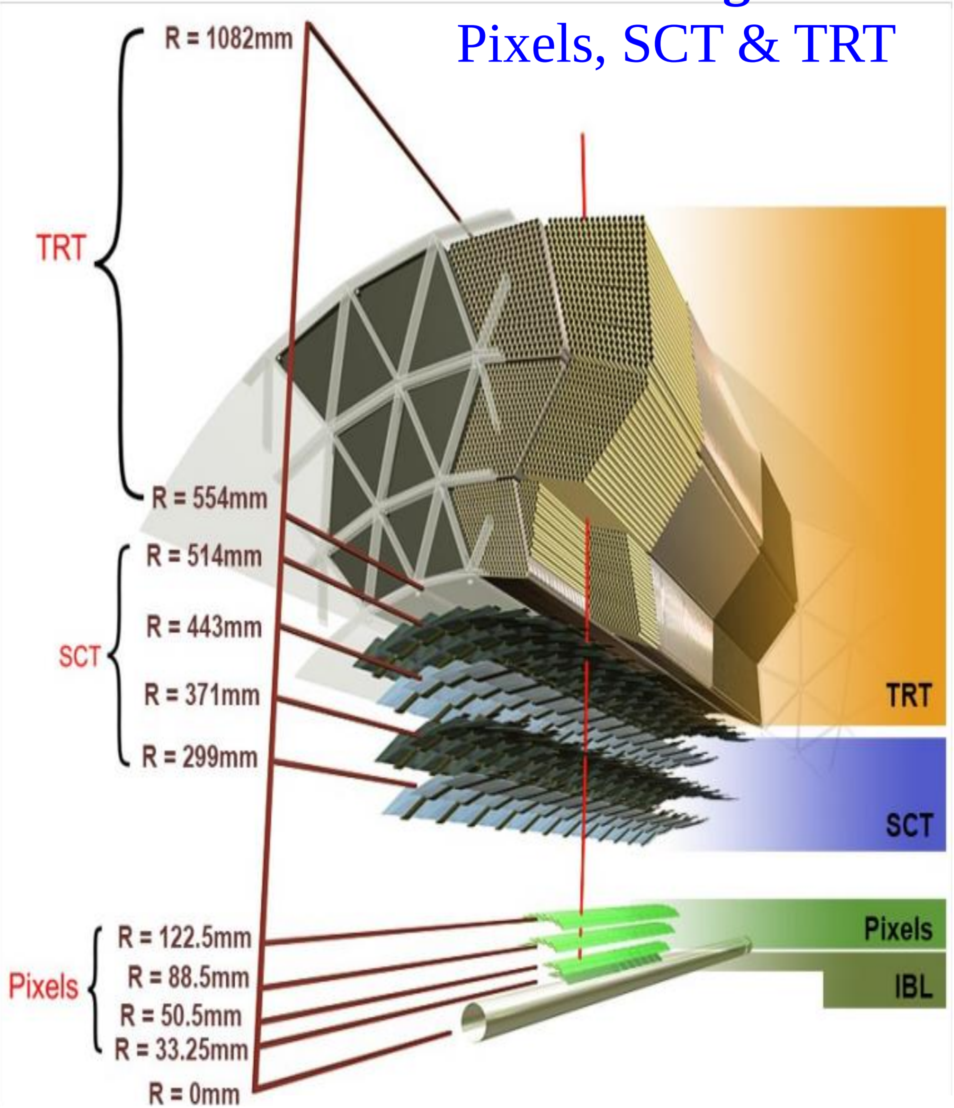

- **New innermost 4-th layer** for the Pixel detector [**IBL** = Insertable B-Layer]
- Required complete removal of the ATLAS Pixel volume
- IBL fully operational

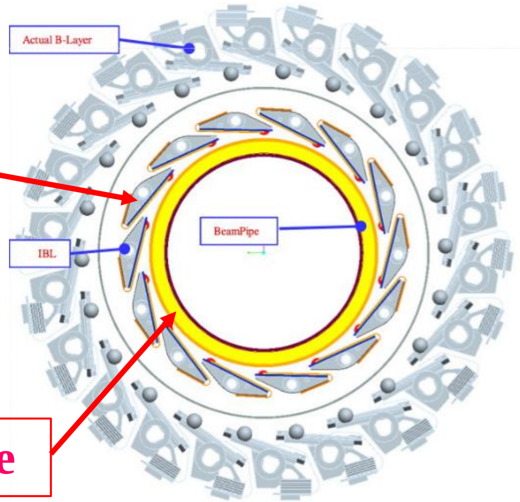

New Be beam pipe

Two times better tracks impact parameters resolution at 13 TeV!

ATLAS CALORIMETERS

- **Lar & TileCal >> Very stable** performance
- **Improved stability** of new Tile power supplies
- **Good operation efficiency: ~100% for LAr & Tile**
- LAr using 4 sample readout to achieve 100 kHz

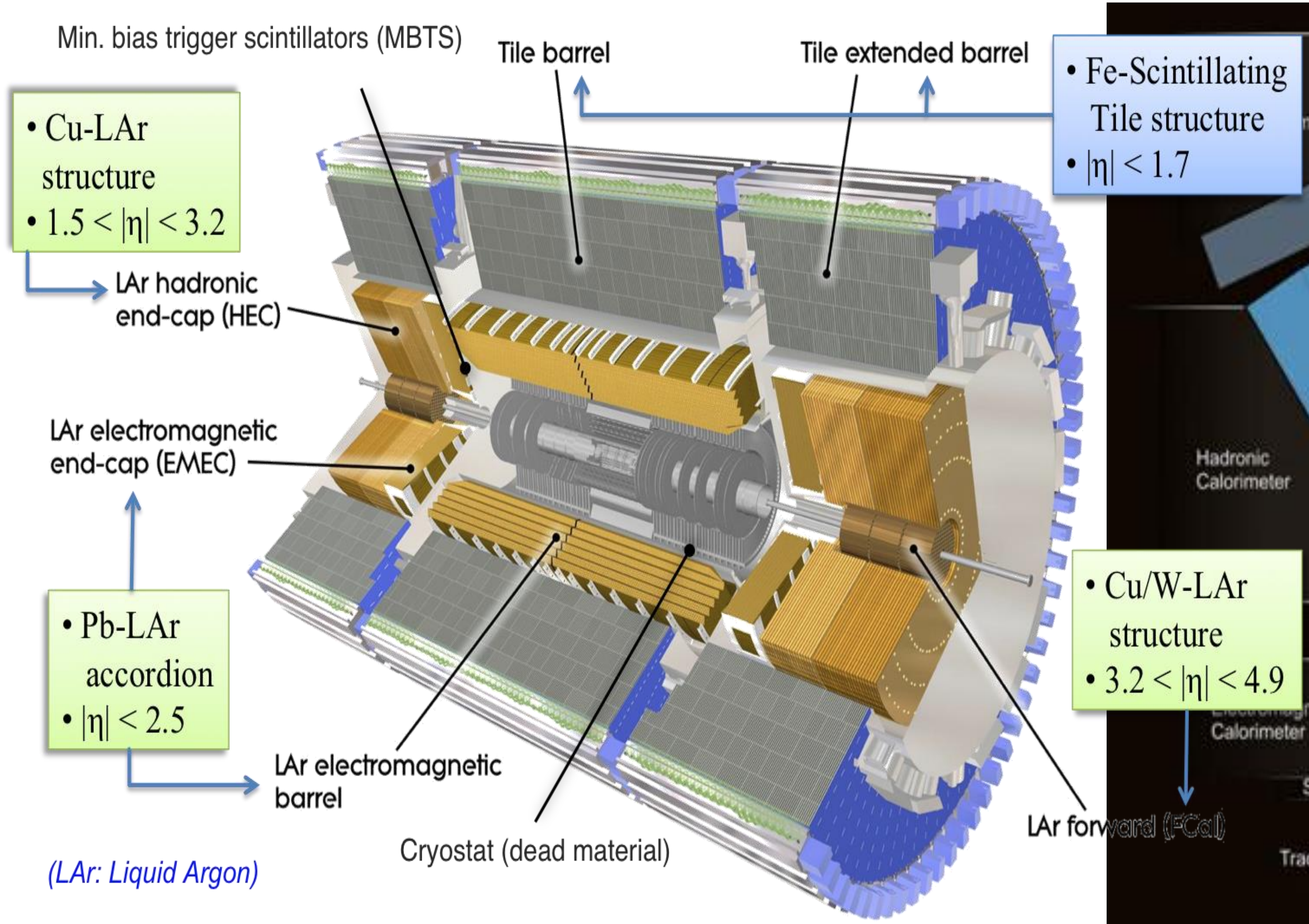

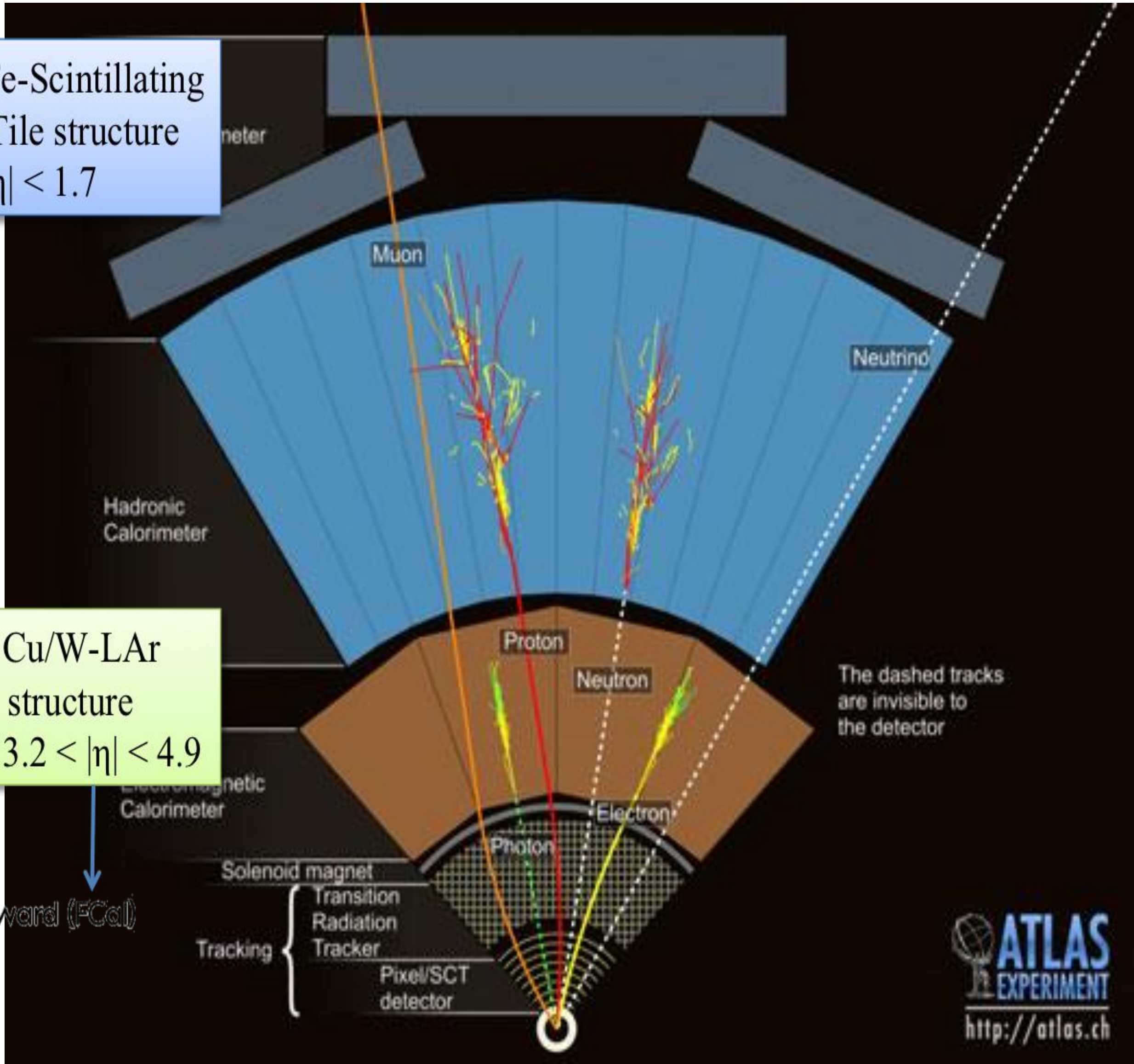

DIRECT PHOTON/ELECTOR RECONSTRUCTION

- ❑ Search for **seed energy clusters** in the EM calorimeter with significant energy
- ➢ For **|η|<2.5** EM LAr calorimeter is divided into 3 layers in depth, which are finely segmented in η and ϕ; a thin LAr presampler layer covering **|η|<1.8**;
- ➢ Form a cluster from cells in a rectangular region **Δη×Δφ=0.125×0.1715** around seed
- ❖ Selected in **barrel** $|\eta^{\gamma}|<1.475$ & **two end-cap** $1.375<|\eta^{\gamma}|<3.2$;
- ❖ **Photon identification**: classify as electron, photon, or converted photon matching cluster with tracks; use lateral and longitudinal energy profiles of the *photon/electron* electromagnetic shower

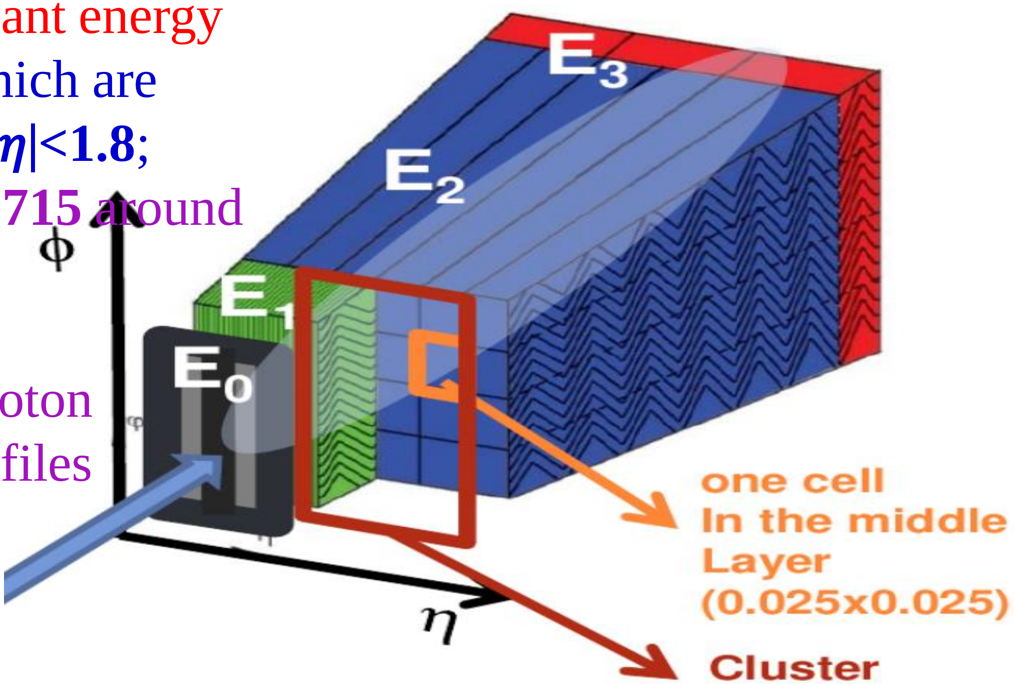

- ❑ **Calorimeter isolation** in region $\Delta R_{\gamma\gamma}>0.4$ around photon with requirement $E_T^{iso}<0.05 \times p_T^{\gamma}$
- ➢ Converted and unconverted *γ*-s are calibrated separately use the tracking information to correct the Calorimeter response for upstream energy losses and leakage
- ❖ **Calculate energy and direction**: photon energy a weighted sum of layer energies, with corrections for detector effects
- ✓ Corrected **for pileup** using jet area method
- ➢ Use 2D-sidebands for remaining background
- ❖ Remove hadron and τ background
- ✓ Small electron background removed using MC

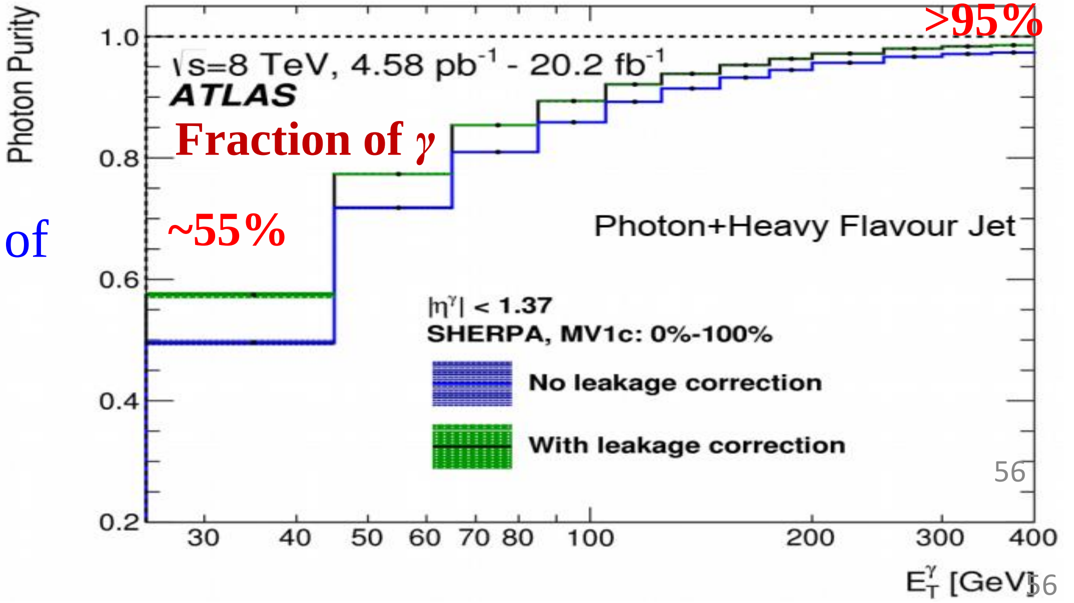

Cross section of $pp \to \gamma\gamma + X$ at 13 TeV #4

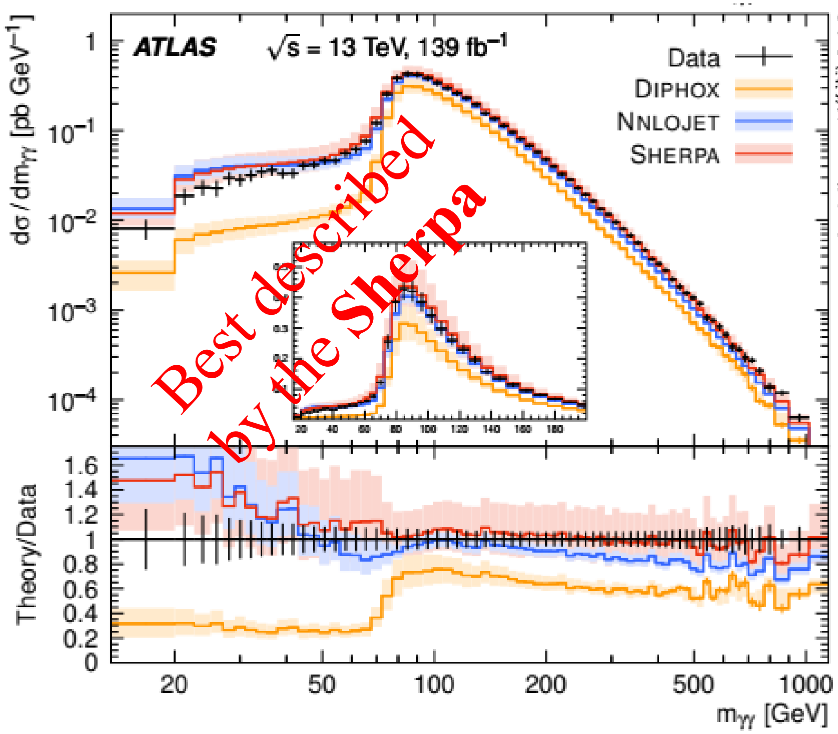

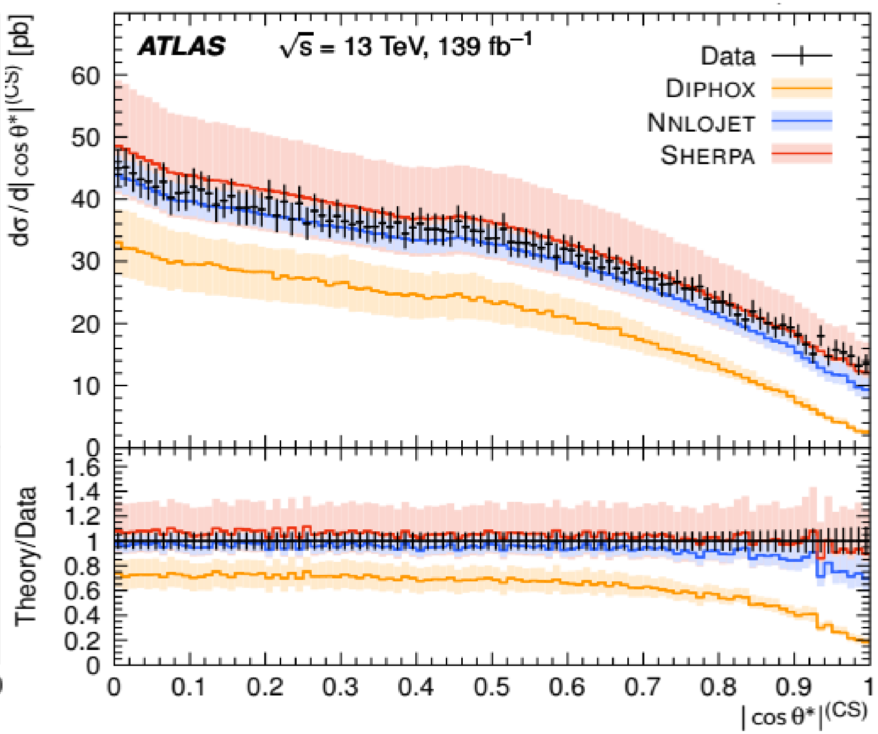

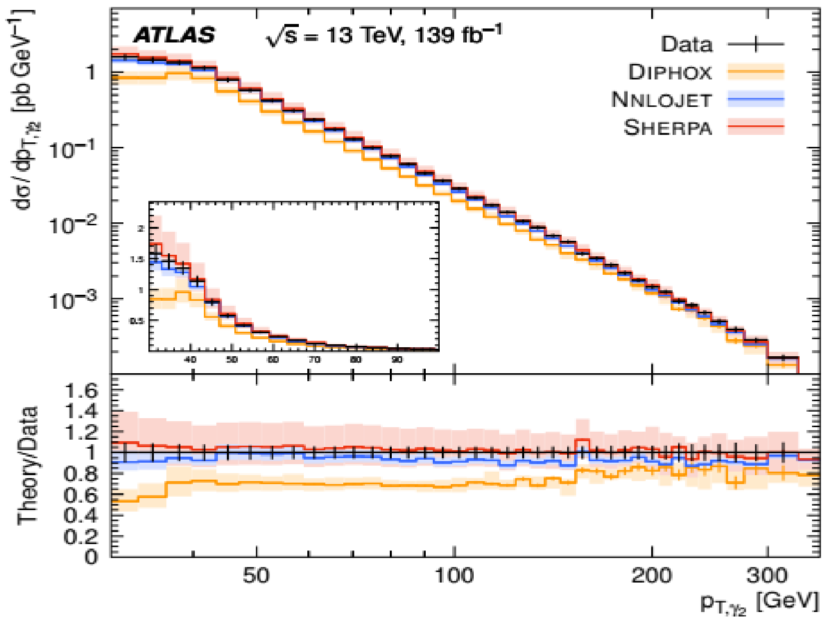

Differential cross sections measured as functions of $\mathbf{m_{\gamma\gamma}}$, $\boldsymbol{p_{T,\gamma 1}}$, $\boldsymbol{p_{T,\gamma 2}}$, $\mathbf{|\cos\theta^*|^{(CS)}}$ compared with the predictions from **Diphox NLO**, **Nnlojet NNLO**, **Sherpa** MEPS@NLO.

$$|\cos\theta^*|^{(CS)} = \left| \frac{\sinh(\Delta\eta_{\gamma\gamma})}{\sqrt{1+(p_{T,\gamma\gamma}/m_{\gamma\gamma})^2}} \cdot \frac{2p_{T,\gamma_1}p_{T,\gamma_2}}{m^2_{\gamma\gamma}} \right| = \left| \frac{p^+_{\gamma_1}p^-_{\gamma_2} - p^-_{\gamma_1}p^+_{\gamma_2}}{m_{\gamma\gamma}\cdot\sqrt{m^2_{\gamma\gamma}+p^2_{T,\gamma\gamma}}} \right|$$

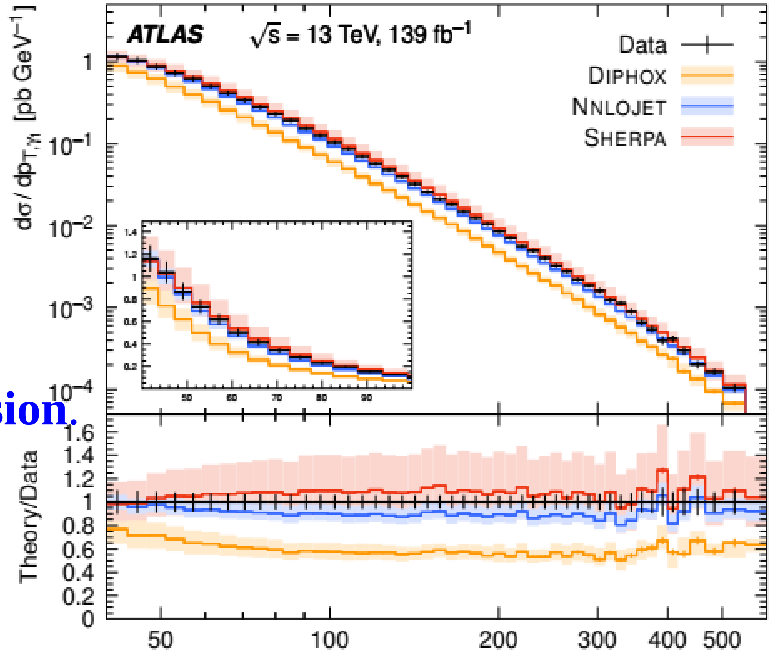

- Good agreement is generally found with the predictions at the **highest theoretical precision**.
- Only the merged approach with **multi-leg matrix elements at NLO**, as implemented by **Sherpa**, and a **fixed-order NNLO** calculation, as implemented by **NNLOJET**, give a **satisfactory description of the data.**

ELECTROWEAK $pp \to Z(\to ll)\gamma\, jj + X$ & $pp \to Z(\to \nu\nu)\gamma\, jj + X$ PRODUCTION #2

Experimental Signature

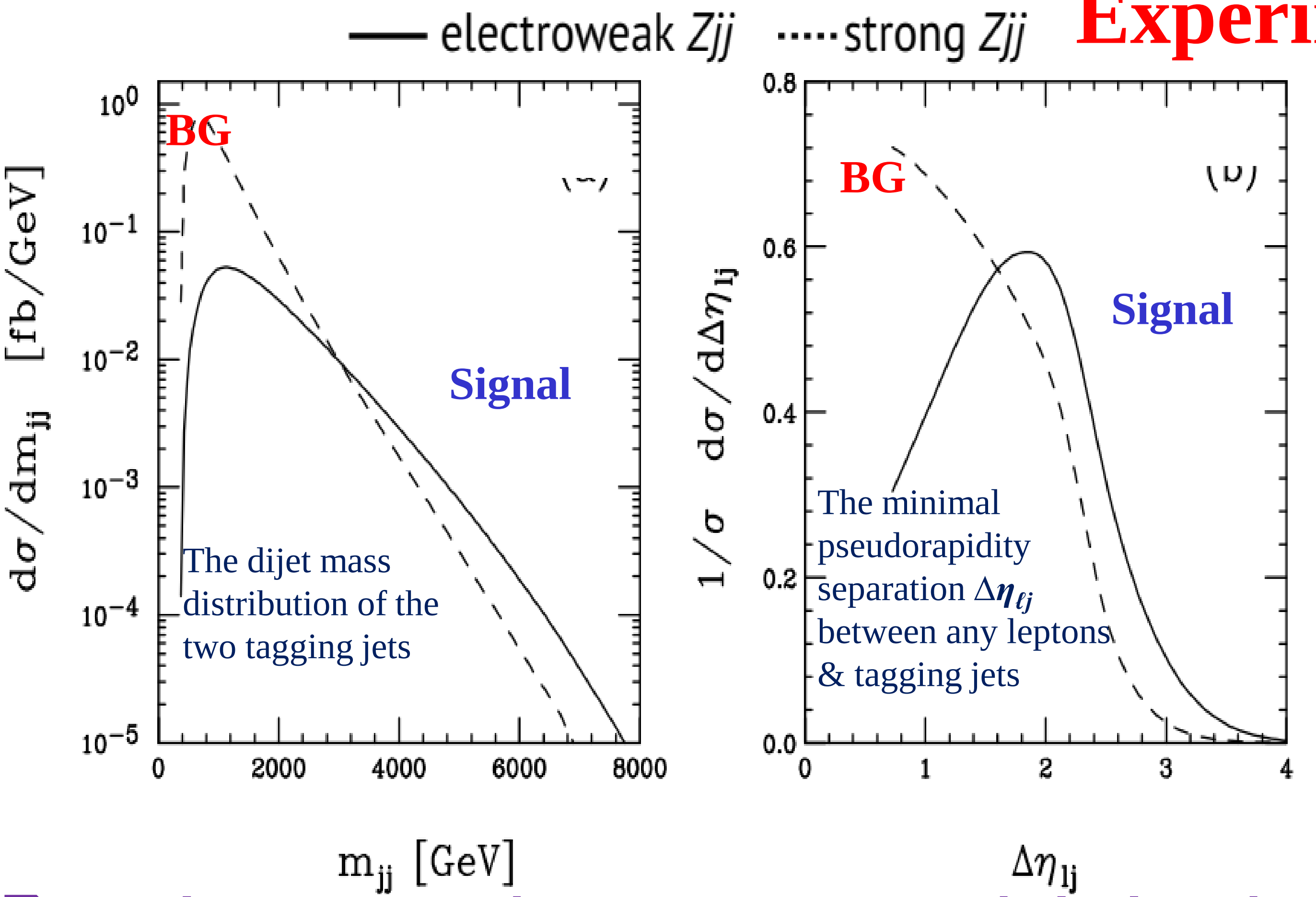

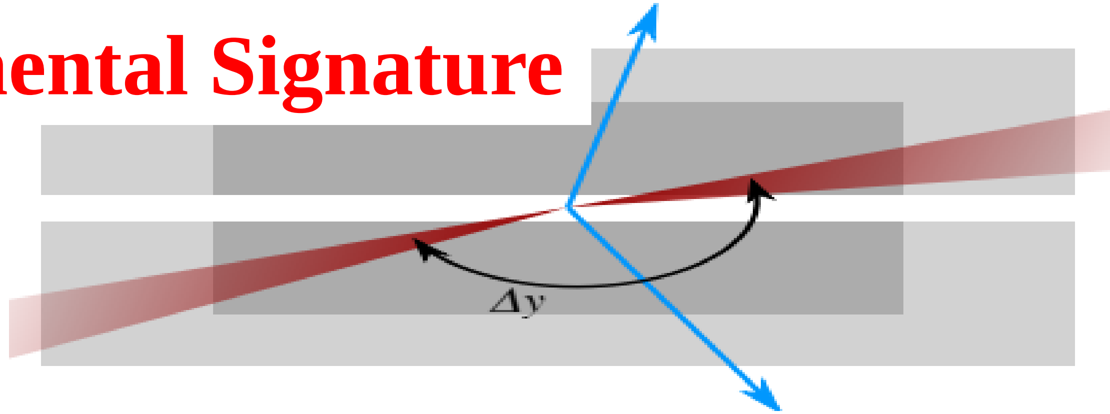

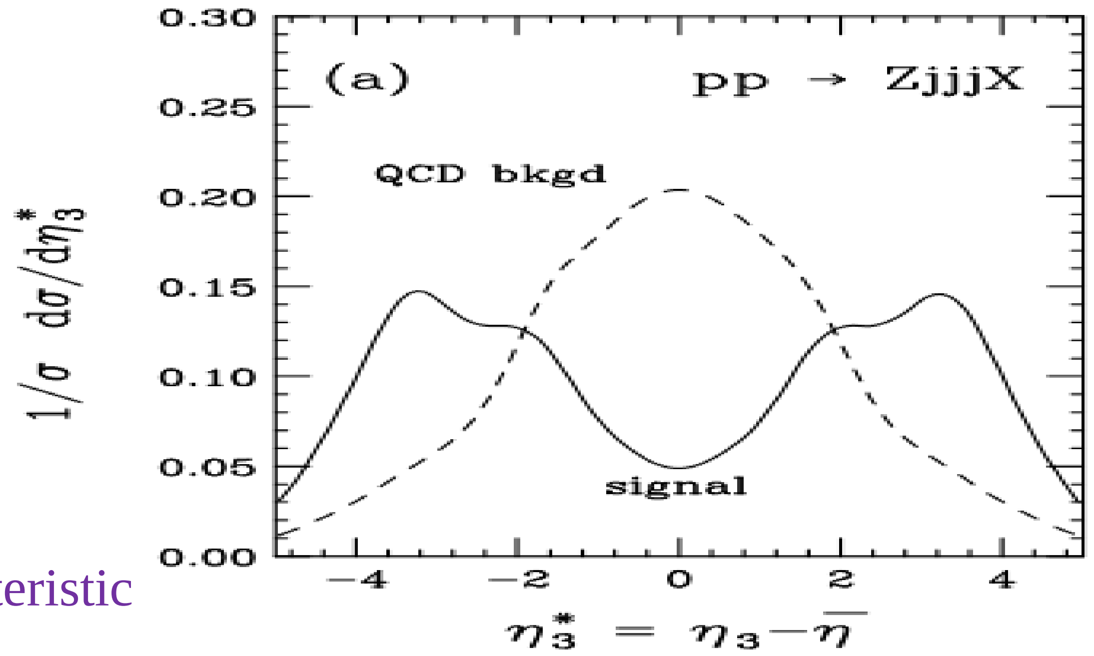

Characteristics of the third - soft jet in Z_{jjj} signal (solid) and background (dashed) events at the LHC. The pseudorapidity η_3^* is measured with respect to the center of the two tagging jets, $\langle\eta\rangle = (\eta_j^{tag1} + \eta_j^{tag2})/2$, and the distributions are normalized to unit area.

- No colour connection between scattering quarks leads to characteristic signature
- Additional activity in the event measured relative to centre of "tagging jets":

$$\zeta_X = \left|\frac{y_X - (y_{j1} + y_{j2})/2}{y_{j1} - y_{j2}}\right|, \quad C_X = \exp\left[-4\left(\frac{\eta_X - (\eta_{j1} + \eta_{j2})/2}{\eta_{j1} - \eta_{j2}}\right)^2\right]$$

COMBINATION OF THE ATLAS MEASUREMENTS

- The combination of **EW** ***Z(→ νν)γjj (E_T^γ>150 GeV) & (15<E_T^γ<110 GeV)*** production yields an observed (expected) **signal significance of 6.3σ (6.6σ)**
- Limits on ***anomalous Quartic Gauge Couplings (aQGC)*** are obtained in the framework of ***Effective Field Theory (EFT)*** with **dimension-8** operators

The effect of new physics introduced by ***aQGCs*** can be realised using an ***EFT*** linearly parameterised by an ***effective Lagrangian***:

$$\mathcal{L} = \mathcal{L}^{SM} + \sum_i \frac{c_i}{\Lambda^2} O_i + \sum_j \frac{f_j}{\Lambda^4} O_j$$

where O_i & O_j are **dimension-6** or **dimension-8** operators induced by integrating ou the new degrees of freedom, while c_i & f_j represent the numerical coefficients that are meant to be derivable from a more complete high-energy theory. The Λ term is a **mass-dimension parameter** associated with the **energy scale** of the new degrees of freedom that have been integrated out.

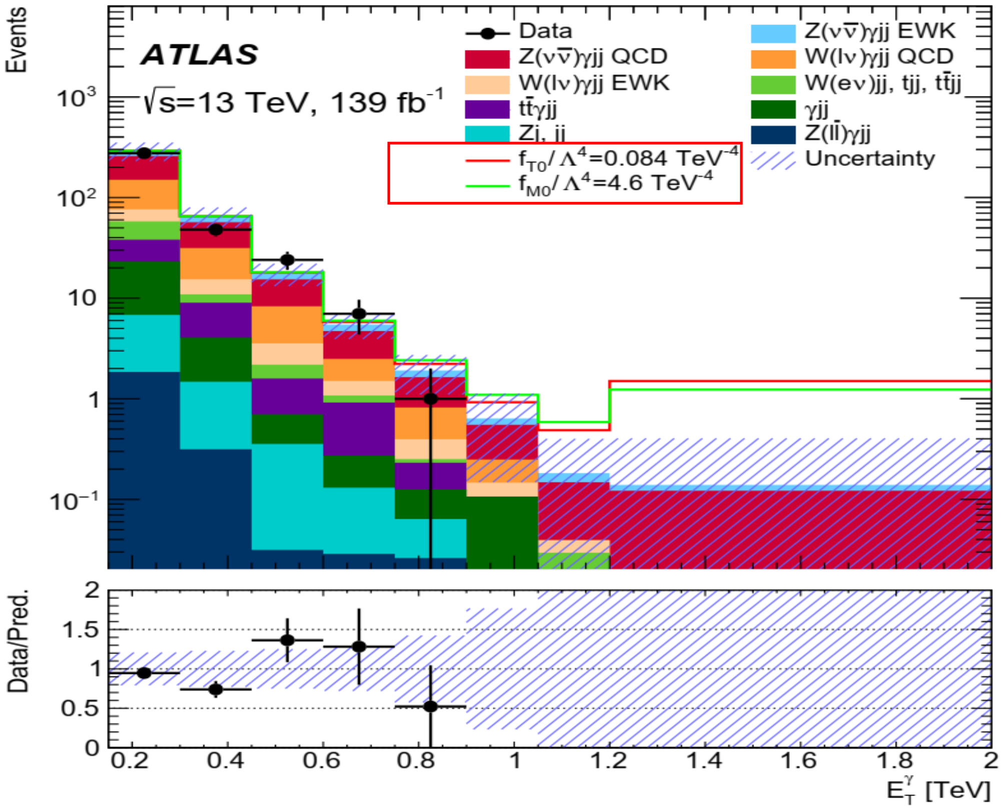

The E_T^γ distribution in the ***SR*** after the fit in the ***CRs***. The red (green) line shows the expected number of events in the case of non-zero ***EFT*** coefficient f_{T0}/Λ^4 (f_{M0}/Λ^4), values shown in the legend.

- ***Having found no significant deviations from SM predictions***, the data are used ***to set limits on anomalous Quartic Gauge Couplings***
- The limits are set on ***Effective Field Theory*** dimension-8 operators (f_{T0}/Λ^4, f_{T5}/Λ^4, f_{T8}/Λ^4, f_{T9}/Λ^4, f_{M0}/Λ^4, f_{M1}/Λ^4 & f_{M2}/Λ^4)
- These constraints are either competitive with or **more stringent** than those previously published by ***CMS***

OBSERVATION OF $pp \to WWW+X$ PRODUCTION #3

Observed (expected) significances and measured signal strengths for the individual and combined channels

Fit	Observed (expected) significances [σ]	$\mu(WWW)$
$e^{\pm}e^{\pm}$	2.3 (1.4)	1.69 ± 0.79
$e^{\pm}\mu^{\pm}$	4.6 (3.1)	1.57 ± 0.40
$\mu^{\pm}\mu^{\pm}$	5.6 (2.8)	2.13 ± 0.47
2ℓ	6.9 (4.1)	1.80 ± 0.33
3ℓ	4.8 (3.7)	1.33 ± 0.39
Combined	8.0 **(5.4)**	**1.66 ± 0.28**

Uncertainty source	$\Delta\sigma/\sigma$ [%]
Data-driven background	5.3
Prompt-lepton-background modeling	3.3
Jets and $E_{\mathrm{T}}^{\mathrm{miss}}$	2.8
MC statistics	2.8
Lepton	2.1
Luminosity	1.9
Signal modeling	1.5
Pile-up modeling	0.9
Total systematic uncertainty	9.5
Data statistics	11.2
WZ normalizations	3.3
Total statistical uncertainty	11.6

- Measured signal strength, overall & in individual channels
- **Background-only hypothesis rejected** with **8.0σ**, where **5.4σ** are expected

➢ The measured cross section, **extrapolated to the total phase space**, is:

$$\sigma_{WWW}^{data} = 820 \pm 100\ (stat) \pm 80\ (syst)\ fb$$

approximately **2.6σ** from the predicted cross section of

$$\sigma_{WWW}^{MC} = 511 \pm 18\ fb$$

calculated at NLO QCD and LO electroweak accuracy

ATL-PHYS-PUB-2021-022 COMBINED EFT INTERPRETATION OF *WW, WZ, 4L & ZJJ* PRODUCTION

Wilson coefficients of **the Standard Model Effective Field Theory (SM EFT)** are constrained in a combined fit of differential cross-section measurements of the productions: ***WW* & *WZ*** in leptonic final states, **4 charged leptons**, a leptonically decaying ***Z* boson** in vector-boson-fusion topology. No significant deviations from the SM expectation are found .

- ❑ Interpretation of multiboson measurements in the SMEFT
- ❑ Expansion of SM Lagrangian in increasing powers of inverse scale of new physics, **1/Λ**

$$\mathcal{L}_{\mathrm{SMEFT}} \approx \mathcal{L}_{\mathrm{SM}}^{(4)} + \sum_i \frac{c_i^{(6)}}{\Lambda^2} O_i^{(6)} + \sum_j \frac{c_j^{(8)}}{\Lambda^4} O_j^{(8)}$$

- ❑ Leading SMEFT effect expected from interference of dim-6 operators with SM:

$$\sigma \propto |\mathcal{M}_{\mathrm{SMEFT}}|^2 = |\mathcal{M}_{\mathrm{SM}}|^2 + \underbrace{\sum_i \frac{c_i^{(6)}}{\Lambda^2} 2\mathrm{Re}\left(\mathcal{M}_i^{(6)} \mathcal{M}_{\mathrm{SM}}^*\right)}_{\text{Linear model}} + \underbrace{\sum_i \frac{\left(c_i^{(6)}\right)^2}{\Lambda^4} \left|\mathcal{M}_i^{(6)}\right|^2}_{\text{Quadratic terms}} + \underbrace{\sum_{i \neq j} \frac{c_i^{(6)} c_j^{(6)}}{\Lambda^4} 2\mathrm{Re}\left(\mathcal{M}_i^{(6)} \mathcal{M}_j^{(6)*}\right)}_{\text{Cross terms}}$$

Linear model | **Quadratic terms** | **Cross terms**

- ❑ Quadratic term at the same order, $O(\Lambda^{-4})$, as SM + dim-8 interference
- ❑ Focus on operators at dim-6: 33 CP-even operators studied, assuming flavour symmetry and neglecting Higgs

Combination of several multiboson measurements

- ➢ **pp → WW → eνμν:** Eur. Phys. J. C 79 (2019) 884 using 36 fb^{-1}
- ➢ **pp → WZ → lll'ν:** Eur. Phys. J. C 79 (2019) 535 using 36 fb^{-1}
- ➢ **pp → 4l→ ' lll'l':** JHEP 07 (2021) 005 using 139 fb^{-1}
- ➢ **pp → Zjj → lljj:** Eur. Phys. J. C 81 (2021) 163 using 139 fb^{-1}
- ❑ Higgs-boson production kinematically suppressed:
  - ❑ see **ATLAS-CONF-2020-053** for dedicated EFT study
  - ❑ see **ATL-PHYS-PUB-2021-010** for a H!WW∗ and WW combination

- ❑ Measurements with high precision and small background contributions
- ❑ Sensitive to a large number of dim-6 operators affecting
  - ❑ gauge-boson self-couplings
  - ❑ couplings of gauge bosons and fermions
  - ❑ four-fermion couplings

NR

COMBINED EFT INTERPRETATION OF *WW*, *WZ*, *4L* & *ZJJ* PRODUCTION

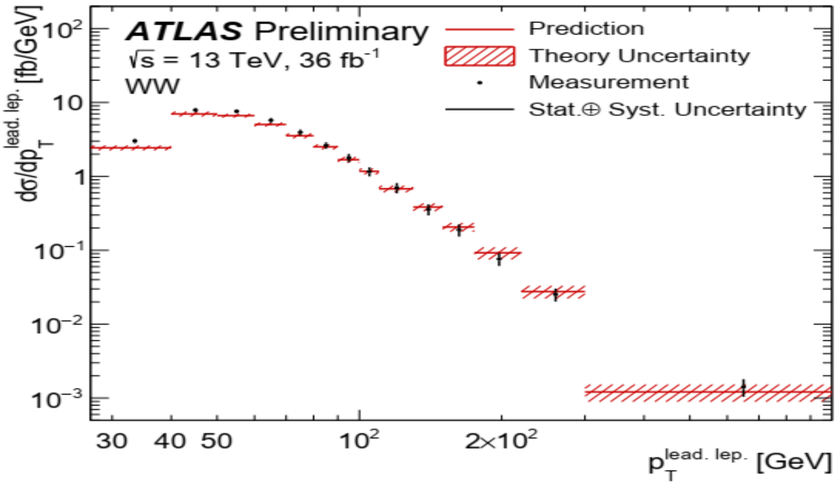

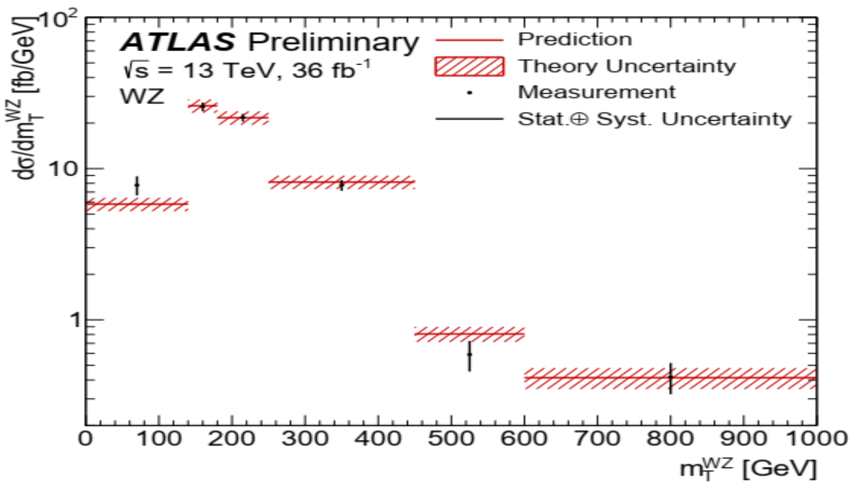

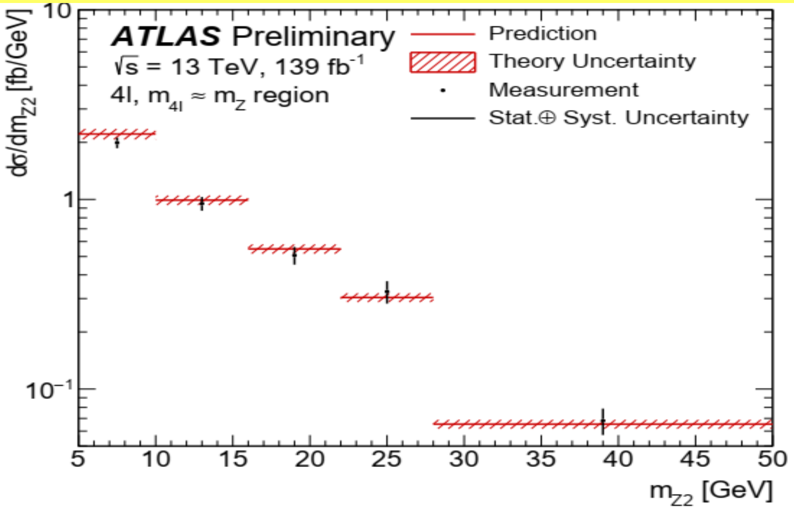

Assuming smooth **EFT** effects have the folding matrix of the SM. Injection of BSM physics has been explicitly tested in $\mathbf{m_{4l}}$

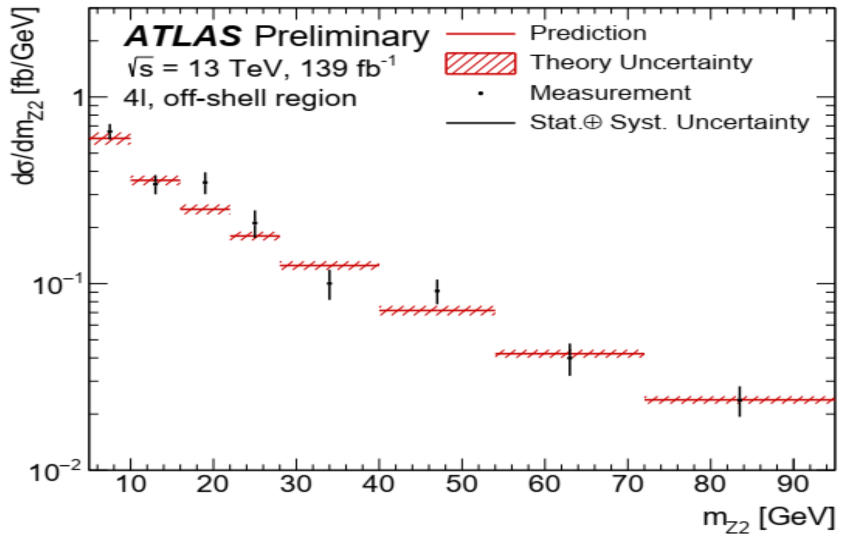

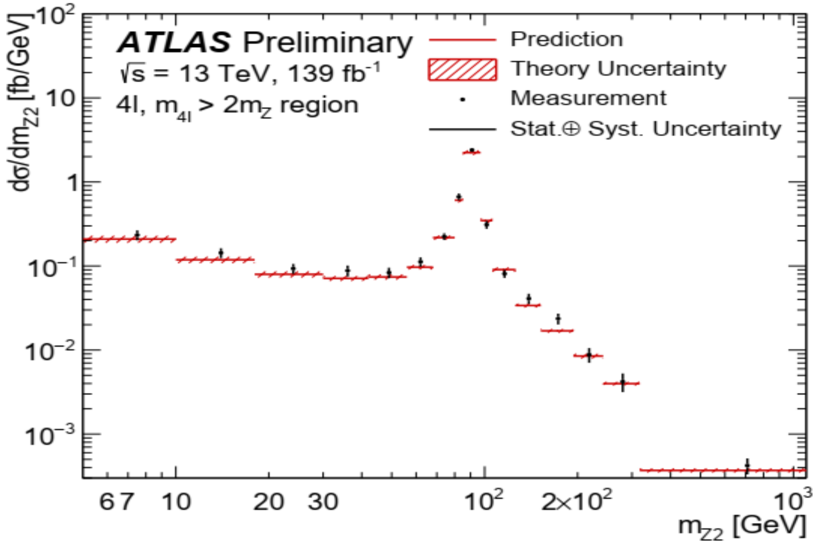

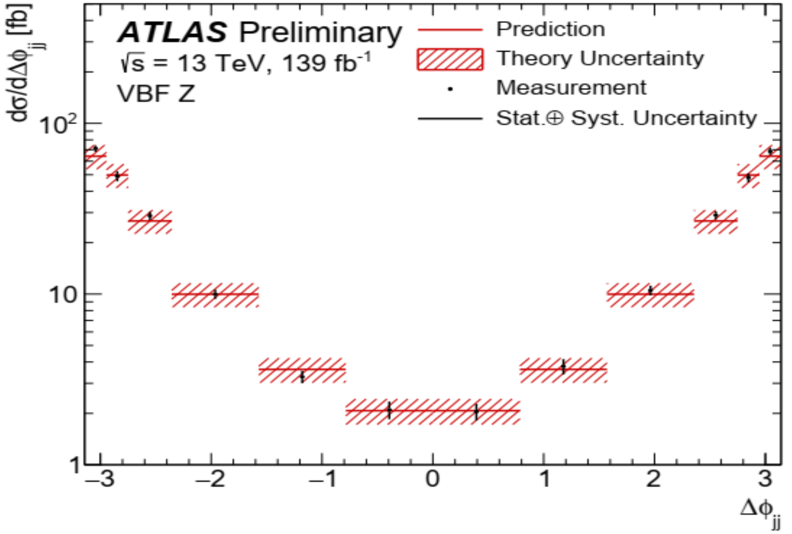

Measured differential cross-sections compared to the SM theory predictions used in this analysis. The $p_T^{lead.lep.}$ in *WW* production, the *WZ* **transverse mass** in *WZ* production, the invariant mass of the secondary lepton pair in the three *4ℓ* analysis regions, the signed azimuthal angle between the two jets in ***Z+jets*** production with a VBF topology.

COMBINED EFT INTERPRETATION OF *WW, WZ, 4L & ZJJ* PRODUCTION

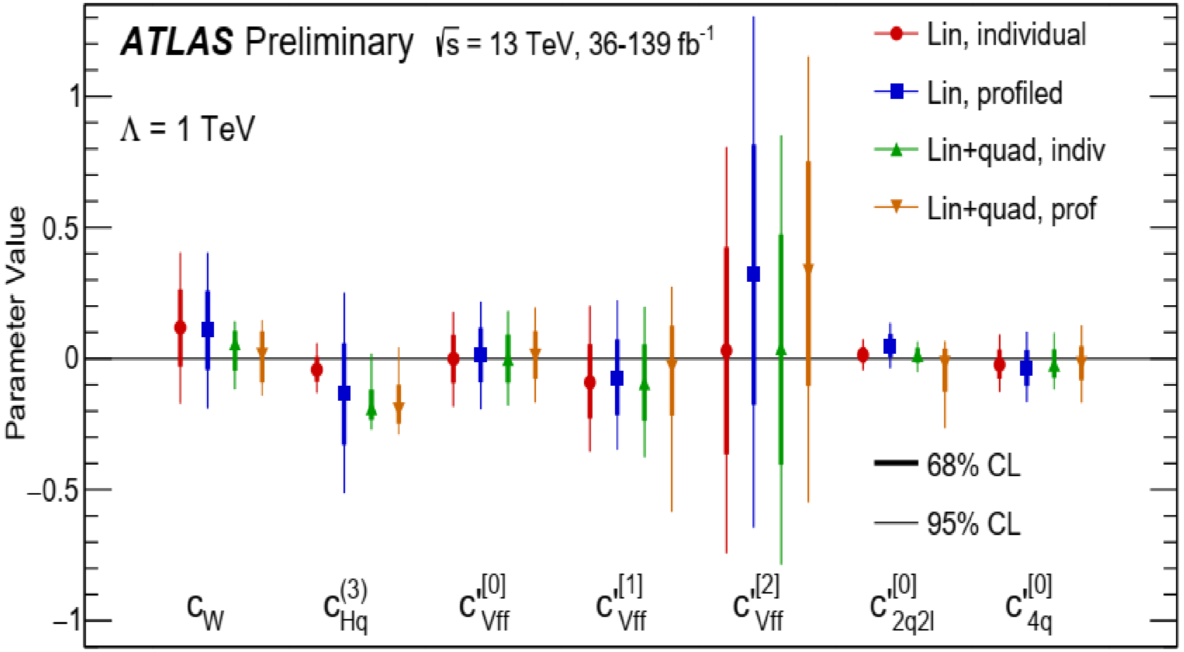

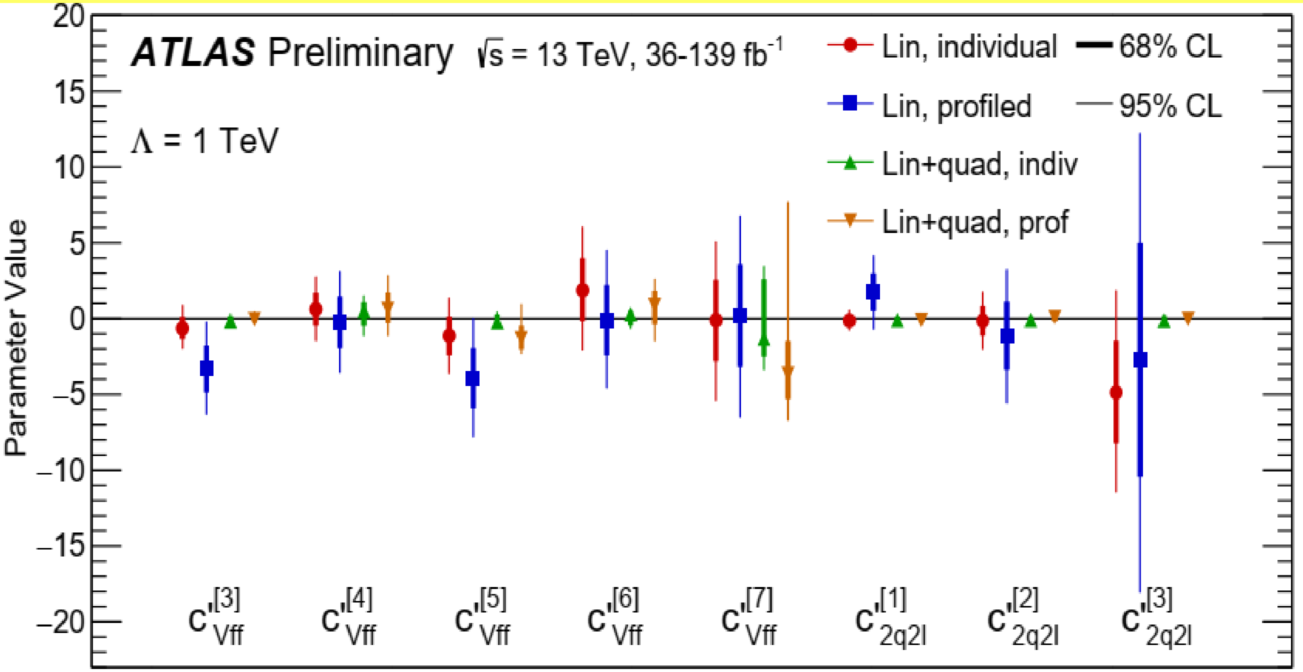

$c'^{[0]}_{Vff} \simeq 0.81c_{HWB} + 0.38c_{HD} + 0.13c^{(1)}_{Hl} + 0.37c^{(3)}_{Hl} - 0.14c^{(1)}_{ll} + 0.12c^{(1)}_{Hq}$

$c'^{[1]}_{Vff} \simeq 0.73c^{(1)}_{Hl} - 0.28c^{(3)}_{Hl} - 0.48c_{He} + 0.38c^{(1)}_{ll} + 0.13c^{(1)}_{Hq}$

$c'^{[2]}_{Vff} \simeq 0.37c_{HWB} + 0.17c_{HD} - 0.31c^{(1)}_{Hl} - 0.53c^{(3)}_{Hl} + 0.25c_{He} + 0.59c^{(1)}_{ll} - 0.21c^{(1)}_{Hq}$

$c'^{[0]}_{2q2l} \simeq -0.37c^{(1)}_{lq} + 0.89c^{(3)}_{lq} - 0.11c_{lu} - 0.21c_{eu} - 0.13c_{qe}$

$c'^{[0]}_{4q} \simeq 0.11c^{(11)}_{qq} + 0.22c^{(18)}_{qq} + 0.95c^{(31)}_{qq} - 0.2c^{(38)}_{qq}$

$c'^{[3]}_{Vff} \simeq -0.19c^{(1)}_{Hl} - 0.14c^{(3)}_{Hl} + 0.86c^{(1)}_{Hq} + 0.41c_{Hu} - 0.17c_{Hd}$

$c'^{[4]}_{Vff} \simeq -0.35c_{HWB} + 0.49c_{HD} + 0.26c^{(1)}_{Hl} + 0.35c^{(3)}_{Hl} + 0.51c_{He} + 0.38c^{(1)}_{ll} + 0.18c^{(1)}_{Hq}$

$c'^{[5]}_{Vff} \simeq 0.25c_{HD} + 0.33c^{(1)}_{Hl} - 0.22c^{(3)}_{Hl} + 0.18c_{He} - 0.35c^{(1)}_{ll} - 0.3c^{(1)}_{Hq} + 0.71c_{Hu} - 0.16c_{Hd}$

$c'^{[6]}_{Vff} \simeq -0.22c^{(1)}_{Hl} + 0.52c^{(3)}_{Hl} - 0.39c_{He} + 0.44c^{(1)}_{ll} - 0.22c^{(1)}_{Hq} + 0.52c_{Hu}$

$c'^{[7]}_{Vff} \simeq -0.28c_{HWB} + 0.71c_{HD} - 0.31c^{(1)}_{Hl} - 0.21c^{(3)}_{Hl} - 0.5c_{He} - 0.14c^{(1)}_{ll}$

$c'^{[1]}_{2q2l} \simeq 0.56c^{(1)}_{lq} + 0.44c^{(3)}_{lq} + 0.61c_{eu} - 0.1c_{ed} + 0.34c_{qe}$

$c'^{[2]}_{2q2l} \simeq 0.68c^{(1)}_{lq} + 0.15c^{(3)}_{lq} + 0.33c_{lu} - 0.51c_{eu} + 0.13c_{ed} - 0.37c_{qe}$

$c'^{[3]}_{2q2l} \simeq -0.27c^{(1)}_{lq} + 0.79c_{lu} - 0.39c_{ld} + 0.26c_{eu} - 0.22c_{ed} - 0.16c_{qe}$

Confidence intervals for the 15 parameters included in the combined maximum likelihood fit. Results are quoted both for fits linear in the parameters and for fits that take into account also quadratic contributions. The first case corresponds to a model in which only the $\mathcal{O}(\Lambda^{-2})$ contributions to the cross-section prediction, the interference between SM and dimension-six operators, is included. The latter case also includes quadratic dimension-six contributions, which are part of the $\mathcal{O}(\Lambda^{-4})$ contributions. Comparisons of the two results can be used to estimate uncertainties due to the truncation of the EFT expansion.

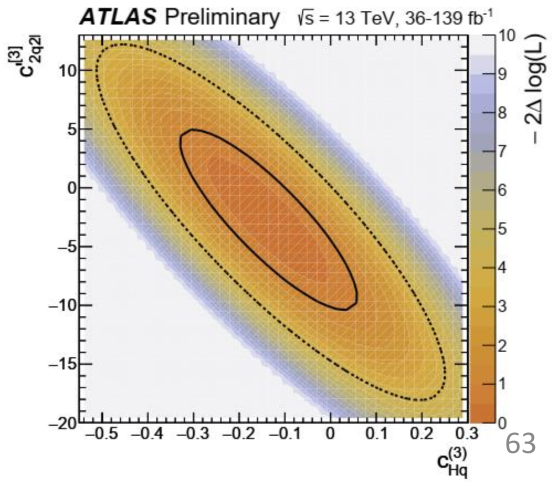

- Limits set at 95% confidence level, both for the "linear" and "linear plus quadratic" models
- Fits of individual coefficients, as well as combined fit

Parton distribution functions at $\sqrt{s}$ = 7, 8, 13 TeV

- An analysis at NNLO order in the theory of QCD for the determination of a new set of parton distribution functions (PDF) using diverse measurements in *pp* collisions at $\sqrt{s}$ = 7, 8 and 13 TeV, performed by the ATLAS at the LHC, together with deep inelastic scattering data from *ep* collisions at the HERA.
- The ATLAS data sets considered are differential cross-section measurements of inclusive $W^{\pm}$ and $Z/\gamma*$ boson production, $W^{\pm}$ and Z boson production in association with jets, $t\bar{t}$ production, inclusive jet production and direct photon production. The resulting set of PDF is called **ATLASpdf21**.
- It is observed that the addition of the **ATLAS** data sets to the **HERA** data brings the PDFs much closer to the **global PDFs** of MSHT, CT and NNPDF than to HERAPDF2.0.
- The **ATLASpdf21** PDFs agree with these global fits as well as they agree with each other.
- Thus, ATLAS data seem to be able to replicate many of the features that the fixed-target deep inelastic scattering and Drell–Yan data plus the Tevatron Drell–Yan data bring to the global PDFs.
- Using only the HERA and ATLAS data allows a detailed treatment of correlated systematic uncertainties.

Eur. Phys. J. C 82 (2022) 7, 608
arXiv: 2202.02218

BOSE-EINSTEIN CORRELATIONS AT 13 TEV #1

Correlations in phase space **between two identical bosons** from symmetry of wave functions.

- ► Enhances likelihood of *two particles close* in phase space
- ► Allows one to 'probe' the source of the bosons *in size* and *shape*
- ► Dependence on particle multiplicity and transverse momentum probes *the production mechanism*

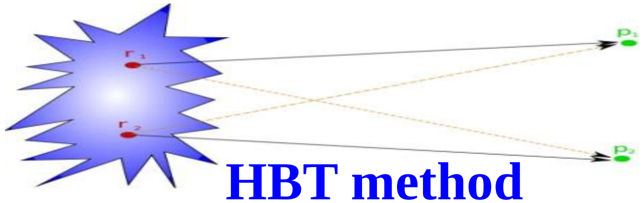

HBT method

Correlation function $C_2(Q)$ a ratio of probabilities:

$$C_2(Q) = \frac{\rho(p_1,p_2)}{\rho_0(p_1,p_2)} = C_0\left(1+\Omega(\lambda,RQ)\right)\cdot\left(1+Q\varepsilon\right),$$

$$\Omega^E(\lambda,RQ) = \lambda e^{-RQ}$$

$$\Omega^G(\lambda,RQ) = \lambda e^{-R^2Q^2}$$

$$Q^2 = -(p_1-p_2)^2$$

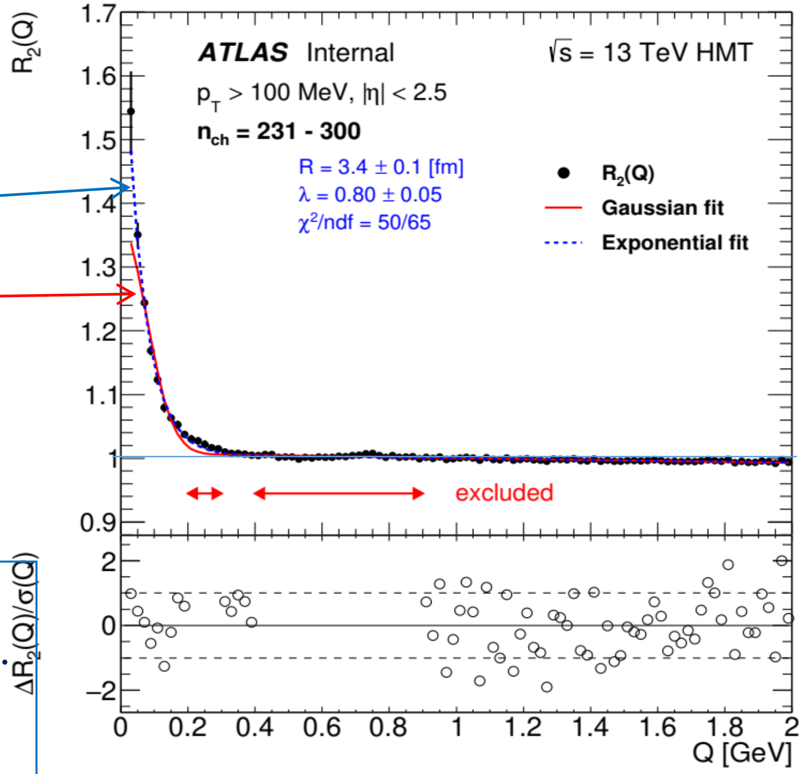

C_0 is a *normalisation*, **ε** accounts for *long range effects*, **R** is the **effective radius parameter of the source**, **λ** is the **strength of the effect parameter**, 0/1 for coherent/chaotic source.

Two possible parameterisation: **Gaussian and Exponential**.

$$C_2(Q) = \frac{N^{++,--}(Q)}{N^{ref}(Q)}$$

N_{ref} without BEC effect from: unlike-charge particles (**UCP**), opposite hemispheres, event mixing. **Basic Reference**: distribution of **UCP** pairs of non-identical particle taken from the same event.

$$R_2(Q) = \frac{C_2^{Data}(Q)}{C_2^{MC}(Q)} = \frac{\rho(++,--)\big/\rho(+-)}{\rho^{MC}(++,--)\big/\rho^{MC}(+-)}$$

29.08.2023

The studies are carried out using the **double ratio correlation function**. The **$R_2(Q)$** eliminates problems with energy-momentum conservation, topology, resonances, hadronic jets, mini-jets etc. **MC without BEC.**